

https://dspace.org/

Elucidating the molecular pathways associated with Cholesteryl Ester Transfer Protein (CETP) knockdown in estrogen receptor positive breast cancer

Pillay, Ruvesh Pascal

2020
https://hdl.handle.net/10539/30978

Downloaded from a DSpace repository. https://dspace.org/



Elucidating the Molecular Pathways associated with Cholesteryl Ester Transfer Protein (CETP) Knockdown in Estrogen Receptor Positive Breast Cancer

by

Ruvesh Pascal Pillay

(1101436)

Dissertation

Submitted in fulfilment of the requirements for the degree

Master of Science

in

Molecular and Cell Biology

in the Faculty of Science, University of the Witwatersrand, Johannesburg, South Africa

Supervisor: Professor Mandeep Kaur

February 2020

Declaration

I declare that this dissertation is my own, unaided work. It is being submitted for the Degree of Master of Science at the University of the Witwatersrand, Johannesburg. It has not been submitted before for any degree or examination at any other University.



27th day of February 2020 at the university of the Witwatersrand

Abstract

The cholesterogenic phenotype, encompassing *de novo* biosynthesis and accumulation of cholesterol aids cancer cell proliferation and survival. Previous studies from our laboratory have implicated the Cholesteryl Ester Transfer Protein (CETP), in the involvement of breast cancer aggressiveness via cholesterol accumulation. Interestingly, the abrogation of CETP resulted in significant cell death in MCF-7 breast cancer cells (estrogen receptor positive), which also sensitised cells to currently available cytotoxic cancer agents, such as Tamoxifen even at low concentrations. Thus, this study displayed CETP's role as potential cancer survival gene and drug resistance marker. The current study investigated the effect of CETP knockdown (in MCF-7 cells) on cholesterol levels and changes in expression of genes that are involved in lipoprotein signalling and cancer drug resistance. The study therefore focused on elucidating the molecular mechanisms underlying CETP's involvement in cancer, particularly, ER+ breast cancer. Intriguingly, CETP knockdown resulted in reduction in cholesterol especially when treated with a cholesterol depletory agent (Acetyl-plumbagin), decreasing the viability of these cancer cells. Furthermore, there was an overall downregulation of genes involved in cholesterol biosynthesis, including genes of the mevalonate pathway (*HMGCS1, HMGCR, MVD*), as well as genes that code transcription factors for cholesterol synthesis (*SREBPF1*), post-CETP knockdown. Additionally, *LDLR*, the principal receptor involved in exogenous cholesterol uptake was also significantly downregulated. Cancer drug resistance gene expression analysis revealed a downregulation of genes coding growth factor receptors (*ESR1, IGF1RHER2*), drug efflux pumps (*ABCB1*) and anti-apoptotic *BCL2*. The principal findings of this study display the possible role of downregulating CETP to limit drug resistance and cholesterol accumulation in cancer cells, thereby reducing breast cancer aggressiveness.

Acknowledgements

- I would like to thank my supervisor, Prof Kaur for all the help and insight into the project, as well as giving me great words of motivation and advice, and the continuous patience she displayed throughout my Master's degree.
- I would like to thank my colleagues in GH527 for all the help they have given me and for making the lab environment fun to be in. A special thank you to Liang, my mentor, for the continuous support over the years.
- I would like to thank my parents, grandmother, brother, friends and extended family for always believing in me, even when I didn't, for all the encouraging words, love and support.
- Lastly, I would like to thank the University of the Witwatersrand for financial support through funding of my degree by the Post-graduate Merit Award (PMA).

Table of Contents

Declaration 2
Abstract 3
Acknowledgements 4
List of figures 7
List of tables 8
List of symbols 9
List of abbreviations 10
1. Introduction 16
1.1. Global cancer statistics and breast cancer occurrence 16
1.2. Cancer and breast cancer hallmarks 16
1.3. Hormone induced breast cancer and existing breast cancer treatments 18
1.4. The role of cholesterol in breast cancer progression 19
1.5. Targeting cholesterol for cancer treatment 26
1.5.1. Cholesterol synthesis inhibitory drugs 27
1.5.2. Cholesterol-depleting agents 28
1.6. Preliminary studies 30
2. Aim and objectives 32
2.1. Aim 32
2.2. Objectives 32
3. Methods 33
3.2. Cell culture 33
3.3. Cell counting 33
3.3. CETP knockdown by siRNA transfection 35
3.4. Reverse-Transcriptase Quantitative Polymerase Chain Reaction (RT-qPCR) 38
3.4.1. RNA isolation 38
3.4.2. cDNA synthesis 40
3.4.3. Quantitative PCR (qPCR) 40
3.5. Western blotting 42
3.5.1. Cell lysis 43
3.5.2. BCA assay 43
3.5.3. SDS PAGE and Western blotting 45
3.6. Immunofluorescence staining 47
3.7. Cholesterol quantification 48
3.7.1. Cholesterol assay 48

3.7.2. Filipin staining 51
3.8. RT^2 Profiler PCR Array (Lipoprotein Signalling and Cancer Drug Resistance) 52
3.8.1. RNA isolation 52
3.8.2. Reverse transcription 52
3.8.3. Real-time PCR 54
3.9. Network maps: OmicsNet and Cytoscape 55
3.10. Statistical analysis 55
4. Results 56
4.1. Confirmation of successful CETP knockdown 56
4.1.1. RT-qPCR anlaysis 56
4.1.2. Western blotting and densitometry analysis 57
4.1.3. Immunofluorescence imaging 58
4.2. CETP knockdown reduces free cholesterol and endogenous CEs in MCF-7 cells 60
4.2.1. Filipin staining 60
4.2.2. Cholesterol Assay 61
4.3. CETP knockdown decreases MCF-7 cell viability 62
4.4. Shift in pathway dynamics post-CETP knockdown: Overall downregulation of genes involved lipoprotein signalling and cancer drug resistance 63
4.4.1. Lipoprotein signalling 64
4.4.2. Cancer Drug resistance 69
5. Discussion 73
5.1. CETP knockdown reduces MCF-7 cell viability and decreases cholesterol and CE content 73
5.2. Altered lipogenic expression profile in MCF-7 post-CETP knockdown 75
5.3. CETP knockdown reduces cancer drug resistance in MCF-7 cells 79
6. Concluding remarks and future perspectives 83
7. Successes and limitations of the study 84
8. Troubleshooting 85
9. References 87

List of figures

Figure 1.1: The biosynthesis of cholesterol, the production of steroid hormones from cholesterol, the role of steroid hormones in oncogenic signalling pathways and the action of current chemotherapeutic drugs in breast cancer.
Figure 1.2: Intracellular uptake and extracellular removal of cholesterol, and the role of CETP in cholesterol homeostasis.
Figure 1.3: Cholesterol homeostasis maintained by several proteins, enzymes, receptors and TFs.
Figure 1.4: Various targets in the cholesterol pathway by available drugs
Figure 3.1: Representation of a Neubauer haemocytometer under a microscope.
Figure 3.2: Mechanism of gene silencing by siRNA.
Figure 3.3: A representative integrity gel of the extracted RNA.
Figure 3.4: A representative BCA protein standard curve.
Figure 3.5: Basis of a cholesterol assay.
Figure 4.1: Successful knockdown of CETP mRNA in MCF-7 cells, confirmed by RT-qPCR.
Figure 4.2: Successful knockdown of CETP protein in MCF-7 cells, confirmed by Western blotting.
Figure 4.3: Successful knockdown of CETP protein in MCF-7 cells, confirmed by immunofluorescence staining.
Figure 4.4: Reduction in CE content post-CETP knockdown in MCF-7 cells, confirmed by filipin staining.
Figure 4.5: CETP knockdown reduces intracellular CE levels in MCF-7 cells.
Figure 4.6: CETP knockdown reduces MCF-7 cell viability.
Figure 4.7: Network map of genes involved in lipoprotein signalling in response to CETP knockdown.
Figure 4.8: Network map of genes involved in cancer drug resitance in response to CETP knockdown.

List of tables

Table 3.1: siRNA transfection reagent mixture.

Table 3.2: 1× TBE buffer (pH 8.0).

Table 3.3: Volumes of RevertAidFirst Strand cDNA Synthesis reagents added to extracted RNA for cDNA synthesis.

Table 3.4: Volumes of SensiFAST™ SYBR® No-ROX reagents added to cDNA templates for qPCR.

Table 3.5: Primer sequences of CETP and GAPDH genes (Ding *et al*., 2015).

Table 3.6: Three-step cycling parameter used for qPCR.

Table 3.7: Ripa/Lysis buffer components.

Table 3.8: SDS-PAGE 10%, 1 mm gel components.

Table 3.9: SDS-PAGE gel buffer components.

Table 3.10: 1× TBST buffer (pH 7.5).

Table 3.11: Cholesterol assay components (Reagent A) per well (mixed in this order).

Table 3.12: Genomic DNA elimination mix.

Table 3.13: Reverse-transcription mix.

Table 3.14: PCR components mix.

Table 3.15: Cycling conditions.

Table 4.1: Gene expression changes of genes involved in lipoprotein signalling in transfected compared to non-transfected MCF-7 cells.

Table 4.2: Gene expression changes of genes involved in cancer drug resistance in transfected compared to non-transfected MCF-7 cells.

List of symbols

β Beta

µ Micro

™ Trademark

℃ Degree Celsius

% Percentage

© Copyright

® Registered Trademark

List of abbreviations

ABCA1	ATP-binding Cassette Transporter
ABCB1	Gene encoding P-gp or MDR1
ABCB1	P-gp or MDR1
ACAT	Acyl-Coenzyme A: Cholesterol Acyltransferase
Acetyl-CoA	Acetyl-coenzyme
Akt	Protein Kinase B
AP	Acetyl – Plumbagin
AP-1	Activator Protein
ApoA – I	Apolipoprotein A – I
APS	Ammonium Persulphate
AR	Androgen Receptor
AR	Gene encoding AR
BCA	Bicinchoninic Acid
BCL-2	B-cell lymphoma 2
BRCA1	Gene encoding Breast Cancer 1 susceptibility protein
BRCA1	Breast Cancer 1 susceptibility protein
BSA	Bovine Serum Albumin
Caspase	Cysteine-Aspartic Proteases
CANSA	Cancer Association of South Africa
CCND1	Gene encoding cyclin D1
cDNA	Complementary Deoxyribonucleic Acid
CDK	Cyclin-dependent kinase
CDK2	Gene encoding Cyclin-dependent kinase 2

CDK2	Cyclin-dependent kinase 2
CDKN2D	Gene encoding Cyclin-dependent kinase inhibitor 2D/p19
CE	Cholesteryl Ester
CETP	Cholesteryl Ester Transfer Protein
CETP	Cholesteryl Ester Transfer Protein (Gene)
CO_2	Carbon Dioxide
CRE	Cholesterol Response Element
Cu^{2+}	Copper Sulphate
dH_2O	Distilled Water
DMEM	Dulbecco's Modified Eagle's Medium
DNA	Deoxyribonucleic Acid
DNase	Deoxyribonuclease
EDTA	Ethylenediaminetetraacetic Acid
EGF	Epidermal Growth Factor
EMT	Epithelial-to-mesenchymal transition
ER	Estrogen Receptor
ERBB2	Gene encoding HER2
ESR1	Gene encoding the Estrogen Receotor
FA	Fatty acid
FBS	Foetal Bovine Serum
GAPDH	Glyceraldehyde 3-Phosphate Dehydrogenase
H_2O_2	Hydrogen Peroxide
HCl	Hydrochloric Acid
HDL	High-Density Lipoprotein

HER2	Epidermal Growth Factor Receptor
HMG-CoA	3-Hydroxy-3-Methyl-Glutaryl-Coenzyme A
HMGCR	Gene encoding HMG-CoA reductase
HMGCS1	Gene encoding HMG-CoA synthase
HRP	Horseradish Peroxidase
IGF	Insulin-like Growth Factor
IGF1R	Gene encoding Insulin-like Growth Factor 1 Receptor
INSIG	Insulin-induced gene-1 protein
INSIG1	Gene encoding Insulin-induced gene-1 protein
JAK	Janus kinase
LCAT	Lecithin-cholesterol acyltransferase
LDL	Low-Density Lipoprotein
LDLR	Low-Density Lipoprotein Receptor
LXR	Liver X Receptor
MAPK	Mitogen-Activated Protein Kinase
MBTPS1	Gene encoding S1P
MβCD	Methyl-β-Cyclodextrin
MCF-7	Michigan Cancer Foundation – 7
MDR	Multi-Drug Resistance
MDR1	Multi-Drug Resistance Protein-1
MMR	Mismatch Repair
MOMP	Mitochondrial outer membrane potential
mRNA	Messenger Ribonucleic Acid
MSH2	Gene encoding MutS homolog 2

MSH2	MutS homolog 2
mTORC1	Mammalian target of raptomycin complex 1
MVD	Gene encoding mevalonate pyrophosphate decarboxylase
MVD	Mevalonate pyrophosphate decarboxylase
MVK	Gene encoding mevalonate kinase
MVK	Mevalonate kinase
NaCl	Sodium Chloride
NF-κB	Nuclear Factor kappa-light-chainenhancer of activated B cells
NIH	National Institute of Health
NSDHL	Gene encoding NAD(P) dependent steroid dehydrogenase-like
NSDHL	NAD(P) dependent steroid dehydrogenase-like
OD	Optical Density
p19	Cyclin-dependent kinase inhibitor 2D
p53	Tumour suppressor p53
PBS	Phosphate Buffered Saline
PCSK9	Proprotein Convertase Subtilisin/kextin type- 9
P-gp	P-glycoprotein
PI3K	Phosphatidylinositol 3 Kinase
PL	Plumbagin
PR	Progesterone Receptor
P-S	Penicillin-streptomycin
P-value	Statistical/ Null Hypothesis
PVDF	Polyvinylidene Fluoride/ Di fluoride
qPCR	Quantitative Polymerase Chain Reaction

Rb	Retinoblastoma protein
RB1	Gene encoding the retinoblastoma protein
RCT	Reverse Cholesterol Transport
RISC	RNA-induced silencing complex
RNA	Ribonucleic Acid
RNAi	RNA inteference
ROS	Reactive Oxygen Species
RT	Reverse Transcription
S1P	Site-1 protease
S2P	Site-2 protease
S.D	Standard Deviation
SCAP	SREBP Cleavage-Activating Protein
SDS	Sodium Dodecyl Sulphate
SDS-PAGE	Sodium Dodecyl Sulphate Polyacrylamide Gel Electrophoresis
SERM	Selective ER Modulator
siRNA	Small Interfering Ribonucleic Acid
SR-B1	Scavenger Receptor Class B Type 1
SRE	Sterol Regulatory Element
SREBP	Sterol Regulatory Element-Binding Protein
SREBPF1	Gene encoding Sterol Regulatory Element-Binding Protein
STAT	Signal transducers and activators of transcription factors
TAM	Tamoxifen
TBE	Tris-borate EDTA
TBST	Tris-buffered saline and Polysorbate 20 (Tween-20)

TEMED	Tetramethylethylenediamine
TG	Triglycerides
TGFβ	Transforming Growth Factor – β
TP53	Gene encoding p53
VLDL	Very-Low-Density Lipoprotein
WHO	World Health Organisation

1. Introduction

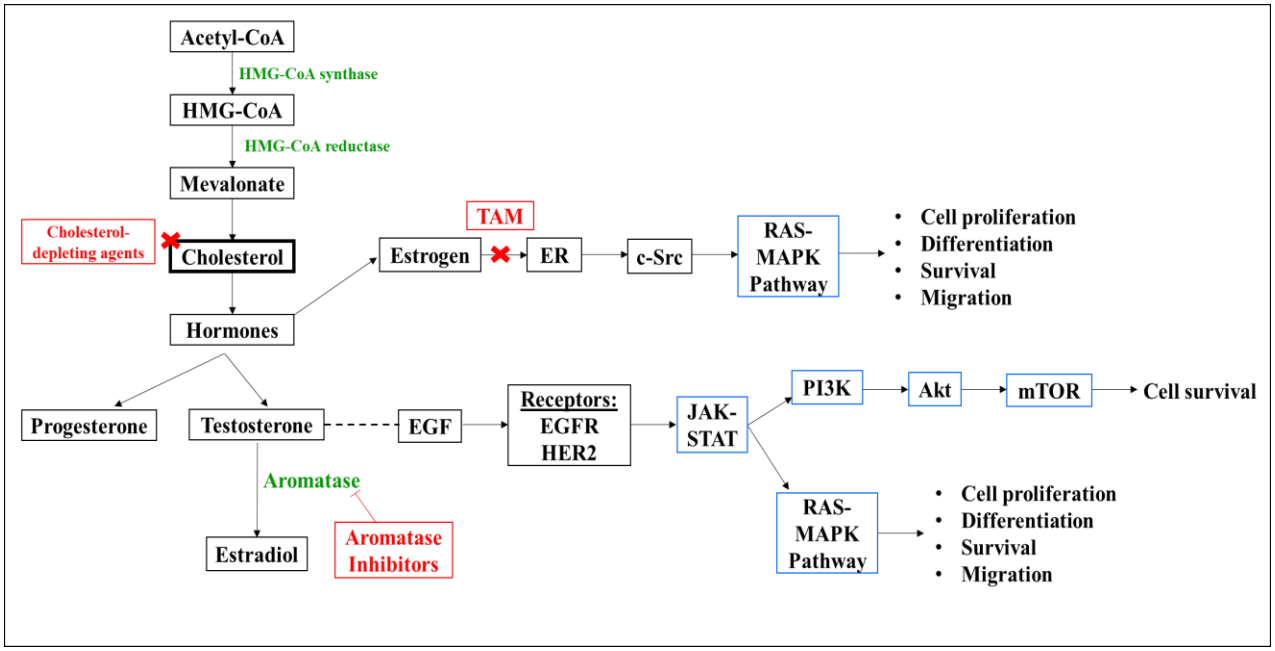
1.1. Global cancer statistics and breast cancer occurrence

Cancer remains a global burden, presenting itself as the second leading cause of death worldwide (WHO, 2019). As reported by the World Health Organisation (WHO), an estimated 8.2 million deaths were caused by cancer in 2012 and approximately 14 million new cases are reported yearly (WHO, 2019). Amongst the global cancer statistics, breast cancer is the second most prevalent cancer type in women, with an estimated total of 521, 000 deaths documented in 2012 (WHO, 2019). Interestingly, breast cancer has become the leading cause of cancer deaths in South African women and according to the Cancer Association of South Africa (CANSA), one in eight South African women are at the risk of developing breast cancer in their lifetime (CANSA, 2019). The high incidence rate of breast cancer and cancer deaths highlights the fundamental need for the development of novel chemotherapeutic strategies or improvements of existing strategies to treat breast cancer.

1.2. Cancer and breast cancer hallmarks

Broadly, cancer can be defined by the abnormal growth of cells as a result of uncontrolled cell division, with the ability of these neoplasms to metastasise or spread (CANSA, 2019). Breast cancer more specifically, is characterised by a malignant tumour that forms in various tissues and/or ducts of the breast (CANSA, 2019). Several key hallmarks define the cancerous state, with evasion of apoptosis, unrestricted cell proliferation and metastasis being the most prominent (Hanahan and Weinberg, 2011). Considering the metastatic potential, resistance to apoptosis and heterogenous nature, breast cancer has become increasingly difficult to treat (Sagar et al., 2014). Apoptosis, a form of programmed cell death, can be activated either extrinsically (death receptor pathway) or intrinsically(mitochondrial-mediated) (Hanahan and Weinberg, 2011). Both pathways activate different cysteine-aspartic proteases called caspases, the executioners of cell death, causing characteristic cell changes, such as cell shrinkage, chromatin condensation, membrane blebbing and chromosomal DNA and nuclear fragmentation, to eliminate the mutated cells (Hanahan and Weinberg, 2011). However, in breast cancer these pathways are suppressed, causing uncontrolled cell proliferation. Additionally, several well-known pathways involved in cell proliferation, survival and migration, namely: the phosphatidylinositol-3-kinase and protein kinase B (PI3K/Akt),

mitogen-activated protein kinase (MAPK), Wnt and Sonic Hedgehog proteins and Janus kinases and signal transducers and activator of transcription factors (JAK-STAT) pathways (Hanahan and Weinberg, 2011) (Figure 1.1), are abnormally activated or up-regulated through its interaction with various steroid hormones and their corresponding cell surface receptors, making breast cancer an aggressive cancer type (Esau et al., 2016; Sagar et al., 2014).



<u>Figure 1.1:</u> The biosynthesis of cholesterol, the production of steroid hormones from cholesterol, the role of steroid hormones in oncogenic signalling pathways and the action of current chemotherapeutic drugs in breast cancer.

The biosynthesis of cholesterol initiates from acetyl-CoA (acetyl-coenzyme A), a by-product from glycolysis, and it is converted to HMG-CoA (3-hydroxy-3-methyl-glutaryl-coenzyme A), which is then reduced by HMG-CoA reductase to form mevalonate. Through a cascade reaction, cholesterol is ultimately produced. The cholesterol is then used in the essential synthesis of various hormones (estrogen, progesterone and testosterone) for maintaining internal homeostasis. Tamoxifen (TAM) acts as selective estrogen modulator (SERM) essentially blocking the interaction between estrogen and its receptor (ER). Aromatase inhibitors supress the synthesis of estrogen by inhibiting the aromatase enzyme that converts testosterone into estrogen. Estrogen, as aforementioned, is involved in cell proliferation, differentiation, survival and migration, through its interaction with various oncogenic signalling pathways, as those seen above.

1.3. Hormone induced breast cancer and existing breast cancer treatments

Steroid hormones, which are derivatives of cholesterol, act as important regulators of cell survival and proliferation in both normal and cancerous cells (Gabitova et al., 2014) (Figure 1.1).

These steroid hormones, such as estrogen and progesterone, play significant roles in behavioural and physiological responses in normal cells, including those in reproduction and development (Cruz et al., 2013). Breast cancer cells, however, are identified based on the presence of surface receptors that bind these steroid hormones which are responsible for cell proliferation (Cleator et al., 2007). Breast cancer cells can therefore be categorised into several groups, namely, estrogen or progesterone receptor positive (ER+; PR+), estrogen receptor negative (ER-) and triple-negative cancerous cells (Breastcancer.org, 2018). ER- breast cancer cells are independent of steroid hormones and alternatively depend on the human epidermal growth factor (EGF) receptor 2 (HER2) for proliferation, survival and migration (Cleator et al., 2007). While triple-negative breast cancer cells lack HER2 and both the steroid hormone receptors, ER and PR, responding to insulin-like growth factors (IGFs) to maintain the cancerous state (Cleator et al., 2007). Despite the numerous types of breast cancers, approximately 75% of all breast cancer incidences are ER+ (National Cancer Institute, 2019), emphasising the importance of estrogen and its receptor in the progression of breast cancer. Elevated levels of estrogen and increased expression of steroid hormone receptors is often associated with breast cancer aggressiveness (Esau et al., 2016; Sagar et al., 2014). These surface receptors can thus act as useful biomarkers to predict various cancer types or be employed to predict effectiveness of various chemotherapeutic drugs (Sagar et al., 2014).

Many cancer interventions and chemotherapeutics have been developed to treat breast cancer. However, limitations in these therapies have resulted in increasing morbidity and mortality rates (Maughan et al., 2010). Given that majority of breast cancers are hormone dependent, hormone or endocrine targeted therapies are the most popular administered treatments for breast cancer (Hodges et al., 2003). Tamoxifen (TAM), the gold standard drug and primary treatment for hormone-induced breast cancer, has been administered over 40 years (Hodges et al., 2003). TAM acts as a selective ER modulator (SERM), displaying an antagonistic role to the estrogen hormone (Maughan et al., 2010) (Figure 1.1). TAM is initially metabolised by a family of cytochrome P450 enzymes (Cronin-Fenton et al., 2014) into various active metabolites namely: endoxifen and 4-hydroxy-tamoxifen, both which competitively bind to the

ERs of BC cells (Lu et al., 2012). The principle metabolite, endoxifen, is then internalised and binds to estrogen dependent genes thus reducing gene expression possibly through the recruitment of corepressors (Hodges et al., 2003). Consequently, this prevents the activity of various transcription factors thus impeding growth promoting signals for cellular replication (Hodges et al., 2003). Conversely, TAM has also been found to have agonist properties, in which it promotes transcription by initiating the activator protein (AP-1) pathway in the uterine endometrium, bone and cardiovascular system (Hodges et al., 2003). Therefore, long-term use of TAM has been reported to cause adverse side effects including early onset of menopausal symptoms, blood clots and endometrial cancer (Acconcia et al., 2006). Ultimately, the continual use of this drug leads to TAM resistance becoming ineffective in preventing breast cancer (Ring and Dowsett, 2004). Interestingly, approximately 40% of patients eventually relapse after ±5 years of using TAM, despite its therapeutic benefits (Ring and Dowsett, 2004) Apart from the large cohort of individuals who are also inherently resistant to TAM (Esau et al., 2016).

Other popular drugs useful in the treatment of ER+ breast cancer include, aromatase inhibitors and 5-Fluorouracil. Aromatase, an enzyme that converts testosterone (synthesised through cholesterol) to estradiol (estrogen), is highly expressed in breast cancer cells, particularly ER+ breast cancer cells (Peng et al., 2009). Therefore, these inhibitors have been found to suppress the growth of ER+ breast cancer cells, by inhibiting the conversion of testosterone to estrogen (Peng et al., 2009). Another popular chemotherapeutic drug is 5-Fluorouracil which acts by disrupting DNA synthesis and impeding breast cancer cell proliferation (Maughan et al., 2010). Although these therapies are effective in the early stages of treatment, many hormone receptor positive breast cancers become resistant to these therapies and ultimately develop hormonal independence (Ring and Dowsett, 2004). Therefore, drug resistance represents a major clinical barrier for the treatment of breast cancer and thus further studies are required to reduce resistance and enhance the response of currently available chemotherapeutic drugs.

1.4. The role of cholesterol in breast cancer progression

Over the past decade the role of cholesterol in breast cancer development has been greatly emphasised. Cholesterol is naturally produced in humans, with approximately 70 – 80% produced exclusively by the body where it plays a role in normal cellular functioning by supporting membrane biogenesis and maintaining cell shape and stability, by forming lipid

rafts. Additionally, it has been established that cholesterol is a precursor for several steroid and sex hormones, including estrogen and progesterone (Cruz et al., 2013). Consequently, breast cancer cells are found to be highly rich in cholesterol, with approximately 6 – 8× higher levels than normal cells (Sagar et al., 2014). The excess cholesterol is essential for the continual supply of estrogen, which allows for the activation of several cell proliferation and survival pathways (Silvente-Poirot and Poirot, 2014), as those shown in Figure 1.1. Apart from the above, many other studies have supported the link between cholesterol and breast cancer progression, including increased cholesterol synthesis and accumulation of oxysterols in breast cancer, cholesterol's role in regulation of cell cycle, apoptosis, metastasis and steroidogenesis, and the overexpression of receptors involved in cholesterol import, such as low-density lipoprotein (LDL) receptor (LDLR) (Gu et al., 2019).

Moreover, cholesterol accumulation generally occurs in specialised microdomains within the cell membrane, known as lipid rafts. Numerous proteins are actively associated with these lipid rafts and are involved in many crucial signalling pathways, including cell proliferation and malignancy (Gu et al., 2019). This could provide a direct link between cholesterol and cancer progression. Additionally, cholesterol metabolites and derivatives of cholesterol (steroid hormones) have been implicated in the activation of several signalling pathways, indirectly contributing to cancer development. Particularly, cholesterol serves an activator for the Sonic Hedgehog (SHH) pathway promoting cell cycle progression, which when upregulated leads to uncontrolled cell proliferation and survival (Luchetti et al., 2006). In addition, cholesterol forms a major component of G-protein coupled receptors, which are implicated in a variety of signalling pathways that are aberrant in cancer (Luchetti et al., 2006). In terms of metastasis, activation of the mitogen-activated protein kinase (MAPK) pathway is dependent on the integrity of lipid rafts, of which receptors for transforming growth factor β (TGFβ) are embedded in, a crucial cytokine involved in epithelial-to-mesenchymal transition (EMT) (Gu et al., 2012). Therefore, the presence of these receptors within lipid rafts, allow TGFβ-induced MAPK activation which promote invasiveness and cancer pathogenesis.

Cellular cholesterol: Biosynthesis and transport

Cholesterol biosynthesis takes place in all cell types, through the mevalonate pathway (Silvente-Poirot and Poirot, 2014). As seen in Figure 1.1, Acetyl-CoA, produced during glycolysis, acts as the precursor molecule for cholesterol synthesis (Buhaescu and Izzedine, 2007). In the first step of the mevalonate pathway, two acetyl-CoA molecules are condensed to yield Acetoacetyl-CoA (Buhaescu and Izzedine, 2007). This is then followed by a second

condensation step, to form hydroxy-methyl glutaryl-coenzyme A (HMG-CoA) and reduction of HMG-CoA then produces mevalonate, which through a series of enzymatic steps is converted to cholesterol (Buhaescu and Izzedine, 2007).

Since cholesterol itself is a lipid molecule, it is only partially soluble in the blood and therefore it cannot be transported by the circulatory system of the body (Sagar et al., 2014). However, these lipid-based molecules are encapsulated in a water-soluble protein coat, known as lipoproteins (Sagar et al., 2014). Lipoproteins are complex amphiphilic molecules, which serve as carriers for the internal transportation of cholesteryl esters (CEs) and the transportation of free cholesterol at the surface of these molecules (Tosi and Tugnoli, 2005). There are four principal classes of lipoproteins, including chylomicrons, high-density lipoproteins (HDLs), low-density lipoproteins (LDLs) and very low-density lipoproteins (VLDLs) (Cruz et al., 2013). However, HDLs and LDLs are the main cholesterol carriers (Cruz et al., 2013). As displayed in Figure 1.2, LDLs are responsible for transporting cholesterol from its site of synthesis (liver) to peripheral tissues (Cruz et al., 2013), while HDLs act in eliminating excess cholesterol from cells either by directly transporting cholesterol to the liver or through reverse cholesterol transport (RCT). In RCT, HDLs shuttle CEs to LDLs and then to the liver where it is converted to bile salts (Ohashi et al., 2005) (Figure 1.2). CEs, a form of esterified cholesterol, allows more efficient transport of free cholesterol by lipoproteins to the liver (Tosi and Tugnoli, 2005).

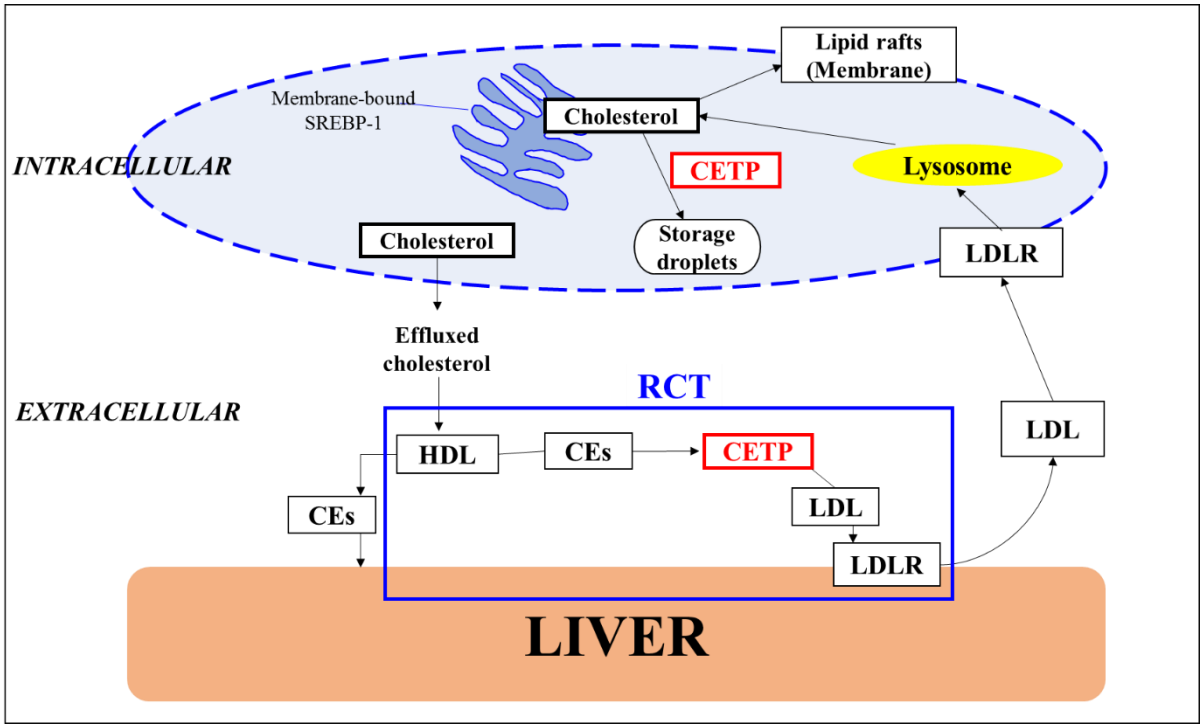


Figure 1.2: Intracellular uptake and extracellular removal of cholesterol, and the role of CETP in cholesterol homeostasis.

[*Self-created Figure*]

Intracellularly, cholesterol is taken up by the cell via binding of LDL to LDL receptor (LDLR), which is produced by the endoplasmic reticulum. Endosomes are then formed due to internalisation of LDL. Lysosomal degradation releases cholesterol into the cytosol of cells, where it is used for various purposes or exported directly out of the cell via HDL and excreted by the liver. Cholesterol can also be removed by RCT, where HDL's shuttle cholesterol to LDL's, which is ultimately converted to bile salts in the liver. RCT is mediated by the action of cholesteryl-ester transfer protein (CETP). In addition, CETP is involved in transporting cholesterol from the site of synthesis (endoplasmic reticulum) to storage droplets of the adipocytes, maintaining intracellular cholesterol homeostasis.

Cholesterol homeostasis: Cholesterol Ester Transfer Protein (CETP), a key player in intracellular and extracellular cholesterol homeostasis

Various proteins, enzymes and gene regulatory elements play a role in both intracellular and extracellular cholesterol homeostasis (Cruz et al., 2013) (Figure 1.3). Extracellularly, free cholesterol synthesised from liver hepatocytes is transported via LDLs to its cell surface receptor, LDLR, where it is internalised and used for various purposes for example to maintain

membrane stability (Esau et al., 2026; Gu et al., 2019). Intracellularly, excess cholesterol is converted to CEs by acyl-CoA: cholesterol acyltransferase (ACAT) in the endoplasmic reticulum and stored as lipid droplets (Willner et al., 2003) (Figure 1.3).

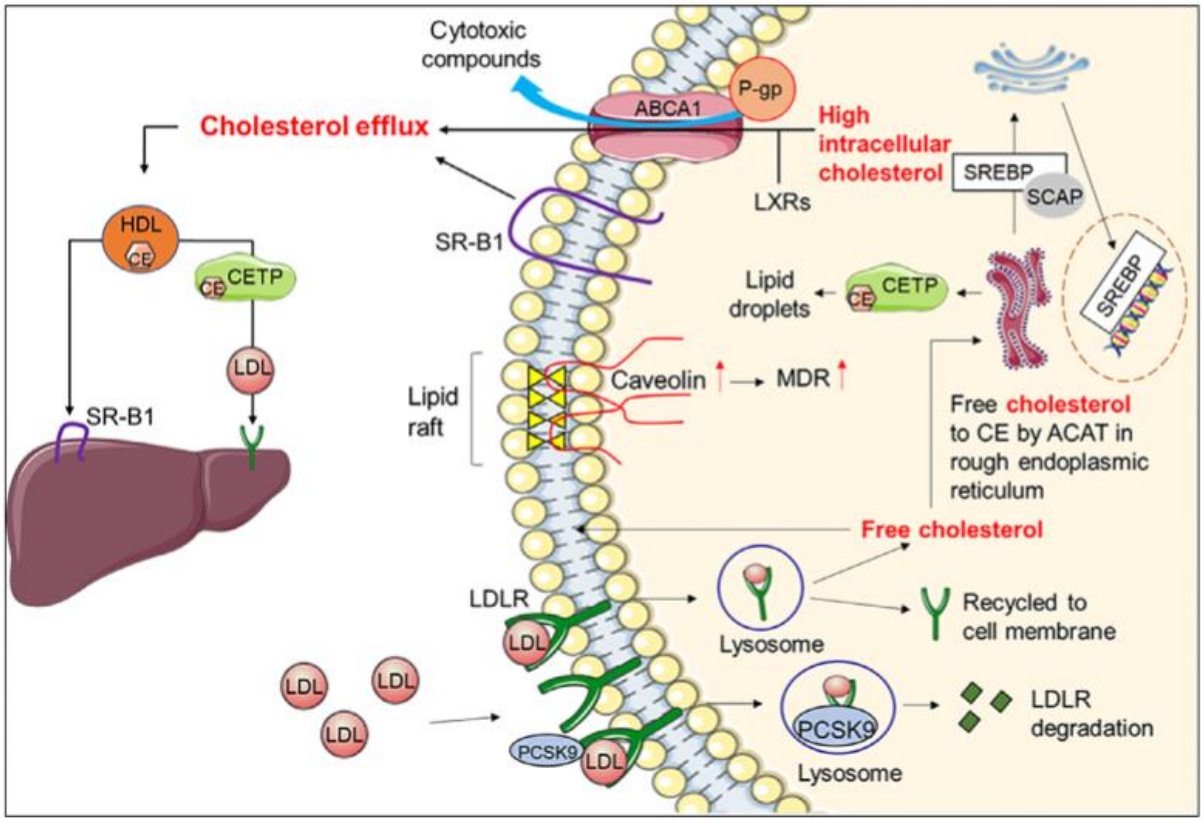
Another regulatory protein involved in cholesterol homeostasis, includes the proprotein convertase subtilisin/kextin type- 9 (PCSK9). PCSK9 is a member of the mammalian serine proprotein convertase family that generally functions in the proteolytic cleavage and maturation of secretory proteins (Frank-Kamenetsky et al., 2008). It is mainly synthesised and secreted by the liver with lower levels of expression in the kidney, brain and intestine (Frank-Kamenetsky et al., 2008). PCSK9 functions as a molecular chaperone by negatively regulating LDLR expression; it binds to LDLR and targets it for lysosomal degradation (Frank-Kamenetsky et al., 2008; Lagace, 2014). Loss of PCSK9 increases liver LDLR levels and reduces plasma LDL cholesterol, however if PCSK9 activity is increased, liver LDLR levels is reduced and plasma LDL increases (Lagace, 2014). Intracellularly, PCSK9 binds to LDLR and directs it from the golgi body for lysosomal degradation (Lagace, 2014). Extracellularly, secreted PCSK9 binds at the cell surface to the first EGF-like repeat (EGF-A) of LDLR and upon internalisation, PCSK9 inhibits the endocytic recycling of LDLR, resulting in lysosomal degradation of both proteins (Lagace, 2014).

In addition, intracellular cholesterol levels are maintained by sterol regulatory element-binding protein1 (SREBP1). SREBP1 are a family of TFs that activate a cascade of enzymes needed for endogenous cholesterol, phospholipid, fatty acid (FA) and triglyceride (TG) synthesis (Eberle et al., 2004; Gabitova et al., 2014). For this reason, SREBP1 can be considered as the master regulators of cholesterogenesis and more broadly lipogenesis. SREBP1 is synthesised as inactive precursors bound to the membrane of the endoplasmic reticulum (Guo et al., 2014) (Figure 1.2 and Figure 1.3). As seen in Figure 1.3, a decrease in sterol levels causes the proteolytic cleavage of the precursor and active SREBP1 is translocated to the Golgi with the aid of the SREBP cleavage-activating protein (SCAP) (Shimano, 2001), which is bound by the Insulin-induced gene (INSIG) and acts as both a chaperone and cholesterol sensor. SREBP1 is then cleaved and activated by site 1 and site 2 proteases (S1P AND S2P), where it stimulates cholesterogenic genes that are involved in cholesterol synthesis (Shimano, 2001). However, in a cholesterol-rich environment, excess cholesterol inhibits the translocation of SREBP1 from endoplasmic reticulum to Golgi by the disruption of the SCAP chaperone (Shimano, 2001).

Cholesteryl Ester Transfer Protein (CETP) is an important protein that is involved in intracellular cholesterol homeostasis and is central to this study. CETP is a 74 kDa plasma glycoprotein that promotes the exchange of neutral lipids, TGs and CEs between distinct lipoprotein classes (Esau et al., 2016; Sagar et al., 2014). CETP has a binary role in maintaining cholesterol homeostasis; intracellularly, CETP facilitates CE and TG uptake from the endoplasmic reticulum into storage droplets of the adipocytes (Izem and Morton, 2007), given that free cholesterol is toxic to cells (Figure 1.2 and Figure 1.3). Extracellularly by RCT, CEs are taken up from HDLs and transferred to the liver to be eliminated from the body via LDLR (Izem and Morton, 2007) (Figure 1.2). Earlier studies have found that CETP deficient cells have lower intracellular cholesterol levels than normal cells and this could possibly be due to the accumulation of CEs at the synthesis site (endoplasmic reticulum) (Esau et al., 2016). Since CE transport is impeded, there is inefficient removal of CEs from the endoplasmic reticulum, signalling sterol abundance. This could possibly lead to downregulation of pathways that synthesise cholesterol and up-regulation of pathways involved in cholesterol removal (Esau et al., 2016). Moreover, in the absence of CETP, LDL levels decrease while HDL levels are elevated in plasma (extracellularly) (Esau et al., 2016). The increased HDL levels could possibly suggest an enhanced clearance of cholesterol in the plasma (Esau et al., 2016). Therefore, the notion of targeting CETP has been investigated as a possible therapeutic against cholesterol-related diseases, such as arteriosclerosis and coronary heart disease (Chen et al., 2017). However, the association between CETP and cancer has not been well-documented.

One key player in intracellular cholesterol homeostasis is the ATP-binding cassette transporter-1 (Kang et al., 2013; Yvan-Charvet et al., 2010). ABCA1 facilitates the transfer of excess cholesterol (in the presence of P-glycoprotein or P-gp) from the inside of cells to HDLs and apolipoprotein A-I (ApoA-I) that are outside of the cells, where cholesterol esterification occurs through lecithin: cholesterol acyltransferase (LCAT) (Fig. 1.4) (Tall et al., 2008). More importantly, overexpression of ABCA1 protein is involved in multi-drug resistance (MDR), where it assists in the export of various hydrophobic compounds such as TAM (Dean et al., 2001), therefore reducing intracellular cytotoxicity. Overexpression of ABCA1 can be stimulated by LXR (liver X receptor), which belongs to the nuclear hormone receptor superfamily of ligand-activated TFs. Both free cholesterol and CEs are incapable of binding and activating LXRs. Rather, increased intracellular cholesterol is believed to drive the synthesis of oxysterols that act as ligands for LXR (Repa and Mangelsdorf, 2002). The interaction between a ligand (lipophilic molecules) and the receptor is followed by a

conformation change in LXRs, which initiates coactivators for transcription of various target genes (Li et al., 2007). Therefore, the activation of LXR is directly proportional to cholesterol availability; where increased intracellular cholesterol enhances LXR activity (Li et al., 2007). LXRs regulate RCT by stimulating the expression of several target genes that are implicated in cellular efflux, plasma transport, and biliary excretion of cholesterol (Ohashi et al., 2005). This includes ABC transporters A1, G1, G5/8, and CETP and SREBP1 (Masson et al., 2004). Activation of LXR induces intracellular cholesterol catabolism, decreasing cholesterol levels and increasing its secretion by the liver (Zhao and Dahlman-Wright, 2010). Cholesterol from peripheral cells is transported to the liver by HDL molecules, where it can be secreted into bile as free sterols or be converted to bile acids that are also secreted into bile, thereby promoting cholesterol efflux (Cao et al., 2002). Furthermore, MDR is associated with high levels of caveolin-1 protein (a membrane protein specialising in lipid raft formation that are rich in signalling molecules, receptors, effector proteins, transducers) as increased level of this protein enhances cholesterol efflux (Fu et al., 2004; Ho et al., 2008; Lavie and Liscovitch, 2000). In contrast to the unidirectional cholesterol transport of ABCA1 and caveolin-1, scavenger receptor class B type 1 (SR-B1) is an additional membrane protein that enables bidirectional, gradient-dependent transfer of free cholesterol (both cholesterol efflux as well as influx) (Ohashi et al., 2005; Rosenson et al., 2012; Yancey et al., 2003). Moreover, SR-B1 mediates selective uptake of CEs, phospholipids and triglycerides in the RCT system, thereby maintaining cholesterol homeostasis both intracellularly and extracellularly (Yancey et al., 2003).



<u>Figure 1.3:</u> Cholesterol homeostasis maintained by several proteins, enzymes, receptors and TFs.

[*Adatped from Gu et al., 2019*]

Extracellular, free cholesterol is transported by LDL to the LDLR. The complex is then endocytosed, and free cholesterol is released intracellularly. PCSK9 regulates LDLR availability in a negative feedback mechanism. Free cholesterol is converted to CEs by the enzyme ACAT, since free cholesterol is toxic to cells. Intracellularly, SREBP1 acts as a transcription factor, where in a cholesterol poor environment, becomes activated to transcribe genes involved in cholesterol biosynthesis. Excess cholesterol is effluxed via ABC transporters.

1.5. Targeting cholesterol for cancer treatment

There are currently two approaches that target cholesterol as a possible strategy to treat breast cancer. This includes blocking cholesterol synthesis using drugs such as statins and/or depleting excess membrane cholesterol using cholesterol depleting agents, such as methyl-beta-cyclodextrin (MβCD)

1.5.1. Cholesterol synthesis inhibitory drugs

As mentioned, several cancers, including breast cancer maintain the cholesterogenic phenotype for continuous cell proliferation and survival and thus targeting cholesterol has become an attractive approach to treat breast cancer. Numerous studies have investigated the use of cholesterol synthesis inhibitory drugs (Mostaghel et al., 2012; NIH, 2016); the most popular of these drugs includes the family of statins (Mostaghel et al., 2012). Statins act by inhibiting HMG-CoA reductase, the key enzyme involved in the synthesis of cholesterol thereby stunting the mevalonate pathway (Stancu and Sima, 2001). Consequently, cholesterol levels decrease, thus statins have shown to be effective in treating coronary heart disease and arthrosclerosis (Stancu and Sima, 2001). Additionally, statins promote cellular senescence by down-regulating growth-promoting signals in RAS, PI3K/AKT, Wnt/β-catenin signalling cascades and also induce proapoptotic signalling pathways, becoming a popular approach to treat cancer (Ampuero and Romero-Gomez, 2015; Tsubaki et al., 2011). Despite the significant anticancer properties, there have been several adverse side effects associated with statin usage. These side effects range from moderate to severe and include liver damage, raising blood sugar levels, which in turn increase the risk of diabetes and cardiovascular diseases, myopathy, idiopathic polyneuropathy and the onset of dementia, as cholesterol is vital for normal cognitive functions (Moosmann and Behl, 2004; Sinzinger et al., 2002). The use of statins and its effects on cancer development have been controversially discussed. Several studies have shown that statins possess anticancer properties (Campbell et al., 2006; Chan et al., 2003; Goard et al., 2010; Van Wyhe et al., 2017). However, numerous studies have also emerged that suggest statins strongly promote cancer development (Boudreau et al., 2010; Duncan et al., 2005; Fujimoto et al., 2015; Goldstein et al., 2008; Ravnskov et al., 2015). Therefore, it is crucial to improve the knowledge of the anti- and/or pro- cancer effects of statins and weigh the adverse side effects for its use on cancer patients. Also, 25% people do not respond to statins (Stroes et al., 2015), thus further emphasizing the need to identify alternative cholesterol lowering therapeutic strategies.

Alternative drugs targeting key proteins in cholesterol homeostasis or the mevalonate pathway may have the potential in treating cholesterol-rich diseases, such as breast cancer, include: lonafarnib and tipifarnib (inhibit farnesyltransferase) (Marcuzzi et al., 2011)), certain bisphosphonates (inhibit farnesyl-diphosphate synthase; an intermediate in mevalonate pathway) (Tsoumpra et al., 2015), Lamisil (potentially inhibit squalene epoxidase; a rate-limiting enzyme in sterol biosynthesis pathway) and 2, 3- oxidosqualene cyclase (inhibits squalene synthase) (Nowosielski et al., 2011). All the above-mentioned drugs are currently

undergoing clinical trials which will establish their efficacy and long-term benefits in patients. Additionally, torcetrapib, one of the most well-known CETP inhibitors has been studied as a potential drug for the treatment of atherosclerosis and lipid-related diseases (Bots et al., 2007; Clark et al., 2004). Torcetrapib mechanistically inhibits CETP and increases HDL levels (Clark et al., 2004). However, the negative effects of torcetrapib have been concerning. These side effects include increased blood pressure, increased cardiovascular events and no significant decrease in coronary artherosclerosis risks (Barter et al., 2007; Bots et al., 2007; Forrest et al., 2008; Nissen et al., 2007). Due to the toxicity and off-target effects of torcetrapib, further research was terminated, which warrants alternative strategies to treat cholesterol-related diseases. In addition, the relationship of CETP in the context of cancer is yet to be investigated.

1.5.2. Cholesterol-depleting agents

On the contrary, due to the high level of cholesterol in cancer cells, especially in ER+ breast cancer cells, depleting the excess cholesterol or disrupting the lipid rafts has been anticipated as an alternative and better method in treating breast cancer or other cholesterol-related diseases. Increasing evidence has proposed that depleting cholesterol in the lipid rafts disrupt cell membranes and thus initiates apoptosis (Esau et al., 2016). Additionally, the removal of excess cholesterol within cell membrane induces chemosensitivity to certain drugs, such as TAM (Mandal and Rahman, 2014; Mohammad et al., 2014).

MβCD is amongst the most extensively studied cholesterol-depleting agents, which has shown significant anticancer activity in several cancers including breast cancer (Mohammad et al., 2014), by effectively decreasing membrane cholesterol through lipid raft disruption (Ahern et al., 2014). MβCD is a well-studied cyclodextrin compound that possesses a hydrophobic cavity, which allows the extraction of cholesterol from cell membranes (Zidovetzki and Levitan, 2007). Studies performed on breast cancer cells also showed that cholesterol-depletion by MβCD induced apoptosis in breast cancer cells through down regulation of caspase-3 activation as well as Akt activity (Li et al., 2006). The structures of membrane microdomains are essential for the modulation of the influx and efflux of cancer drugs (Mohammad et al., 2014). Therefore, cholesterol-depletion in the membrane disrupts lipid raft integrity and simultaneously increases membrane permeability for drug passage (Mohammad et al., 2014). Although MβCD has been shown to be less toxic as compared to most drugs, it is not cancer

specific and thus it negatively impacts on normal cell proliferation (Mahammad and Parmryd, 2015).

Recently, a new cholesterol depleting agent, acetyl-plumbagin (AP), has emerged and is currently being investigated. AP is a derivative of the highly toxic cholesterol-lowering agent, plumbagin (PL) (Sagar et al., 2014). In several studies, PL has been found to induce apoptosis by a number of pathways. These include, signalling the production and release of radical oxygen species (ROS) and NF-κB (nuclear factor kappa-light-chainenhancer of activated B cells), thereby inhibiting the activation of cyclin D, inducing apoptosis (Sagar et al., 2014; Sandur et al., 2006; Srinivas et al., 2004; Wang et al., 2008). Due to the high toxicity of this molecule, various derivatives of PL were developed, one being AP (Sagar et al., 2014; Sakao et al., 2009). AP was observed to be several folds less cytotoxic compared to PL, especially in normal fibroblasts *in vitro* and *in vivo* (Esau et al., 2016). Though the exact mechanistic activity of AP has not been well studied, the depletion of cholesterol using AP resulted in a decrease in CETP mRNA expression, as well as a significant increase in mitochondrial mediated apoptosis (Esau et al., 2016). A study carried out by Gu (Master's dissertation, 2018) also demonstrated that the combination of CETP knockdown with AP treatment induce apoptosis and decrease breast cancer cell viability, through cytotoxicity. Gu's study (Master's dissertation, 2018) thus illustrated the potential of CETP knockdown (and the combination of CETP knockdown together with AP treatment) as a chemotherapeutic approach for breast cancer. However, the molecular mechanisms involved in CETP knockdown is yet to be elucidated. Therefore, the present study aimed to investigate the change in gene expression and pathways involved in CETP knockdown, particularly in MCF-7 cells (ER+ breast cancer type).

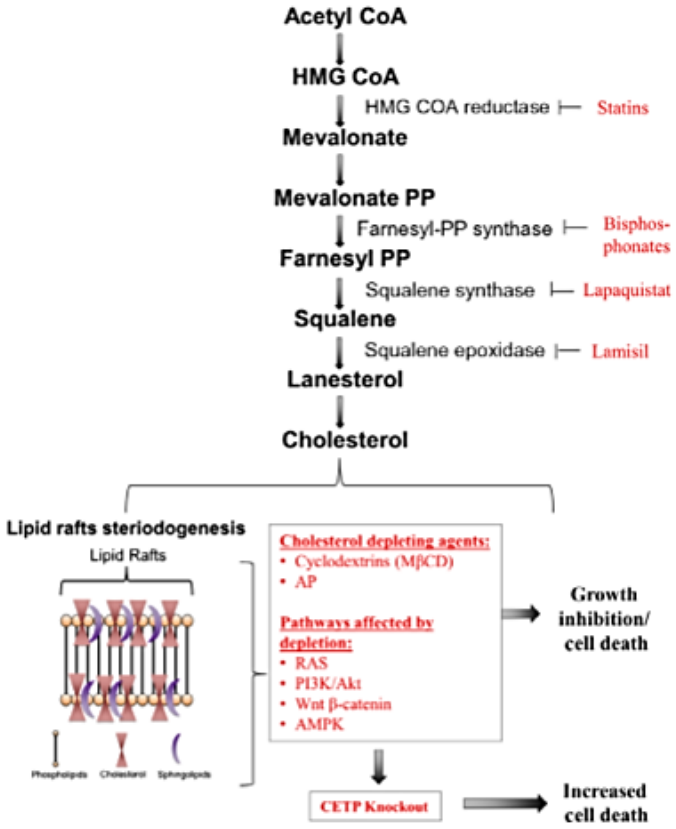


Figure 1.4: Various targets in the cholesterol pathway by available drugs.

[*Adapted from Gu et al., 2019*]

The Figure illustrates the steps in the cholesterol synthesis pathway that can be targeted by drugs/compounds. This includes statins, biophisphonates and lamsil. Cholesterol depletory agents, such as MβCD and AP, deplete excess cholesterol in cancerous cells and cause cell death. Pathways that could possibly be affected by this depletion, include RAS, PI3K/Akt, Wnt β-catenin and AMPK pathways.

1.6. Preliminary studies

More recently, CETP's role as a molecular target against breast cancer has been established; studies executed by Esau et al (2016) and Sagar et al (2014) link cholesterol accumulation to breast cancer occurrence and administration of cholesterol-depleting agents such as, MβCD and AP has shown to be effective in promoting cell death in breast cancer cells (Esau et al., 2016; Sagar et al., 2014; Gu, 2018). AP was found to deplete membrane cholesterol, which resulted in a significant decrease in CETP mRNA expression (Esau et al., 2016). Additionally, CETP knockdown in MCF-7 breast cancer cells triggered an increase in caspase 3/7 activity, which sensitised the cancerous cells to mitochondrial-mediated apoptosis (Esau et al., 2016;

Gu, 2018). These studies therefore exhibited the role of CETP as a possible drug resistance marker that could be used to monitor the therapeutic effects of drugs such as TAM in cholesterol-rich cancers. Furthermore, the studies anticipated the use of combination treatment (knocking down CETP plus administration of a cholesterol-depleting agent) in combating cholesterol rich-hormone receptor positive breast cancers and its possibility in decreasing drug resistance (Esau et al., 2016). CETP knockdown is central in these studies and presents itself as a possible therapeutic approach in combatting ER+ breast cancer. However, the molecular pathways involving CETP knockdown is yet to be elucidated. The present study aimed to investigate changes in expression of genes involved in lipoprotein signalling and cancer drug resistance, as well as quantify cholesterol content post-CETP knockdown. The results presented in this study is novel and will possibly provide insight into the mechanistic anti-cancer effect of CETP, as well as the role of cholesterol in drug resistance.

2. Aim and objectives

2.1. Aim

Elucidating the molecular mechanisms underlying CETP's involvement in ER+ BC and its role in cholesterol-mediated cancer drug resistance.

2.2. Objectives

- To successfully knockdown CETP in MCF-7 cells.
- To quantify cholesterol, particularly CEs pre- and post- CETP knockdown in MCF-7 cells.
- To analyse pathway specific gene changes involved in lipoprotein signalling and cancer drug resistance post – CETP knockdown in MCF-7 cells.

3. Methods

The methodology, presented below, was used to achieve the objectives of the study. These experimental procedures were performed on both transfected (CETP knockdown) and non-transfected MCF-7 cell lines and each experiment was conducted at least three times, in triplicates.

3.2. Cell culture

An ER+ breast cancer cell line MCF-7 (Michigan Cancer Foundation – 7) was cultured in Dulbecco's Modified Eagle's Medium (DMEM) (Sigma Aldrich, UK and Gibco: Life Technologies, UK) supplemented with 10% foetal bovine serum (FBS) (Celtic Molecular Diagnostics, SA and Biowest, UK) 1% Penicillin-Streptomycin (Sigma Aldrich, UK) and incubated at 37°C in the presence of 5% CO_2. DMEM provided the necessary nutrients for cell survival and growth. The antibiotics (Penicillin-Streptomycin) ensured the cultures were free of bacterial and fungal contamination, while incubation at 37°C in the presence of 5% CO_2 ensured a constant pH is maintained by means of a carbon dioxide-bicarbonate buffer system, mimicking *in vivo* conditions and allowing the optimum growth of the cells.

3.3. Cell counting

Cell density and viability analysis was performed using the Neubauer haemocytometer and selective staining with trypan blue. This procedure was imperative to allow an accurate number of cells to be seeded prior to transfection (CETP knockdown) and for downstream assays. Firstly, media was removed and cells (approximately 70% confluency) were washed with 1× phosphate-buffered saline (PBS) (Sigma Aldrich, UK). This was followed by trypsinisation with 1× trypsin-EDTA (2 ml in a 25 cm^2 culture flask) (Sigma Aldrich, UK) and incubation at 37°C for approximately 10-15 minutes. When the cells were detached, trypsin containing cells were added to 0.4% trypan blue (Sigma Aldrich, UK) in a 1:1 ratio (100 µl cells in trypsin added to 100 µl trypan blue) and mixed thoroughly. Trypan blue is a vital stain that relies on cell membrane integrity. Viable cells have intact membranes and thus do not take up the dye, remaining unstained. On the contrary, nonviable (dead) cells do not have intact and functional cell membranes and stain blue. Therefore, trypan blue allows for easy differentiation between viable and non-viable cells. Subsequently, 10 µl of the mixture was added onto a

haemocytometer and both viable and dead cells in all four quadrants (containing 16 mini squares) were counted under a microscope. Cells on the top right-hand corners of the four quadrants were included in the total count (Figure 3.1).

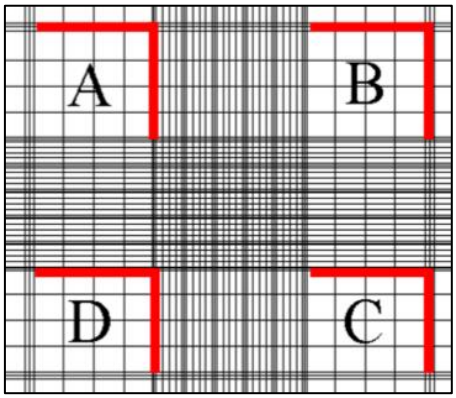


Figure 3.1: Representation of a Neubauer haemocytometer under a microscope.

A haemocytometer, is a thick glass microscope slide with a hollow chamber of precise dimensions, allowing for a defined volume of cell suspension to be deposited so that the number of cells in a sample can be counted. The gridlines engraved on the slide and the Neubauer factor (10^4) which accounts for the volume and dimensions of the indented chamber, *allows for an accurate determination of cell number. Cells in the top-right hand corner were included in the total cell count, however, cells on the bottom-left hand corner were not included in the total cell count.*

Cellular viability of ≥95% was used in downstream experiments and was calculated as follows:

% Cell viability = Number of viable cells (unstained)/ Total cells counted (viable and non-viable) × 100

Cells were then seeded at a desired density as follows:

10 000 µl (10 ml) × Total number of 10 cm^2 culture dishes = Total volume of media required **(a)**

300, 000 cells/ culture dish × Total number of culture dishes = Total number of cells required

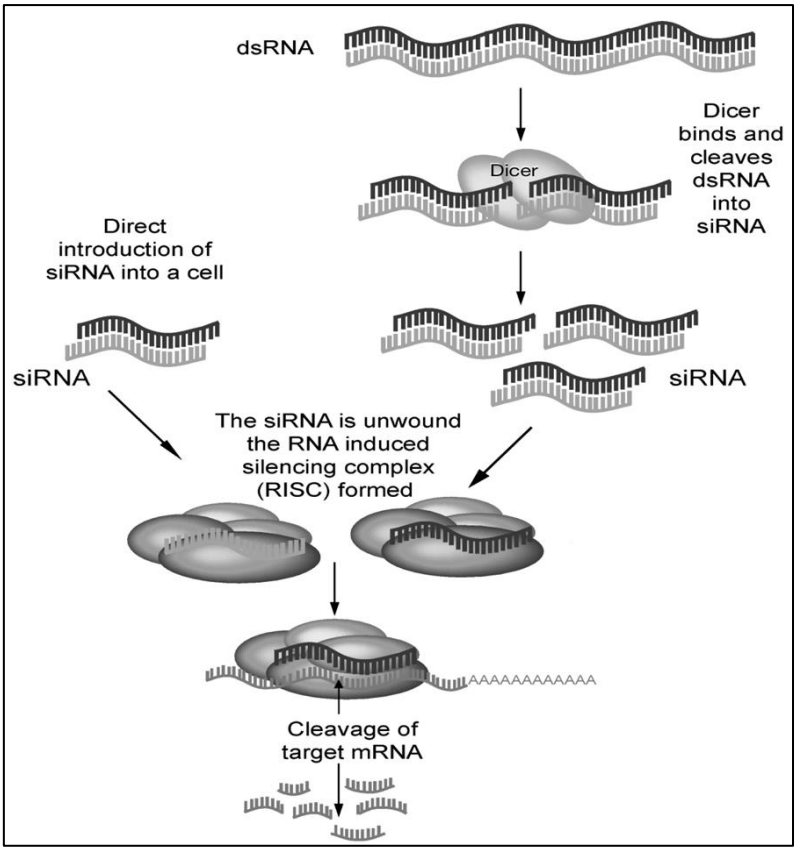
(Total volume in flask (µl) × Total number of cells required)/Total number of cells counted in flask = Volume of cells required from flask **(b)**

a - b = Media to be added to cells

10 000 µl (10 ml) was then pipetted into each culture dish with approximately 300 000 cells/culture dish

3.3. CETP knockdown by siRNA transfection

Transfection is the process of artificially introducing nucleic acids, such as small interfering RNA (siRNA), into eukaryotic cells leading to an altered expression of a particular gene or gene product. A popular method of reducing gene expression post-transcriptionally by mRNA degradation involves the use of siRNA molecules. These 20 – 25 nucleotide sequences are involved in the RNA interference pathway (RNAi), which induces short term silencing of protein coding genes. The antisense strand (guide strand), of the duplex siRNA is integrated into the RNA-induced silencing complex (RISC). RISC not only prevents the interaction of the large and small ribosomal subunits but also inhibits the binding of elongation factors to the mRNA. The siRNA-RISC complex then elicits gene silencing by binding, through complementarity, to a single marked mRNA sequence, targeting it for cleavage and degradation (Dharmacon™, GE Lifesciences SA). The process can be seen in Figure 3.2.



<u>Figure 3.2:</u> Mechanism of gene silencing by siRNA.

[Adapted from Tuzmen et al., 2007]

The dicer enzyme,an RNase III cleaves dsRNA into smaller siRNA's. The antisense strand of the siRNA is then integrated into the RISC complex. Subsequently, the siRNA-RISC complex elicits gene silencing by binding, through complementarity, to a single target mRNA sequence, thereby targeting it for cleavage and degradation.

CETP knockdown was accomplished using the Silencer® Select Pre-designed CETP siRNA (Ambion®, Life Technologies, USA) and the DharmaFECT™ transfection reagent (Dhramcon™, GE Healthcare, UK; Inqaba Biotec™), a non-liposomal lipid mediated transfection reagent (polymer-based). Cells were briefly trypsinised (2 ml 1× trypsin-EDTA), followed by re-suspension in media, to deactivate the trypsin. Cells were then seeded in 10 cm^2 culture dishes, at a density of 300 000 cells/dish. Transfection was carried out as follows (Volumes of reagents used can be seen in table 3.1): In two separate tubes, the required amount of 5 μM CETP siRNA (tube 1) and of DharmaFECT™ transfection reagent (tube 2) was added to the appropriate volume of serum-free media. The tubes were then allowed to sit at room temperature for 5 minutes. Subsequently, the contents of tube 2 was added and gently mixed

with the contents of tube 1 and allowed to incubate for 20 minutes. This allowed the non-liposomal lipids of the transfection reagent to encapsulate the siRNA, forming micelles that can be transported into the cells and CETP knockdown to take place. In addition, cells were transfected with a siRNA control, to ensure that CETP siRNA, in particular, was involved in CETP knockdown; this served as a negative control for the transfection procedure. Following incubation, the siRNA and transfection reagent mixture was added to each culture dish and incubated for 72 hours before the cells could be harvested for downstream processes.

Table 3.1: siRNA transfection reagent mixture.

Volumes of siRNA and DharmaFECT™ reagent added to each 10 cm culture dish containing approximately 300,000 cells. The volume of 10 ml yielded a final siRNA concentration of 10 nM.

Cell seeding		**Tube 1:** *CETP* siRNA/siRNA negative control (µl/dish)		**Tube 2:** DharmaFECT™ reagent (µl/dish)		
Cell density	Complete media (µl)	5µM siRNA (µl)	Serum-free media (µl)	DharmaFECT™ reagent (µl)	Serum-free media (µl)	Total volume per 10 cm culture dish (µl)
300, 000	9 600	20	180	3	197	10, 000 (10 ml)

In addition, both negative and untreated controls were included in the siRNA experiment.. The siRNA negative control helped distinguish sequence-specific effects from the effects of experimental conditions on cellular responses. On the contrary, the untreated control provided a useful reference for cell phenotype and normal gene expression profile of the non-transfected cells. This polymer-based (non-liposomal) method of transfection uses cationic polymer reagents that strongly bind the negatively-charged phosphate backbone of the siRNA and easily mediates interaction with the cell membrane, where the siRNA and polymer complex is taken up via endocytosis (Dharmacon™, GeLifesciences, SA). The reagent itself can become cytotoxic to cells if more than the specified amount is used (Dharmacon™, GeLifesciences, SA). However, this delivery method is highly efficient, reproducible and simple to perform.

3.4. Reverse-Transcriptase Quantitative Polymerase Chain Reaction (RT-qPCR)

RT-qPCR was performed to confirm successful knockdown of CETP and to quantify CETP mRNA expression in transfected and non-transfected cells.

3.4.1. RNA isolation

RNA isolation was perfomed using the Direct-zol™ RNA MiniPrep kit (Zymo Research, Inqaba Biotec™, SA). Firstly, 300 µl of TRIzol® reagent (Ambion®, Life Technologies, USA) was added to cell pellets (~ 1×10^6 cells) and mixed thoroughly. This chemical reagent is used to disrupt cell membranes allowing for the isolation of intact RNA, DNA and proteins from cells (Simões et al., 2013). Subsequently, an equal amount of ethanol (99.9%) was added to the samples so the nucleic acids, DNA and RNA, could be precipitated. Thereafter, the samples were transferred to a Zymo-Spin™ IIC Column in a collection tube, centrifuged at 16 000 ×g for 30 seconds (as well as for subsequent centrifugation steps) and the flow through was discarded. A DNase step was then included to digest DNA in the samples; 5 µl DNase I was added to 75 µl DNA digestion buffer and incubated for 15 minutes at room temperature. Afterwards, two wash steps were performed using 400 µl of Direct-zol™ RNA PreWash and 700 µl of RNA wash buffer, respectively. These additional wash steps ensured the samples were free of DNA contamination. Lastly, RNA was eluted and re-suspended in 50 µl of DNase/RNase-Free water (Direct-zol™ RNA MiniPrep kit; Zymo Research, Inqaba Biotec™, SA) and stored at -80°C, since RNA is prone to rapid breakdown by commonly occurring nucleases.

Prior to cDNA synthesis and RT-qPCR, it is necessary to examine RNA quality (purity and integrity). Purity analysis (A260/280 and A260/230 ratios) and RNA quantification (ng/µl) was performed using the Nanodrop 1000 spectrophotometer (Thermo Fisher Scientific, USA). Extracted RNA with an A260/A280 ratio of approximately 2.0 was used for downstream processes. RNA has an absorption maximum at 260 nm and the ratio of the readings at 260 nm and 280 nm (A260/A280) provides an estimate of the purity of the RNA with respect to contaminants that absorb in the UV region, such as proteins. Pure RNA has an A260/A280 of approximately 2.1. Following extraction and quantification, the integrity of each RNA sample

was examined. This was achieved by combining 500 ng of RNA with 2 µl 2× RNA loading dye (Thermo Scientific, USA)and loading it onto a 1% (w/v) agarose gel (5 g agarose powder + 50 ml 1× Tris-borate EDTA (TBE)+ 5 µl Ethdium bromide, Thermo Scientific, USA)) for 30 minutes at 100 mV. Thereafter, an image of the gel was captured using the ChemiDoc™ MP system and examined for patterns of 28S and 18S bands.

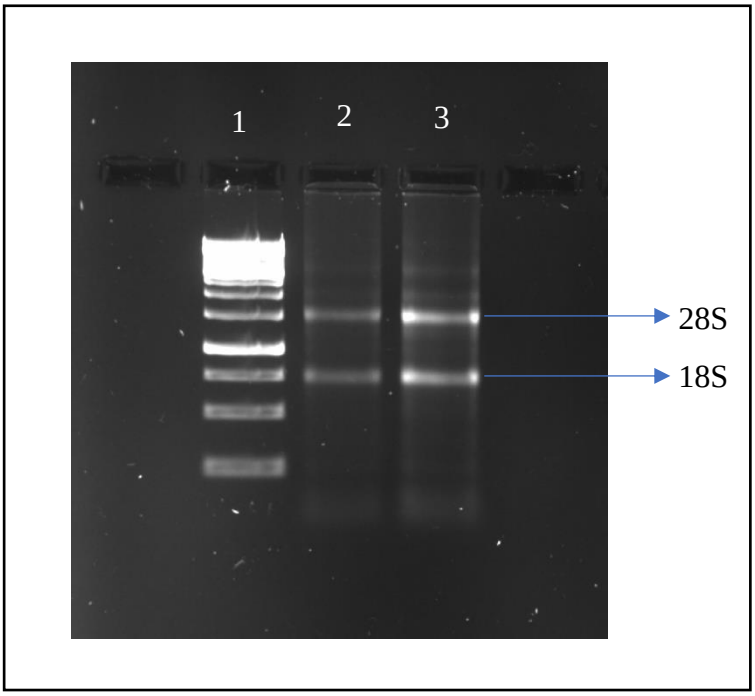


Figure 3.3: A representative integrity gel of the extracted RNA.

Extracted RNA was subjected to agarose gel electrophoresis on a 1% (w/v) agarose gel (100 V for 30 minutes). The image shows the intact 28S and 18S rRNA (labelled above), with minimal smearing. Lane 1 (MW marker), Lane 2 (RNA extracted from transfected cells), Lane 3 (RNA extracted from non-transfected cells).

Table 3.2: 1× TBE buffer composition (pH 8.0) (All reagents from Sigma Aldrich, UK)

Component	Amount
Tris	10.8 g
Boric acid	5.5 g
EDTA	0.75 g
dH_2O	1 L

3.4.2. cDNA synthesis

The RevertAidFirst Strand cDNA Synthesis kit (Thermo Fisher Scientific, USA) was used to convert the extracted RNA to cDNA, in preparation for qPCR. As seen in table 3.2, the isolated RNA together with Oligo-dT18 primers (allows cDNA synthesis of all mRNA present. In order to perform cDNA synthesis of a particular gene of interest specific primers, in this case CETP mRNA, would be required), dNTP Mix (to allow for extension of the cDNA, by the addition of nucleotides), RevertAid M-MuLV reverse transcriptase (to allow synthesis of cDNA from the extracted RNA) and DNase/nuclease-free water (free of DNases/nucleases that might degrade the synthesised cDNA) was added to a tube, gently mixed and centrifuged briefly prior to incubation at 42°C for 1 hour using the MultiGene PCR machine (Labnet International, UK). The reaction was then terminated at 70°C and stored at -20°C till further use.

Table 3.3: Volumes of RevertAidFirst Strand cDNA Synthesis reagents added to extracted RNA for cDNA synthesis.

The reagents below, together with extracted RNA (2 µg) were added to produce a reaction mixture with a final volume of 20 µl for cDNA synthesis.

Reagent	Volume (µl)
Template RNA	2 µg (volume dependent on RNA concentration)
Oligo $(dT)_{18}$ primer	1
Nuclease-free water	To make volume 12
Volume	**12**
Master Mix	
5× Reaction Buffer	4
RiboLock RNase Inhibitor	1
10mM dNTP Mix	2
RevertAid M-MuLV RT (200U/µl)	1
Volume	**8**
Total Volume	**20**

3.4.3. Quantitative PCR (qPCR)

Quantitative PCR (qPCR) is a biological technique that monitors the amplification of a targeted DNA molecule, in this study CETP cDNA, in real-time and not at its end was monitored, like

traditional PCR. The SensiFAST™ SYBR® No-ROX kit was used to determine CETP cDNA expression in transfected as well as non-transfected cells (Assuming that there is a correlation between mRNA and cDNA). SYBR green, a fluorescent cyanine dye, intercalates into double stranded DNA during the annealing and extension steps of PCR. Therefore, SYBR green detection (Cq/Ct – initial detectable signal of SYBR green) is directly correlated to the amount of template and extension during the qPCR process, allowing the change in relative CETP mRNA expression levels to be determined by the $2^{-\Delta\Delta Ct}$ method (Livak and Schmittgen, 2001). The reaction components at the required volumes, as seen in table 3.3, were added to white, opaque 8-well PCR strips (BIOPlastics, Netherlands; Celtic Diagnostics, SA) and thoroughly mixed. Primers were synthesised by Integrated DNA Technologies (IDT- Illinois, USA) and the sequences can be seen in table 3.4. Finally, a 3-step cycling parameter was set on the Bio-Rad CFX-96 system (Bio-Rad, USA) (Table 3.5) and Cq/Ct values were generated using the CFX Maestro software (Bio-Rad, USA).

Table 3.4: Volumes of SensiFAST™ SYBR® No-ROX reagents added to cDNA templates for qPCR.

The reagents below, together with the synthesised cDNA templates were added to produce a reaction mixture with a final volume of 10 µl for qPCR.

Reagent	Volume (µl)	Final Concentrations
2× SensiFAST™ SYBR® No-ROX mix	5	1×
10 µM Forward Primer	0.4	400 nM
10 µM Reverse Primer	0.4	400 nM
cDNA Template	2	-
dH_2O	2.2	-
Final Volume	**10**	-

Table 3.5: Primer sequences of CETP and GAPDH genes (Ding *et al*., 2015).

Gene	Sequence (5′-3′)	Annealing Temperature (°C)	GC Content (%)
CETP (Forward)	GAGTCCCATCACAAGGGTCA	57.1	55
CETP (Reverse)	GGAAGACTCGCTCAGAGAACC		57.1

GAPDH (Forward)	CGTGTCGGTTGTGGATCTGA		55
GAPDH (Reverse)	TGACGAAGTGGTCGTTGAGG		55

Table 3.6: Three-step cycling parameter used for qPCR.

Cycles	Temperature (°C)	Duration	PCR Step
1	95	2 minutes	Polymerase activation
45	95	6 seconds	Denaturation
	57.1	10 seconds	Annealing
	72	20 seconds	Extension

GAPDH was used as a reference gene. Since GAPDH is a reference gene, it is constitutively expressed in the cell and its inclusion in the qPCR experiment allowed the normalisation of the results obtained, ensuring the accurate determination of CETP mRNA expression levels in both transfected and non-transfected cells. GAPDH was chosen as reference gene since it functions optimally at the temperature cycles chosen and has been used in previous studies (Gu Master's Dissertation, 2018). In addition, the no-template control (negative control), from the cDNA synthesis procedure, was also included in the qPCR experiment. This control ensured that the extracted RNA (which was converted to cDNA) and no other contaminants was being amplified during the qPCR process.

3.5. Western blotting

Western blotting was performed as described in Sagar et al., (2014) to confirm successful knockdown of CETP and to quantify CETP protein expression in transfected, non-transfected and siRNA negative control cells.

3.5.1. Cell lysis

The chemical method of cell disruption was employed in the present study, using lysis buffer. Transfected, non-transfected and siRNA negative control cells were harvested (~ 3×10^6 cells) and centrifuged at 4000 ×g for 5 minutes, with the supernatant being discarded. This was then followed by a lysis step, using 1× RIPA or lysis buffer (100 µl/1×10^6 cells) (Table 3.6) the pellet was thoroughly mixed with lysis buffer and briefly vortexed in 5 minutes intervals over 20 minutes. Samples were kept on ice during the entire procedure, as lysis buffer functions optimally at-4^{o}C. Lysis buffer disrupts cell membranes allowing cell contents, including internal proteins, to be released from the cells.

Table 3.7: 1× RIPA buffer/Lysis buffer componets (All reagents from Sigma Aldrich, UK).

	Component (for 100 ml)
1× RIPA/Lysis buffer	• 300 mM NaCl = 0.876 g • 1% Triton-X-100 = 1 ml • 1% Deoxycholate = 1 g • 0.1% SDS 1 ml of 10 % SDS • 50 mM Tris = 1.21 g • 10 mM EDTA = 1 ml

3.5.2. BCA assay

Thereafter, a bicinchoninic acid (BCA) assay was performed to determine the total protein concentrations of each cell sample. A BCA assay is a colorimetric quantification method that relies on the peptide bonds in proteins to reduce copper sulphate (Cu^{2+}) to Cu^{+} ions. Two molecules of BCA then chelate with each Cu^{+} ion leading to the formation of a purple coloured complex that absorbs at a wavelength of 562 nm. The amount of Cu^{2+} reduced and hence the purple complex formed is directly proportional to the protein present in the sample. Unknown protein concentrations may then be determined by measuring absorbance at 562 nm of known protein standards subjected to a BCA assay.

Prior to SDS polyacrylamide gel electrophoresis (SDS-PAGE), it is essential to determine protein concentration in a sample to ensure equal loading, especially when observing gene knockdown in a sample. Bovine serum albumin (BSA) concentrations of 3 mg/ml, 2 mg/ml, 1 mg/ml, 0.8 mg/ml, 0.6 mg/ml, 0.4 mg/ml, 0.2 mg/ml and 0 mg/ml (blank and negative control) were added in triplicates to a 96-well plate (25 µl/well); this was used to generate a BSA standard curve. Thereafter, 5 µl protein lysate of each sample and 20 µl 1× lysis buffer (1:5 dilution) were added to the plate in triplicates. Subsequently, 200 µl of BCA reagent, consisting of 196 µl of BCA (Sigma Aldrich, UK) and 4 µl copper sulphate (Sigma Aldrich, UK) (50:1), was added to each well. This was then followed by incubation at 37°C for 30 – 45 minutes, depending on the intensity of purple colour. Absorbance of each sample was then measured at 562 nm, using the microtiter plate reader-Multiskan GO Microplate Reader (Thermo Fisher Scientific, SkanIt™ software). The BSA standard curve and protein concentration of each cell lysate was then calculated in Microsoft Office Excel© as seen below:

Average absorbance of samples – Average of blank = **(a)**

Regression line equation of BSA standard curve:

Substituted y-value with **(a)** in the y = mx + c formula above in BSA protein standard

∴ Calculated x-value

x-value × 5 (for dilution) = Protein lysate concentration (mg/ml)

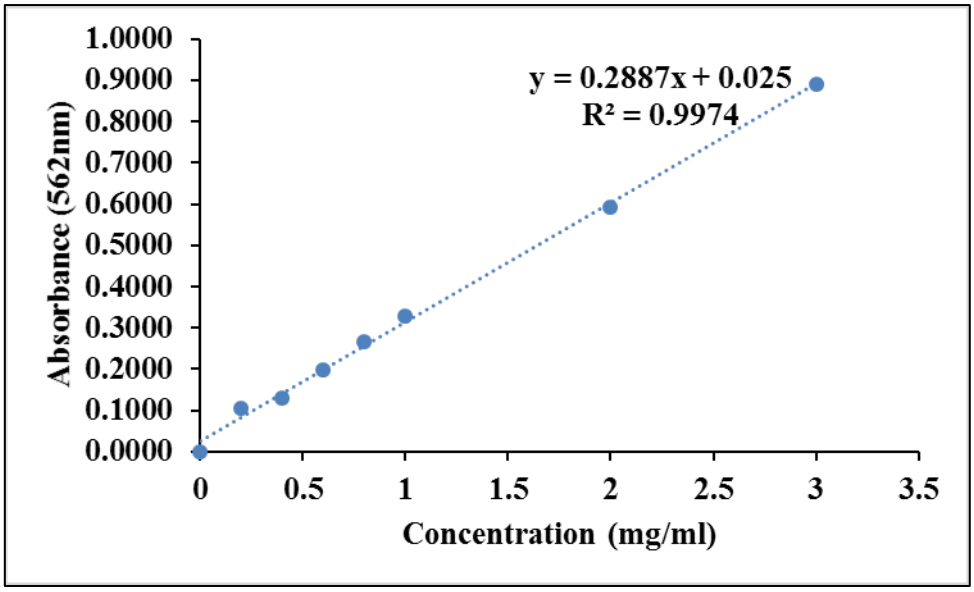


Figure 3.4: A representative BCA protein standard curve.

A BSA protein standard curve was created using known concentrations of BSA (ranging from 0.2 mg/ml to 3 mg/ml) subjected to a BCA assay. The standard curve was then used to quantify the total protein in transfected, non-transfected and siRNA negative control cell lysates.

3.5.3. SDS PAGE and Western blotting

Lysates were then subjected to SDS-PAGE; cell lysates of equal total protein concentrations were loaded onto a 1 mm 10% polyacrylamide gel (table 3.7 and table 3.8) in triplicates, with the Precision Plus Protein™ unstained molecular weight marker (Bio-Rad, USA) and electrophoresed at a voltage of 120 V for 1.5 hours. Proteins were then transferred onto a 0.22 µM polyvinylidene fluoride or polyvinylidene difluoride (PVDF) membrane using the Trans-Blot®Turbo™ Transfer System (Bio-Rad, USA), a semi-dry transfer system (at 25V for 30 minutes). Next, the membranes were transferred into a 10 % skim milk (in 1× tris-buffered saline with Tween-20 or TBST; Sigma Aldrich, UK) blocking solution on a shaker for an hour. Following transfer, it is necessary to block the membrane before the blot can be processed for detection. Considering that membranes have a high affinity for binding proteins and therefore antibodies, blocking prevents non-specific binding of both primary and secondary antibodies to the membrane (Kurien and Scofiled, 2006). Thereafter, primary antibody in 10% skim milk in 1× TBST (anti-β-tubulin; diluted 1:2000; Sigma Aldrich, UK, anti-CETP; diluted 1:1000; Sigma Aldrich, UK) were added to the membranes and incubated overnight at 4 ℃ on a shaker. After overnight incubation, primary antibody solutions were removed, followed by 5× 5 minute

washes with 1× TBST to remove unbound antibodies and prevent background. Subsequently, membranes were incubated with horseradish peroxidase (HRP) – conjugated secondary antibody in 10% skim milk in 1× TBST for 1 hour on a shaker (Anti-mouse; diluted 1:2000; Bio-Rad, SA, anti-rabbit; 1:2000; Bio-Rad, SA). This was then followed by 5× 5 minute washes with 1× TBST (table 3.10) to remove unbound antibodies. Lastly, Clarity ECL substrate (Bio-Rad, USA), a horseradish peroxidase-conjugated substrate for chemiluminescence detection was added (1:1 ratio of reagent A and reagent B; 1 ml reagent A and 1ml reagent B) and the membranes were viewed using the ChemiDoc™ MP system (Bio-Rad, South Africa). Protein expression levels were determined by performing densitometry analysis of the Western blots, using Image Lab™ 4.0 Software (Bio-Rad, USA).

Monoclonal anti-β-tubulin antibody produced in mouse (T4026, Sigma Aldrich) was used as a loading control. Since β-tubulin is constitutively expressed in cells, the protein expression level of β-tubulin was used to normalise the results obtained from protein expression levels of CETP.

Table 3.8: SDS-PAGE 10%, 1 mm gel components.

	Resolving Gel	Stacking Gel
Resolving gel buffer with SDS	3 ml	-
Stacking gel buffer with SDS	-	750 µl
30% Bis-acrylamide (Sigma Aldrich, UK)	3 ml	500 µl
Distilled Water (dH2O)	3 ml	1.75 ml
10% Ammonium Persulfate (APS) (Sigma Aldrich, UK)	100 µl	30 µl
Tetramethylethylenediamine (TEMED) (Sigma Aldrich, UK)	10 µl	3 µl

Table 3.9: SDS-PAGE gel buffer components

	Component
Resolving Gel Buffer	• 36.2 g Tris-HCL • 0.8 g SDS

	• Dissolve in 150 ml dH_2O • pH to 8.9 • Make up to 200 ml with dH_2O
Stacking Gel Buffer	• 5.9 g Tris • 0.4 g SDS • Dissolve in 70 ml dH_2O • pH to 6.8 • Make up to 100 ml with dH_2O
30% Bis-acrylamide (Sigma Aldrich, UK)	• 30 g Acrylamide • 0.8 g Bisacrylamide • 0.1 g SDS • Make up to 100 ml dH_2O
10% APS (Sigma Aldrich, UK)	• 100 mg APS in 1 ml dH_2O

Table 3.10: 1× TBST buffer (pH 7.5) (All reagents from Sigma Aldrich, UK)

Component	Amount
Tris	6.05 g
NaCl	8.76 g
Tween-20	1 ml
dH_2O	1 L

3.6. Immunofluorescence staining

In addition to RT-qPCR and Western blotting, immunofluorescence staining was performed to confirm successful knockdown of CETP in transfected MCF-7 cells. 50 000 cells (transfected, non-transfected and siRNA negative control) were seeded into a 6-well plate in 2 ml of media and incubated at 37 °C for 24 hours. Torcetrapib was used as positive control, since it's a known inhibitor of CETP; cells were treated with 25 µM torcetrapib for 24 hours. Subsequently, media was removed, and cells were washed 3× with 1× PBS. Subsequently, cells were fixed with 4%

formalin (HT501128, Sigma Aldrich, UK) at room temperature for 10 minutes, followed by three 1× PBS washes. Formalin fixation involves cross-linking proteins, primarily through the basic amino acid, lysine, converting the normal semi-fluid consistency of cells to an irreversible semi-solid. Fixation thus allows the preservation of proteins and cellular organelles. Cells were then permeabilised with 0.1% triton™ X-100 (T8787, Sigma Aldrich, UK) in 1 ml PBS and incubated at room temperature for 20 minutes, allowing antibody access and binding in subsequent steps. This was followed by three washes with 1× PBS washes and cells were then blocked with 0.05% BSA (AM 0332, Inqaba Biotec™) for 20 minutes. Cells were then incubated with CETP primary antibody (Anti-CETP; diluted 1:1000; Sigma Aldrich, UK) overnight at 4 ℃. Cells were then washed three times with 1× PBS and incubated with goat anti-rabbit IgG secondary antibody, Texas red (T-2767, Thermo Fischer Scientific, US) for 1 hour in the dark at 4 ℃. This was followed by three 1× PBS washes and a 5 minutes incubation with 0.01 mg/ml DAPI (nuclear stain), at room temperature. Lastly, cells were washed with 1× PBS and the FLoid™ cell imaging system (Thermo Fischer Scientific, USA) was used to observe fluorescence. The immunofluorescence intensity was calculated using ImageJ1 software (NIH, USA).

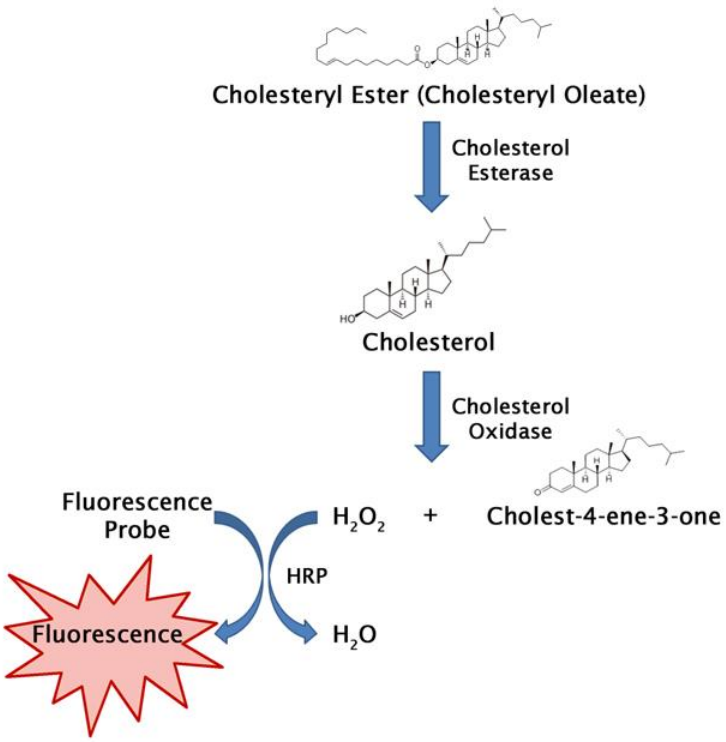
3.7. Cholesterol quantification

A cholesterol assay was used to quantify cholesterol, in particular CEs, in transfected and non-transfected MCF-7 cells. In addition, Filipin staining allowed the visualisation of lipid content in the cells.

3.7.1. Cholesterol assay

The cholesterol assay was used to determine the effects of CETP knockdown on intracellular cholesterol levels. The cholesterol assay involves the hydrolysis of CEs to cholesterol by the enzyme, cholesterol esterase. Cholesterol is then oxidised by cholesterol oxidase, resulting in the formation of two products: cholest-4-ene-3-one and hydrogen peroxide (H_2O_2). A highly specific colorimetric probe, Amplifu Red (Sigma Aldrich, UK) then detects H_2O_2. Subsequently, HRP catalyses the reaction between these two components which binds in a 1:1

ratio (Figure 3.3). The reaction results in pink colour formation, which can be measured at 570 nm (Bioscience, UK).



<u>Figure 3.5:</u> Basis of a cholesterol assay.

[*Adapted from http://cellbiolabs.com/total-cholesterol-assay-kit*]

In the first step of the cholesterol assay, cholesterol esterase hydrolyses CEs to cholesterol. Cholesterol is then oxidised by cholesterol oxidase, resulting in the formation of two products: cholest-4-ene-3-one and hydrogen peroxide (H_2O_2). A highly specific colorimetric probe, amplifu red (Sigma Aldrich, UK) then detects H_2O_2. Subsequently, HRP catalyses the reaction between these two components which binds in a 1:1 ratio.

Transfected and non-transfected cells were seeded in a 96-well plate at a density of 5 000 cells/well in two sets; one measuring total cholesterol and the other free cholesterol. The seeded cells were incubated at 37°C for 24 hours and treated with 10 µM AP for 24 hours accompanied by cholesterol standards of known cholesterol mass. Thereafter, media was removed, and each well was washed with 50 µl 1× PBS. Subsequently, 10 µl of 100 U/ml catalase (Sigma Aldrich, UK) was added to each well and incubated for 15 minutes at 37°C. Catalase degrades excess H_2O_2 to water, protecting cells from reactive oxygen species (ROS) and preventing background

noise when measuring the absorbance. Reagent 'A' was prepared using the following components:

Table 3.11: Cholesterol assay components (Reagent A) per well (mixed in this order)

Reagent A	Total Cholesterol (with esterase) (µl/well)	Free Cholesterol (without esterase) (µl/well)
1 M Potassium phosphate buffer (KPO_4) (Sigma Aldrich, UK)	2.5	2.5
1 M Sodium Chloride (NaCl) (Sigma Aldrich, UK)	6.25	6.25
100mM Cholic acid (Sigma Aldrich, UK)	1.25	1.25
100% Triton-X-100 (Sigma Aldrich, UK)	0.25	0.25
20 U/ml cholesterol oxidase (Sigma Aldrich, UK)	2.5	2.5
150 U/ml HRP (Sigma Aldrich, UK)	1.44	1.44
25 U/ml cholesterol esterase (Inqaba Biotec™, SA)	3.33	-
Isopropanol:NP-40 (9:1) (Merck, SA)	6.48	9.81
10 mM Ampliflu Red (Sigma Aldrich, UK)	1	1

Following the 15 minutes incubation, 25 µl of reagent A (with esterase and without esterase) was added to the respective wells, mixed using a plate shaker (500 rpm) and incubated for 30 minutes at 37°C. The absorbance at 570 nm of each well was measured with the microtiter plate reader-Multiskan GO Microplate Reader (Thermo Fisher Scientific, SkanItTM software) and cholesterol concentration was calculated in comparison to the known cholesterol standards (5, 10, 15, 20 and 0 µg/ml). CEs were calculated as follows:

Average of samples – average of blanks = **(a)**

Substituted y-value with **(a)** in the y = mx + c formula above in the cholesterol standard curve

∴ Calculated x-value for total cholesterol and free cholesterol

x-value = cholesterol concentration (µg/ml)

µg/ml converted to µg/µl → x-value/1000 × total volume in well = cholesterol concentration (µg/µl)

Total cholesterol – free cholesterol = CE

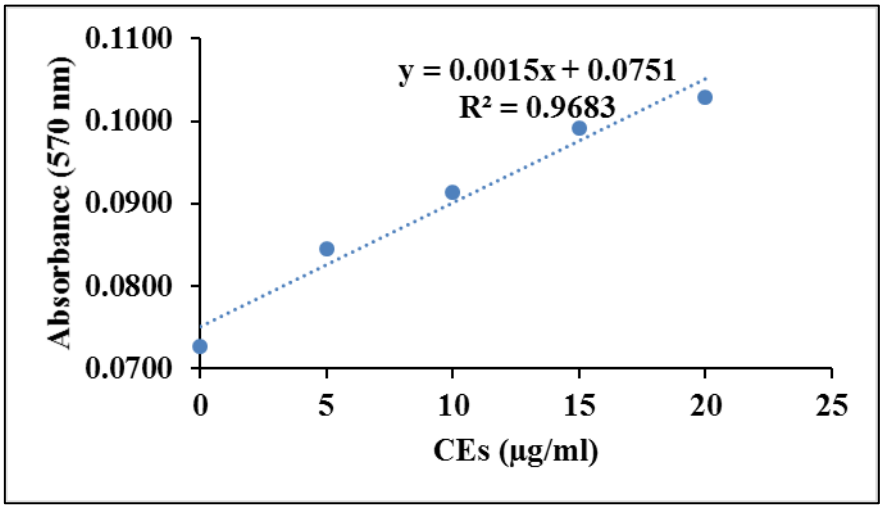


Figure 3.6: A CE assay standard curve

A CE standard curve was created using known concentrations (ranging from 5 µg/ml to 20 µg/ml) subjected to a cholesterol assay. The standard curve was then used to quantify the CEs in transfected, non-transfected and siRNA negative control cell lysates.

3.7.2. Filipin staining

Transfected, non-transfected and siRNA negative control cells were seeded into a 6-well plate at a density of 50 000 cells/well and incubated at 37 ℃ for 24 hours. A positive control was included; cells were treated with 1 mM MβCD for 24 hours at 37 ℃. Thereafter, media was removed followed by three 1× PBS washes. The cells were then fixed with 4% formalin (HT501128, Sigma Aldrich, UK) for 10 minutes at room temperature and this was followed by

three 1× PBS washes. Filipin was then added to each well (0.05 mg/ml in PBS) and incubated at 37 ℃ for 1 hour followed by another three 1× PBS washes. Filipin is a naturally fluorescent polyene antibiotic dye that binds to cholesterol and not esterified sterols. Thus, filipin staining is useful for detecting free cholesterol in cells. Filipin fluoresces with UV excitation approximately at 360 nm and emission at 480 nm. Filipin binding perturbs the membrane bilayer structure, so filipin cannot be used on living cells. Subsequently, one drop of NucRed™ Dead (Thermo Scientific, USA), a nuclear stain was added to each well and incubated for 2 minutes at room temperature. Lastly, cells were washed three times with 1× PBS. Cells were then visualised using the FLoid™ Cell Imaging Station (ThermoFisher Scientific, USA).

3.8. RT^2 Profiler PCR Array (Lipoprotein Signalling and Cancer Drug Resistance)

RT^2 Profiler PCR Arrays (QIAGEN, Germany) were used to assess changes in the expression of genes involved in lipoprotein signalling and cancer drug resistance. RT^2 Profiler PCR Arrays was used on both transfected and non-transfected MCF-7 cells, where a total of 84 genes were evaluated from each array ie. Lipoprotein signalling and cancer drug resistance. Fold change up- or down- regulation of genes was measured between transfected and non-transfected MCF-7 cells.

3.8.1. RNA isolation

Pre- and post-CETP knockdown RNA isolation was performed as above (3.4.1). Thereafter, RNA quality was assessed, as stated above (3.4.1). A total amount of 500 ng of RNA was used for reverse transcription.

3.8.2. Reverse transcription

Prior to reverse transcription, a DNA elimination step was performed, to ensure complete removal of genomic DNA. Reagents were mixed according to table 3.10 and briefly centrifuged. This was then followed by a 5 minutes incubation at 42 ℃. Thereafter, the DNA elimination mix was immediately placed on ice for a minute. Subsequently, the reverse transcription mix was prepared according to table 3.11 and 10 µl of the reverse transcription

mix was added to 10 µl of DNA elimination mix and gently mixed. This was followed by a 15 minutes incubation at 42 ℃, to allow reverse transcription of the isolated RNA. The reaction was immediately stopped by incubation at 95 ℃ for 5 minutes. Lastly, 91 µl of RNase-free water was added to the reaction. Tubes were placed on ice prior to real-time PCR. Concentration of cDNA was measured using the Nanodrop 1000 spectrophotometer (Thermo Fisher Scientific, USA) and approximately 200 ng/µl was used for real-time PCR.

Table 3.12: Genomic DNA elimination mix

Component	Amount
RNA	500 ng
Buffer GE	2 µl
RNase-free water	Variable
Total volume	**10 µl**

Table 3.13: Reverse-transcription mix

Component	Volume (µl)
5× Buffer BC3	4
Control P2	1
RE3 Reverse Transcriptase Mix	2
RNase-free water	3
Total volume	**10**

3.8.3. Real-time PCR

The RT^2 SYBR Green Mastermix was used to determine the expression of several genes involved in cancer drug resistance and lipoprotein signalling pre- and post-CETP knockdown. The real-time PCR reaction was prepared by mixing the components in table 3.12. Thereafter, 25 µl of the PCR component mix was dispensed into each well of the RT^2 Profiler PCR Array, each well representing a different gene. Thereafter, the array was tightly closed with a clear seal and centrifuged for 1 minute at 1000 ×g, to remove any air bubbles. The RT^2 Profiler PCR Array was kept on ice, while setting up the cycling programme. Lastly, a 2-step cycling parameter was set on the Bio-Rad CFX-96 system (Bio-Rad, USA) (Table 3.13) and Cq/Ct values were generated using the CFX Maestro software (Bio-Rad, USA). The Ct values for all wells were then exported to an Excel® spreadsheet and the SABiosciences PCR Array Analysis Template (available at www.SABiosciences.com/pcrarraydatanalysis.php) was used to calculate fold change in gene expression between transfected (CETP knockdown) and non-transfected MCF-7 cell lines. Log_2 was used to normalise the expression of the genes of each array, allowing to model proportional changes.

Table 3.14: PCR components mix

Component	Volume (µl)
2× RT^2 SYBR Green Mastermix	1350
cDNA synthesis reaction	102
RNase-free water	1248
Total volume	**2700**

Table 3.15: Cycling conditions

Cycle	Temperature (ºC)	Duration	Comments
1	95	10 minutes	HotStart DNA *Taq* Polymerase is activated
40	95	15 seconds	Perform fluorescence data collection
	60	1 minute	

3.9. Network maps: OmicsNet and Cytoscape

OmicsNet (http://www.omicsnet.ca/faces/home.xhtml) was used to identify the targets of the differentially expressed genes in each array (lipoprotein signalling and cancer drug resistance) and this was imported as a network on the Cytoscape interface. The GeneMANIA plugin through Cytoscape (http://cytoscape.org, version 3.7.2) was used to create gene expression networks, where each gene (node) was coloured according to Log_2 fold change (transfected/non-transfcted MCF-7 cells) and interactive genes were connected by grey lines. Cytoscape is platform used for visualising molecular interactions and biological pathways, while integrating these networks with gene expression profiles and annotations. The GeneMANIA plugin displays an interactive functional association network by extending the query gene list (input genes) with genes that are functionally similar, illustrating relationships amongst genes in a given data set. Each network is assigned a weight based primarily on how well-connected genes are to each other compared to their connectivity to non-query genes. Mapped interactions were considered statistically significant when $q < 0.05$. A q-value of 0.05 indicates that there is a 5% chance of a false-positive result.

3.10. Statistical analysis

Statistical significance was determined using the student's t-test at 95% confidence interval ($P<0.05$). All statistical calculations were performed on Microsoft Office Excel©.

4. Results

4.1. Confirmation of successful CETP knockdown

CETP knockdown was confirmed by RT-qPCR, Western blotting and immunofluorescent staining.

4.1.1. RT-qPCR anlaysis

Transfected MCF-7 cells showed a visible decrease in CETP mRNA expression compared to the non-transfected and siRNA negative control MCF-7 cells. As illustrated in Figure 4.1, qPCR analysis revealed 72.36% decrease in CETP mRNA expression and hence successful knockdown of CETP, in the transfected cell line. Furthermore, melt curve analysis revealed optimal amplification and primer specificity.

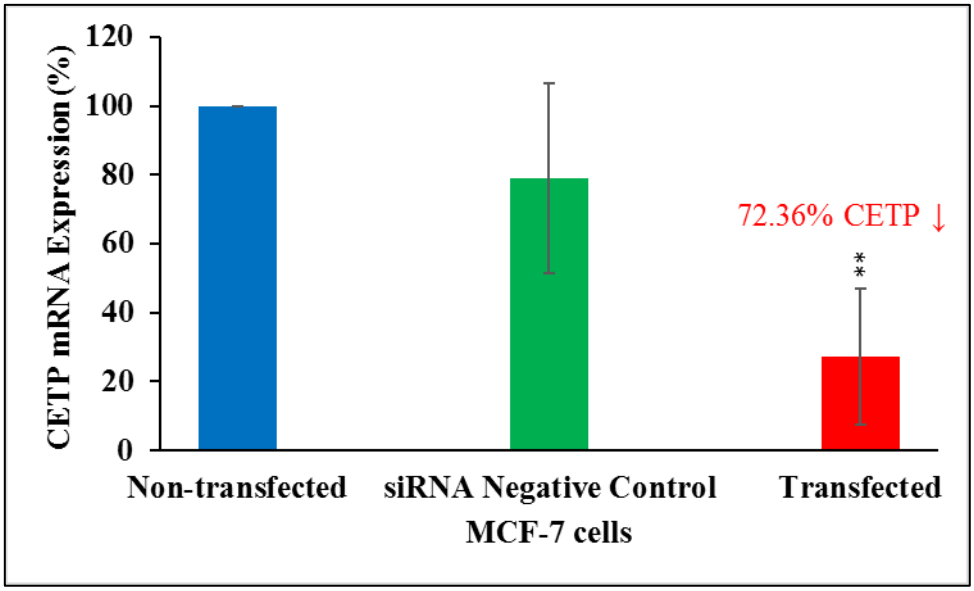


Figure 4.1: Successful knockdown of CETP mRNA in MCF-7 cells, confirmed by RT-qPCR.

*RT-qPCR analysis exhibited a decrease in CETP mRNA expression level (72.36%) in the transfected MCF-7 cells compared to the non-transfected and siRNA negative control cells. RT-qPCR additionally confirmed CETP knockdown. Data represents the mean ± standard deviation (SD). n=3. *P≤0.05, **P≤0.01, ***P≤0.001, no* non-significant.*

4.1.2. Western blotting and densitometry analysis

Western blotting confirmed successful knockdown of CETP protein (~ 70 kDa) in transfected MCF-7 cells, with equal loading of β-tubulin at ~ 50 kDa for all samples (Figure. 4.4A). Furthermore, densitometry analysis revealed significant CETP protein knockdown, with a 69.7% decrease in CETP protein expression in transfected MCF-7 cells as compared to non-transfected cells (Figure 4.4B).

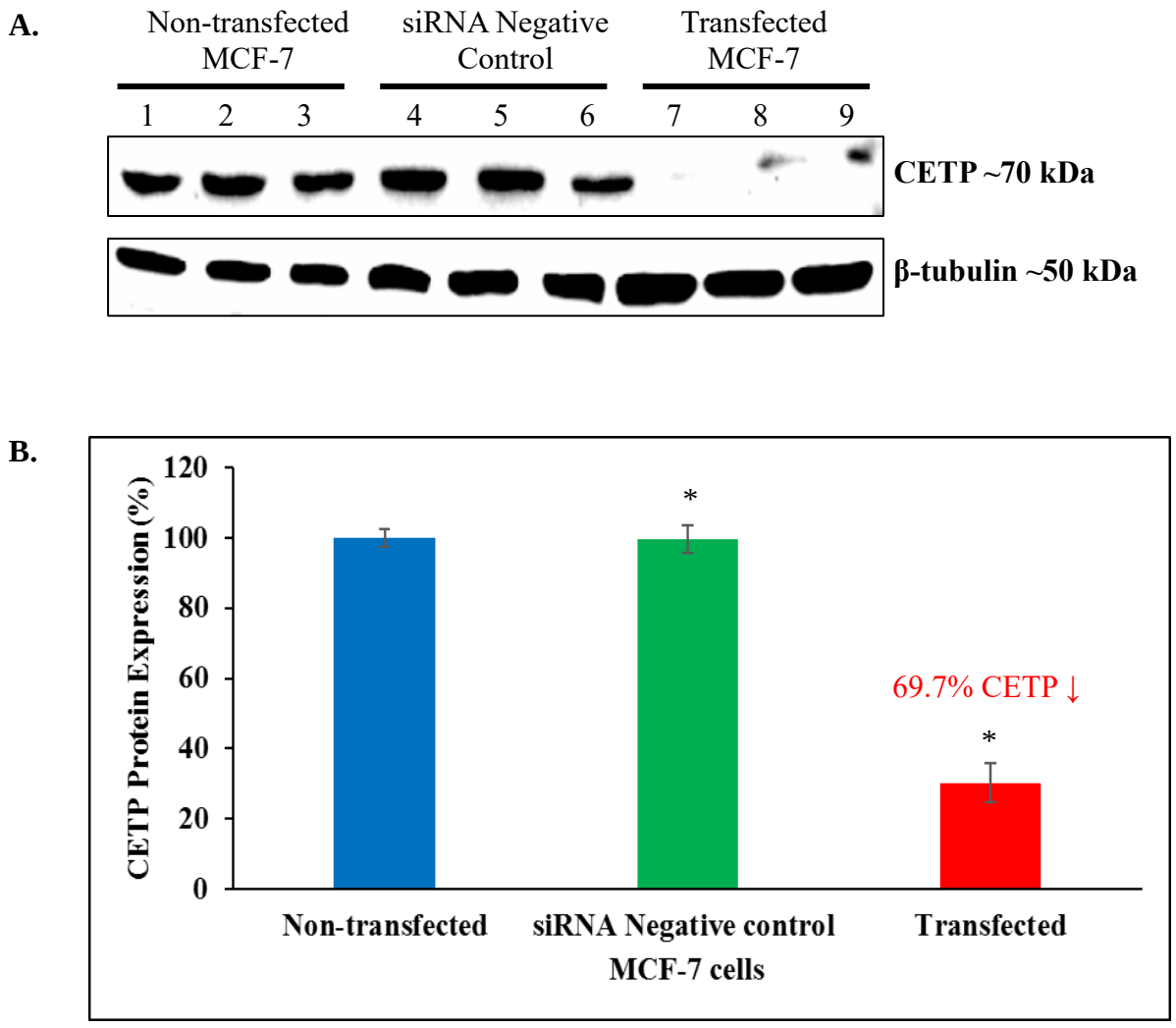


Figure 4.2: Successful knockdown of CETP protein in MCF-7 cells, confirmed by Western blotting.

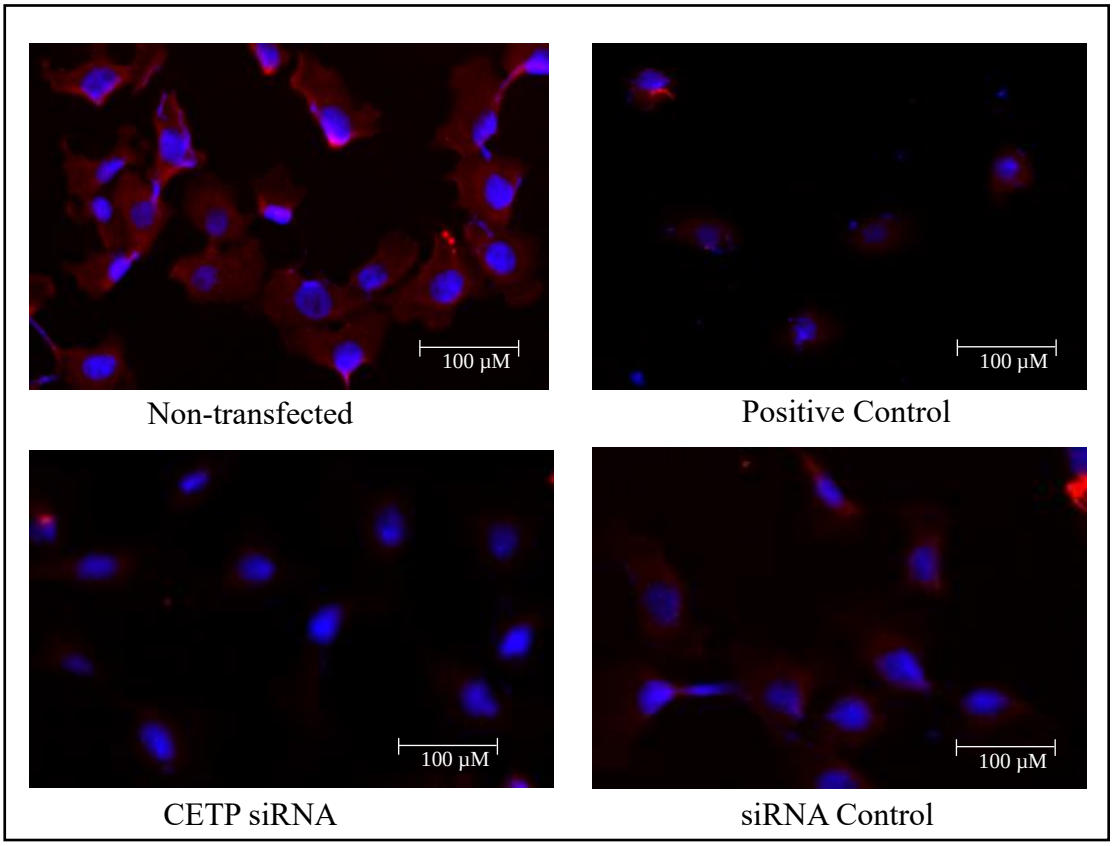
Figure 4.4A illustrates the protein bands of the Western blots viewed using the Chemidoc. Fainter bands are depicted in the transfected MCF-7 cells, justifying CETP protein (~ 70 kDa) knockdown, with equal loading of β-tubulin (~50 kDa). Figure 4.4B displays the densitometry results of the Western blots. A 69.7% knockdown is seen in transfected MCF-7 cells relative to

*the non-transfected MCF-7 cells. Data represents the mean ± standard deviation (SD). n=3. *P≤0.05, **P≤0.01, ***P≤0.001, no* non-significant.*

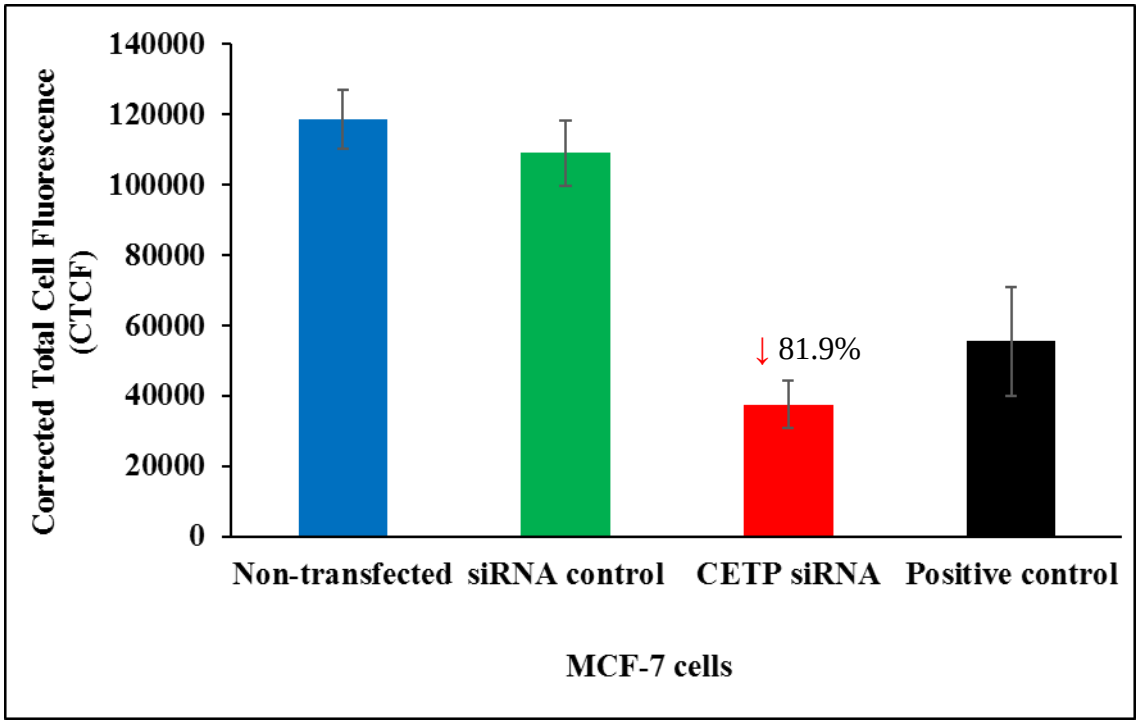
4.1.3. Immunofluorescence imaging

MCF-7 cells exhibited typical 2D morphology, growing in mostly flat monolayers, with some cell aggregates. Immunoflourescence imaging further validated successful CETP knockdown; imaging analysis of the MCF-7 cells stained with Texas Red (CETP) and DAPI (nuclear) revealed a higher fluorescence intensity in non-transfected cells, with the former staining more strongly than the transfected MCF-7 cells. Imaging displayed diffused, but uniform cytoplasmic staining across the non-transfected cells while very limited and punctate staining was observed in transfected MCF-7 cells (Figure 4.3A). Image J1 analysis further confirmed the above result, showing an 81.9% reduction in corrected total cell fluorescence (CTCF) in transfected MCF-7 cells relative to the non-transfected MCF-7 cells (Figure 4.3B).

A.



B.



<u>Figure 4.3:</u> Successful knockdown of CETP protein in MCF-7 cells, confirmed by immunofluorescence staining.

*Figure 4.3A displays the immunofluorescence staining images using the FLoid® Cell Imaging system of transfected, non-transfected, siRNA negative control and positive control (25 µM Torcetrabip) MCF-cells. Cells stained with Texas Red (CETP) and DAPI (nuclear) reveal a higher fluorescence intensity in non-transfected cells, as compared to the transfected cells, confirming CETP knockdown in the latter. Figure 4.3B displays the calculated CTCF values using Image J1 analysis. An 81.9% reduction in CTCF was observed in the transfected cells compared to the non-transfected MCF-7 cells. Similar fluorescence intensities were measured in non-transfected and siRNA negative control cells. Additionally, the siRNA approach was more effective than the 25 µM torcetrabip treatment in knocking down CETP, as shown by CTCF values. Data represents the mean ± standard deviation (SD). n=3. *P≤0.05, **P≤0.01, ***P≤0.001, no* non-significant.*

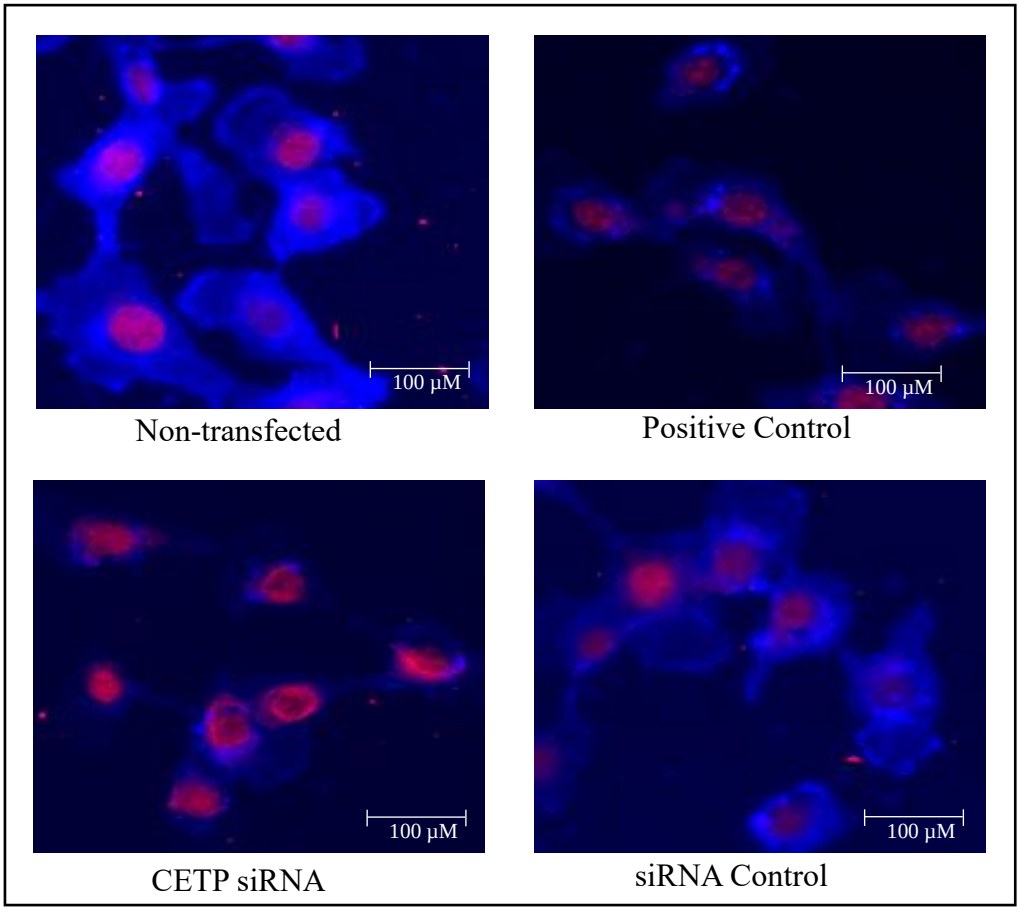
4.2. CETP knockdown reduces free cholesterol and endogenous CEs in MCF-7 cells

Filipin staining was used to quantify free cholesterol and CE content was measured using a cholesterol assay.

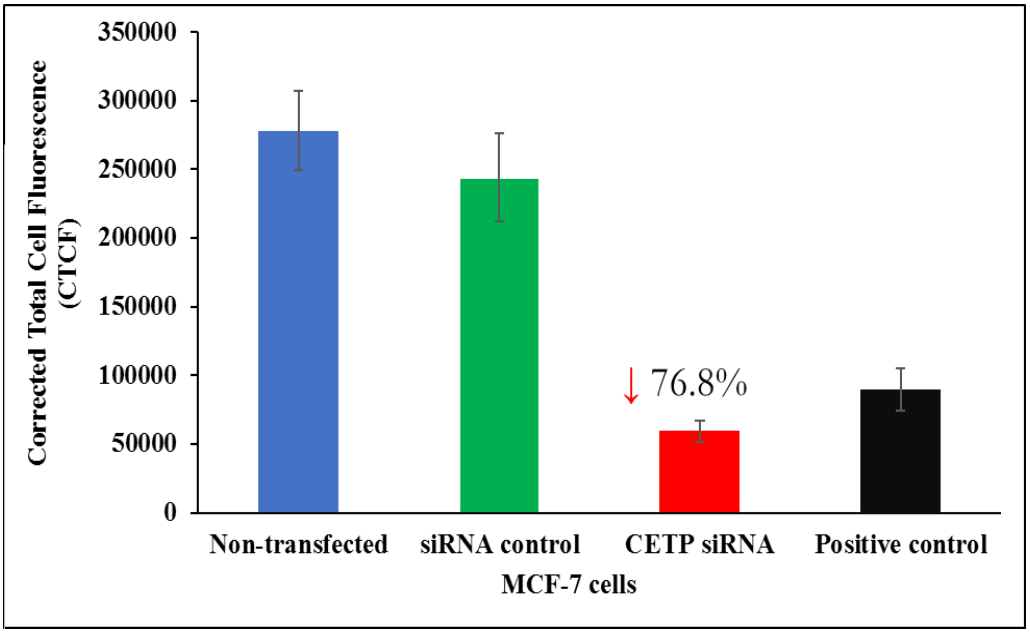
4.2.1. Filipin staining

Numerous studies have linked altered cholesterol metabolism to breast cancer aggressiveness, particularly the accumulation of cholesterol and CEs in breast cancer cells (Esua *et al.*, 2016). In an attempt to measure cholesterol content post-CETP knockdown, filipin staining was performed. In this instance, MCF-7 cells displayed atypical morphology, adopting a rounded shape. This could be attributed to cellular stresses post-CETP knockdown, as well as steps in the staining process, namely fixation. Imaging analysis of MCF-7 cells stained with Filipin (staining cholesterol) and NucRed™ Dead (nuclear) revealed a higher fluorescence intensity and therefore a higher total cholesterol content in the non-transfected MCF-7 cells. On the contrary, CETP knockdown resulted in a significant reduction in cholesterol content, indicated by the 78.6% decrease in CTCF in the non-transfected MCF-7 cells.

A.



B.



<u>Figure 4.4:</u> Reduction in cholesterol content post-CETP knockdown in MCF-7 cells, confirmed by filipin staining. *Figure 4.4A displays the immunofluorescence staining images using the FLoid® Cell Imaging system of transfected, non-transfected, siRNA negative control and positive control (1 mM MβCD) MCF-cells. Filipin (staining cholesterol) and NucRed™ Dead (nuclear) revealed a higher fluorescence intensity in non-transfected as compared to the transfected MCF-cells, displaying the cholesterol depletion effects of CETP knockdown in MCF-7 cells. Cells displayed an atypical cell morphology, possibly due to the cellular stress exerted by CETP knockdown, as well as fixation during the staining process. Figure 4.4B displays the calculated corrected total cell fluorescence (CTCF) using Image J analysis. A 76.8% reduction in CTCF was observed in the transfected cells compared to the non-transfected MCF-7 cells. Similar fluorescence intensities were measured in non-transfected and siRNA negative control cells. Additionally, the siRNA approach was more effective than the 1 mM MβCD treatment in knocking down CETP, as shown by CTCF values. Data represents the mean ± standard deviation (SD). n=3. *P≤0.05, **P≤0.01, ***P≤0.001, no* non-significant.*

4.2.2. Cholesterol Assay

To further validate the above result, a cholesterol assay was used to quantify CEs post-CETP knockdown. As predicted, there was a 54% reduction in CE content in untreated transfected

MCF-7 cells. Furthermore, the AP treated transfected MCF-7 cells showed a further reduction in CE content as compared to the non-treated cells, indicating a possible interaction between CETP and AP. This can be confirmed by the study of Esau et al., 2016 where there was a reduction in CETP mRNA and protein expression upon AP treatment. Additionally, AP was able to significantly increase the thermal stability of CETP as shown by the cellular thermal shift assay, suggesting a potential CETP-AP interaction (Esau *et al*., 2016).

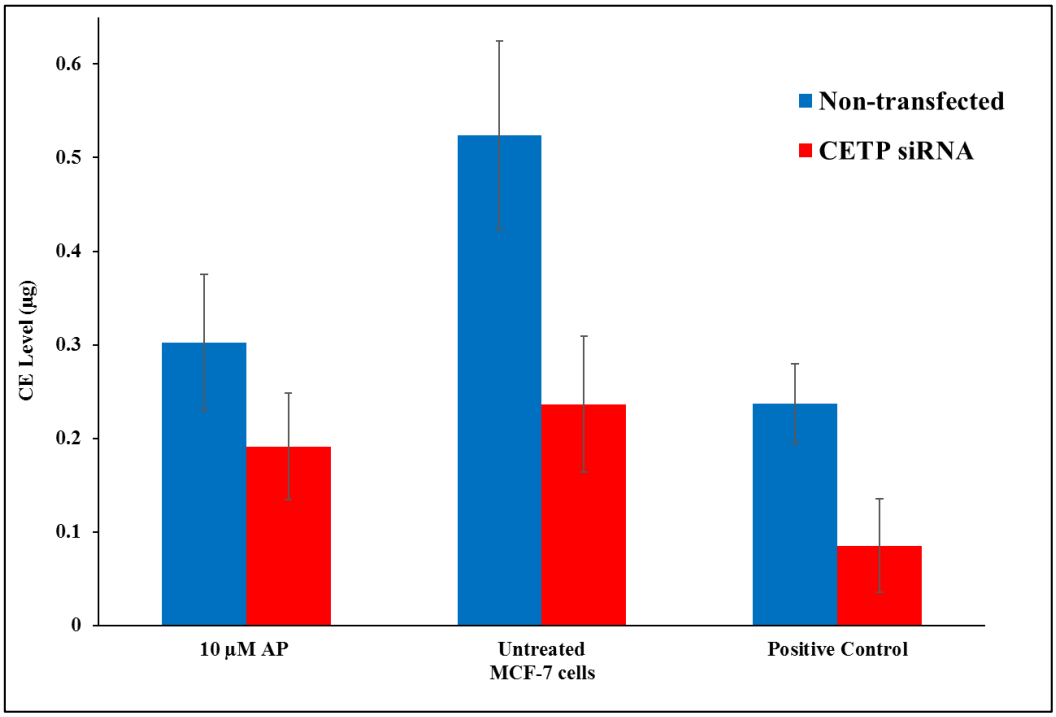


Figure 4.5: CETP knockdown reduces intracellular CE levels in MCF-7 cells.

*CEs fuel breast cancer aggressiveness and CETP knockdown resulted in a 54% reduction in CE content, with a further reduction in AP-treated transfected cells, MβCD was used as a positive control. Data represents the mean ± standard deviation (SD). n=3. *P≤0.05, **P≤0.01, ***P≤0.001, no* non-significant.*

4.3. CETP knockdown decreases MCF-7 cell viability

It was observed from previous results, namely staining, that there was a reduction in the number of transfected cells. Since CETP plays an essential role in cholesterol modulation and cholesterol is an integral component for the synthesis of cell membranes and thus cellular proliferation, it was predicted that CETP knockdown will result in cellular growth stagnation. A viable cell count is essential to evaluate cell growth. As seen in Figure 4.6, a 68.2% reduction

in cell number was observed in transfected MCF-7 cells as compared to the non-transfected cells.

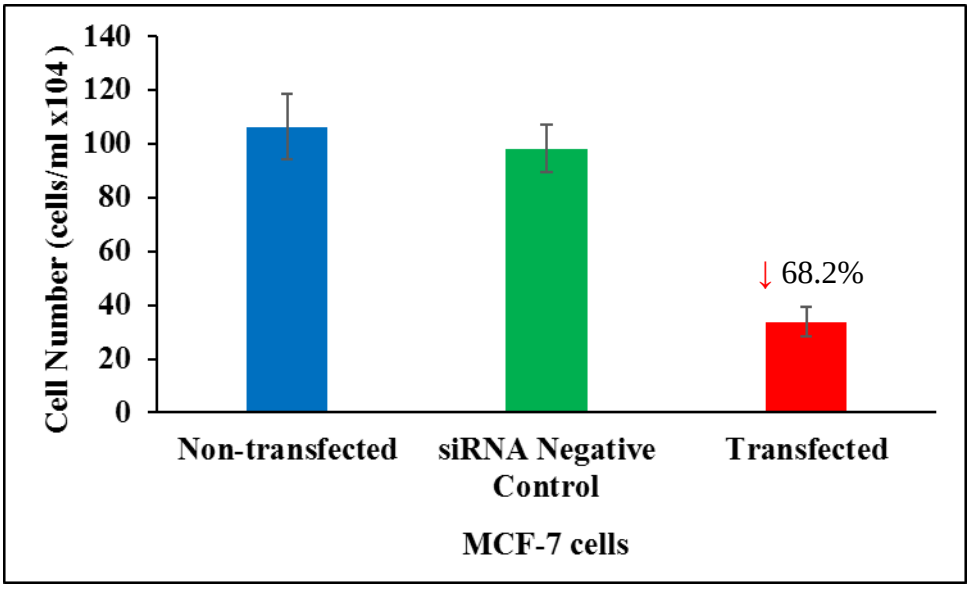


Figure 4.6: CETP knockdown reduces MCF-7 cell viability.

*Post-CETP knockdown a cell count was performed and 68.2% reduction in cell number was observed in transfected MCF-7 cells as compared to the non-transfected cells. CETP knockdown thus results in a decrease in cell number in MCF-7 breast cancer cells, as a result of increase in cell death. Cell count was performed 72 hours after transfection. Data represents the mean ± standard deviation (SD). n=3. *P≤0.05, **P≤0.01, ***P≤0.001, no* non-significant.*

4.4. Shift in pathway dynamics post-CETP knockdown: Overall downregulation of genes involved lipoprotein signalling and cancer drug resistance

RT-qPCR analysis using the RT^2 Profiler PCR Arrays was performed to determine differences in gene expression between transfected (CETP knockdown) and non-transfected MCF-7 cells, namely genes involved in lipoprotein signalling and cancer drug resistance. Modulation of lipoprotein signalling-related genes and cancer drug resistance-related genes by CETP in MCF-7 cells was investigated by RT-qPCR using the respective arrays. These RT^2 Profiler PCR Arrays contain a panel of 84 genes known to be associated with lipoprotein signalling and cancer drug resistance. Fold change values were calculated using non-transfected (untreated) MCF-7 cells compared to CETP knockdown MCF-7 cells.

4.4.1. Lipoprotein signalling

Gene expression analysis revealed a downregulation of 70 genes involved in lipoprotein signalling post-CETP knockdown, with 14 genes being undetectable. These genes might have been detected later in the PCR process ie. at a later cycle. A total of 66 genes were downregulated by more than two-folds post CETP knockdown. Additionally, gene expression of *ABCG1* (fold change = -5.09), *APOA4* (fold change = -7.66), *APOL1* (fold change = -4.07), *APOL5* (fold change = -6.21), *CEL* (-7.75), *CELA3A* (fold change = -5.48), *LCAT* (fold change = -4.49), *LEP* (fold change = -6.39), *LIPE* (fold change = -4.24), *MBTPS1* (fold change = -10.70), *MVD* (fold change = -22.88), *PMVK* (fold change = -4.40), *PRKAA2* (fold change = -11. 59), *PRKAG2* (fold change = -4.70), *STAB1* (fold change = -8.75), *STAB2* (fold change = -4.91), *STARD3* (fold change = -14.26), *TM7SF2* (fold change = -9.05) and *TRERF1* (fold change = -5.34) was substantially downregulated in transfected MCF-7 cells. Complete gene expression analysis is summarised in table 4.1. The expression profiles of genes identified post-CETP knockdown were subjected to OmicsNet and Cytoscape, and a network map of potential interactions and pathways were generated (Figure 4.7). Cytoscape representation showed a general downregulation of pathways involved in cholesterol biosynthesis, cholesterol metabolism, cholesterol catabolism, cholesterol transport, cholesterol efflux, HDL associated proteins, LDL associated proteins, LDLR and LDLR associated proteins post-CETP knockdown. Notably, several of the highly downregulated genes are involved in the cholesterol biosynthesis pathway, supporting the hypothesis that CETP knockdown results in a reduction in cholesterol in breast cancer cells. These genes included *MVD, HMGCR* and *NSDHL*, all of which play a role in the mevalonate pathway. As well as *LDLR*, which is involved in intracellular cholesterol uptake and *SREBPF1*, the TF involved in endogenous cholesterol synthesis.

Table 4.1: Gene expression changes of genes involved in lipoprotein signalling in transfected compared to non-transfected MCF-7 cells.

Table 4.1 summarises the gene expression analysis following RT-qPCR using the lipoprotein signalling RT^2 Profiler PCR Array. Results display an overall downregulation of 70 genes involved in lipoprotein signalling, with 66 genes downregulated by more than two-folds post-CETP knockdown.

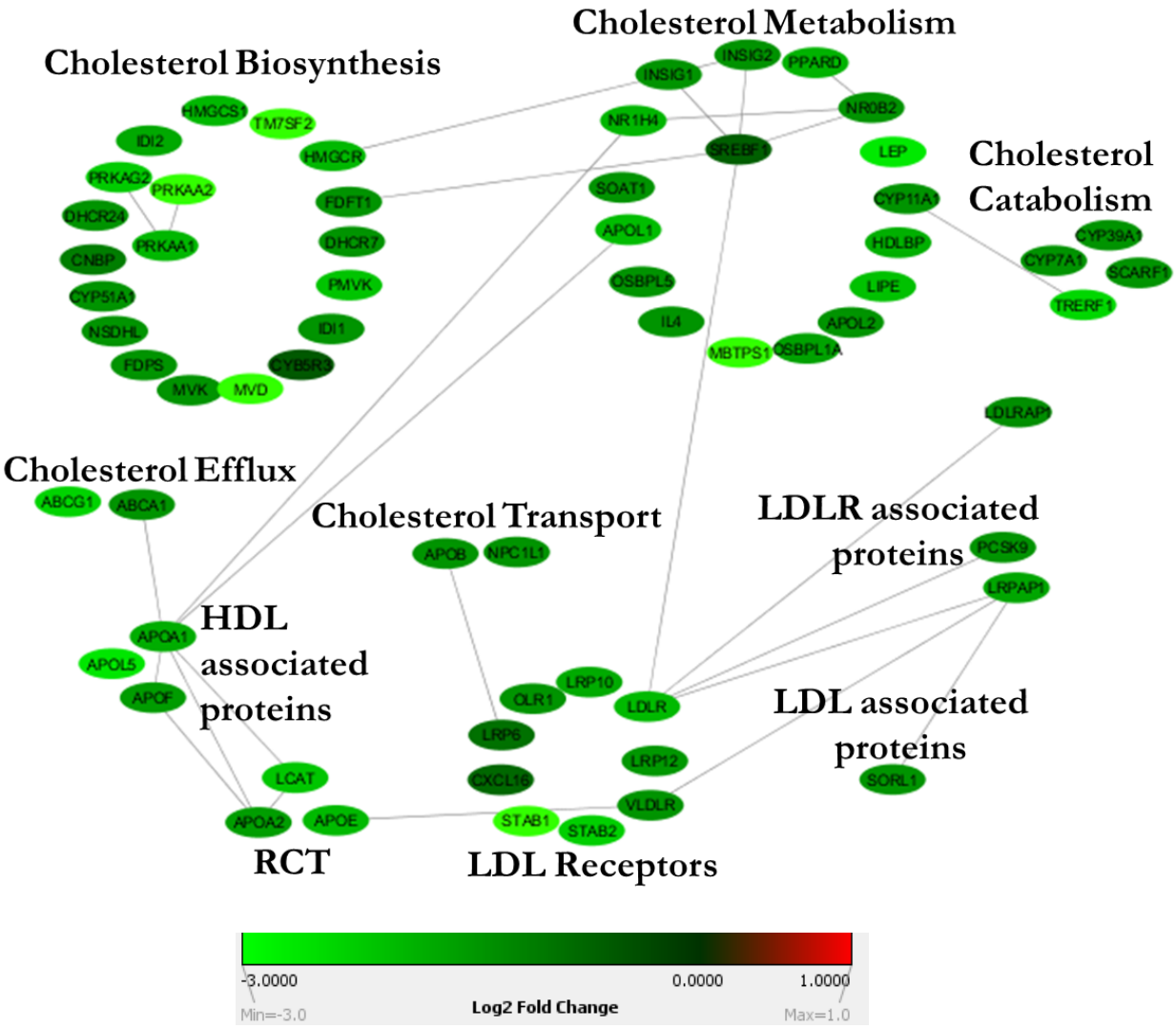
Gene Symbol	Description	Mode of Action	Fold Change (Up- or Down-Regulation; transfected/non-	Log2 Fold Change (Up- or Down-Regulation;

			transfected MCF-7 cells)	transfected/non-transfected MCF-7 cells)
ABCA1	ATP-binding cassette, sub-family A (ABC1), member 1	Cholesterol efflux pump to remove lipids/ cholesterol transporter/ reverse cholesterol transport/cholesterol homeostasis	-2.700404059	-1.433175292
ABCG1	ATP-binding cassette, sub-family G (WHITE), member 1	Cholesterol efflux pump to remove lipids/ cholesterol transporter/cholesterol homeostasis	-5.087940615	-2.347081832
AKR1D1	Aldo-keto reductase family 1, member D1 (delta 4-3-ketosteroid-5-beta-reductase)	cholesterol catabolism	-2.700404059	-1.433175292
APOA1	Apolipoprotein A-I	HDL associated protein/Cholesterol efflux pump to remove lipids/ cholesterol transporter/reverse cholesterol transport/cholesterol homeostasis	-3.453293976	-1.787973155
APOA2	Apolipoprotein A-II	reverse cholesterol transport/cholesterol homeostasis	-2.971064546	-1.570979948
APOA4	Apolipoprotein A-IV	LDL associated proteins/ cholesterol efflux/reverse cholesterol transport/cholesterol homeostasis	-7.655211456	-2.936442229
APOB	Apolipoprotein B (including Ag(x) antigen)	cholesterol transport/ cholesterol metabolism	-2.700404059	-1.433175292
APOE	Apolipoprotein E	cholesterol transporter/ cholesterol efflux/reverse cholesterol transport/cholesterol catabolism/cholesterol homeostasis	-3.965664141	-1.987562499
APOF	Apolipoprotein F	HDL associated protein/cholesterol metabolism	-2.921982223	-1.546947401
APOL1	Apolipoprotein L, 1	cholesterol metabolism	-4.071881768	-2.025695671
APOL2	Apolipoprotein L, 2	HDL associated protein/cholesterol metabolism	-2.700404059	-1.433175292
APOL5	Apolipoprotein L, 5	HDL associated protein	-6.212038923	-2.635066869
CEL	Carboxyl ester lipase (bile salt-stimulated lipase)	cholesterol absorption /cholesterol catabolism	-7.752300954	-2.954624579
CELA3A	Chymotrypsin-like elastase family, member 3A	cholesterol metabolism	-5.481791502	-2.454647457
CELA3B	Chymotrypsin-like elastase family, member 3B	cholesterol metabolism	-2.700404059	-1.433175292
CNBP	CCHC-type zinc finger, nucleic acid binding protein	cholesterol biosynthesis	-2.146649019	-1.102086327
CXCL16	Chemokine (C-X-C motif) ligand 16	LDL receptor	-1.717194958	-0.780053842
CYB5R3	Cytochrome b5 reductase 3	cholesterol biosynthesis	-1.479809697	-0.565411658
CYP11A1	Cytochrome P450, family 11, subfamily A, polypeptide 1	cholesterol metabolism	-2.700404059	-1.433175292
CYP39A1	Cytochrome P450, family 39, subfamily A, polypeptide 1	cholesterol catabolism	-2.700404059	-1.433175292

CYP46A1	Cytochrome P450, family 46, subfamily A, polypeptide 1	cholesterol catabolism	-2.951834427	-1.561611801
CYP51A1	Cytochrome P450, family 51, subfamily A, polypeptide 1	cholesterol biosynthesis	-2.700404059	-1.433175292
CYP7A1	Cytochrome P450, family 7, subfamily A, polypeptide 1	cholesterol catabolism	-2.700404059	-1.433175292
DHCR24	24-dehydrocholesterol reductase	cholesterol biosynthesis	-2.700404059	-1.433175292
DHCR7	7-dehydrocholesterol reductase	cholesterol biosynthesis	-2.700404059	-1.433175292
FDFT1	Farnesyl-diphosphate farnesyltransferase 1	cholesterol biosynthesis	-2.700404059	-1.433175292
FDPS	Farnesyl diphosphate synthase	cholesterol biosynthesis	-2.700404059	-1.433175292
HDLBP	High density lipoprotein binding protein	cholesterol metabolism	-3.561533724	-1.832498651
HMGCR	3-hydroxy-3-methylglutaryl-CoA reductase	cholesterol biosynthesis	-3.887319746	-1.958775779
HMGCS1	3-hydroxy-3-methylglutaryl-CoA synthase 1 (soluble)	cholesterol biosynthesis	-3.869322593	-1.952081014
IDI1	Isopentenyl-diphosphate delta isomerase 1	cholesterol biosynthesis	-2.700404059	-1.433175292
IDI2	Isopentenyl-diphosphate delta isomerase 2	cholesterol biosynthesis	-3.333517586	-1.737045338
IL4	Interleukin 4	cholesterol metabolism	-2.700404059	-1.433175292
INSIG1	Insulin induced gene 1	cholesterol metabolism	-2.700404059	-1.433175292
INSIG2	Insulin induced gene 2	cholesterol metabolism	-2.66793787	-1.41572507
LCAT	Lecithin-cholesterol acyltransferase	reverse cholesterol transport/cholesterol homeostasis	-4.488136824	-2.166116658
LDLR	Low density lipoprotein receptor	cholesterol transport /cholesterol absorption /cholesterol homeostasis	-3.963706908	-1.986850288
LDLRAP1	Low density lipoprotein receptor adaptor protein 1	LDL receptor associated proteins/cholesterol homeostasis	-2.528811306	-1.338459391
LEP	Leptin	cholesterol metabolism	-6.39259729	-2.676402212
LIPE	Lipase, hormone-sensitive	cholesterol metabolism	-4.241056709	-2.084423774
LRP10	Low density lipoprotein receptor-related protein 10	LDL receptor	-3.393693251	-1.762856169
LRP12	Low density lipoprotein receptor-related protein 12	LDL receptor	-2.796002842	-1.483365827
LRP6	Low density lipoprotein receptor-related protein 6	LDL receptor	-1.88999879	-0.918385311
LRPAP1	Low density lipoprotein receptor-related protein associated protein 1	LDL receptor associated proteins/	-3.235114035	-1.693816567

MBTPS1	Membrane-bound transcription factor peptidase, site 1	cholesterol metabolism	-10.70387036	-3.420060643
MVD	Mevalonate (diphospho) decarboxylase	cholesterol biosynthesis	-22.88153822	-4.516112136
MVK	Mevalonate kinase	cholesterol biosynthesis	-2.700404059	-1.433175292
NPC1L1	NPC1 (Niemann-Pick disease, type C1, gene)-like 1	cholesterol transport /cholesterol absorption /cholesterol biosynthesis	-2.700404059	-1.433175292
NR0B2	Nuclear receptor subfamily 0, group B, member 2	cholesterol metabolism	-2.700404059	-1.433175292
NR1H4	Nuclear receptor subfamily 1, group H, member 4	cholesterol metabolism	-3.783398448	-1.919682722
NSDHL	NAD(P) dependent steroid dehydrogenase-like	cholesterol biosynthesis	-2.700404059	-1.433175292
OLR1	Oxidized low density lipoprotein (lectin-like) receptor 1	LDL receptor	-2.700404059	-1.433175292
OSBPL1A	Oxysterol binding protein-like 1A	cholesterol metabolism	-3.115657665	-1.639536725
OSBPL5	Oxysterol binding protein-like 5	cholesterol transport /cholesterol metabolism	-2.700404059	-1.433175292
PCSK9	Proprotein convertase subtilisin/kexin type 9	LDL receptor associated proteins/cholesterol homeostasis	-2.700404059	-1.433175292
PMVK	Phosphomevalonate kinase	cholesterol biosynthesis	-4.399436872	-2.13731887
PPARD	Peroxisome proliferator-activated receptor delta	cholesterol metabolism	-3.684101408	-1.881312773
PRKAA1	Protein kinase, AMP-activated, alpha 1 catalytic subunit	cholesterol biosynthesis	-3.856905444	-1.947443777
PRKAA2	Protein kinase, AMP-activated, alpha 2 catalytic subunit	cholesterol biosynthesis	-11.58955521	-3.534753294
PRKAG2	Protein kinase, AMP-activated, gamma 2 non-catalytic subunit	cholesterol biosynthesis	-4.697258281	-2.231818923
SCARF1	Scavenger receptor class F, member 1	LDL associated proteins/cholesterol catabolism	-2.700404059	-1.433175292
SOAT1	Sterol O-acyltransferase 1	cholesterol metabolism	-2.700404059	-1.433175292
SORL1	Sortilin-related receptor, L(DLR class) A repeats containing	LDL associated proteins/cholesterol metabolism	-2.700404059	-1.433175292
SREBPF1	Sterol regulatory element binding transcription factor 1	cholesterol metabolism	-1.572032519	-0.652631062
STAB1	Stabilin 1	LDL receptor	-8.75428771	-3.129989799
STAB2	Stabilin 2	LDL receptor	-4.912201537	-2.296369753
STARD3	StAR-related lipid transfer (START) domain containing 3	cholesterol transporter/cholesterol metabolism	-14.25544712	-3.833441385

TM7SF2	Transmembrane 7 superfamily member 2	cholesterol biosynthesis	-9.052848571	-3.178371822
TRERF1	Transcriptional regulating factor 1	cholesterol catabolism	-5.343698739	-2.417838675
VLDLR	Very low density lipoprotein receptor	LDL receptor/cholesterol metabolism	-2.700404059	-1.433175292



<u>Figure 4.7:</u> Network map of genes involved in lipoprotein signalling in response to CETP knockdown.

A network map of genes involved in lipoprotein signalling post-CETP knockdown was created using Cytoscape. Nodes (genes) were coloured according to Log_2 fold change (transfected/non-transfected MCF-7 cells) and potential gene interactions (links; coloured in grey) were generated using OmicsNet and visualised in Cytoscape. Genes were grouped according to the major pathway they act in. Figure 4.7 displays several intra-pathway and inter-pathway interactions. Many of the genes in the lipoprotein signalling array are involved in cholesterol biosynthesis and cholesterol metabolism and these also contained most of the

highly downregulated genes post-CETP knockdown. Furthermore, all pathways were downregulated.

4.4.2. Cancer Drug resistance

Gene expression analysis revealed an overall downregulation of 32 genes involved in cancer drug resistance post-CETP knockdown, with *TOP1* (Fold change = 1.34) being the only gene that was upregulated. A total of 30 genes were downregulated by more than two-folds in transfected MCF-7 cells. Additionally, gene expression of *CDKN2D* (Fold change = -1405.56) was drastically reduced post-CETP knockdown, with a significant downregulation in, *ABCB1* (Fold change = -4.15), *ABCC5* (Fold change = -26.13), *AR* (Fold change = -8.73), *BCL2* (Fold change = -20.69), *BRCA1* (Fold change = -8.73), *CLPTM1L* (Fold change = - 13. 82), *CYP2B6* (Fold change = -8.73), *EPHX1* (Fold change = -65.28), *ERBB2* (Fold change = -12.96), *ERBB3* (Fold change = -8.73), *ESR1* (Fold change = -14.50), *ESR2* (Fold change = -8.73), *FOS* (Fold change = - 151.63), *GSK3A* (Fold change = -5.36), *IGF1R* (Fold change = -8.73), *MSH2* (Fold change = -8.54), *MYC* (Fold change = -18. 10), *NAT2* (Fold change = -8.73), *PPARD* (Fold change = - 8.73), *RARA* (Fold change = -6.08) and *TP53* (Fold change = -8.73). Complete gene expression analysis is summarised in table 4.2. Cytoscape analysis showed interactive crosstalk between genes and pathways, as seen in Figure 4.8. Interestingly, there was a downregulation of *ABCB1* and *ABCC5* post-CETP knockdown. These genes encode drug efflux pumps involved in MDR, which serves as a major barrier in the successful treatment of breast cancer. Furthermore, there was a significant downregulation of genes encoding the ER and AR in transfected MCF-7 cells and as mentioned, the presence of these receptors fuel breast cancer aggressiveness through interactions with their respective hormones, which also act as precursors for cholesterol synthesis. Additionally, there was a notable reduction in gene expression of the TFs involved in cell proliferation, which are aberrantly expressed in many cancers, this included FOS and MYC. Lastly, there was a significant downregulation of anti-apoptotic *BCL2,* displaying the apoptotic inducing potential of CETP knockdown in ER+ breast cancer. Cytoscape analysis also showed a drastic decrease in genes encoding growth factor receptors and cell cycle related-genes, exhibiting the anti-proliferative effects of CETP knockdown in MCF-7 cells.

Table 4.2: Gene expression changes of genes involved in cancer drug resistance in transfected compared to non-transfected MCF-7 cells.

Table 4.2 summarises the gene expression analysis following RT-qPCR using the cancer drug resistance RT^2 Profiler PCR Array. Results display an overall downregulation of 32 genes involved in cancer drug resistance, with 30 genes downregulated by more than two-folds post-CETP knockdown. TOP1 was the only upregulated gene post- CETP knockdown.

Gene Symbol	Description	Mode of Action	Fold Change (Up- or Down-Regulation; transfected/non-transfected MCF-7 cells)	Log2 Fold Change (Up- or Down-Regulation; transfected/non-transfected MCF-7 cells)
ABCB1	ATP-binding cassette, sub-family B (MDR/TAP), member 1	Drug resistance	-4.14944	-2.05292
ABCC5	ATP-binding cassette, sub-family C (CFTR/MRP), member 5	Drug resistance	-26.1294	-4.7076
AP1S1	Adaptor-related protein complex 1, sigma 1 subunit	Transcription Factors	-2.40772	-1.26767
AR	Androgen receptor	Hormone Receptors	-8.7333	-3.12653
BAX	BCL2-associated X protein	Drug resistance	-1.63102	-0.70577
BCL2	B-cell CLL/lymphoma 2	Drug resistance	-20.6884	-4.37075
BRCA1	Breast cancer 1, early onset	DNA damage and repair	-8.7333	-3.12653
CCND1	Cyclin D1	Cell cycle	-2.19944	-1.13713
CDK2	Cyclin-dependent kinase 2	Cell cycle	-1.01401	-0.02008
CDKN2D	Cyclin-dependent kinase inhibitor 2D (p19, inhibits CDK4)	Cell cycle	-1405.56	-10.4569
CLPTM1L	CLPTM1-like	Drug metabolism	-13.824	-3.78911
CYP2B6	Cytochrome P450, family 2, subfamily B, polypeptide 6	Drug metabolism	-8.7333	-3.12653
EPHX1	Epoxide hydrolase 1, microsomal (xenobiotic)	Drug metabolism	-65.2763	-6.02849
ERBB2	V-erb-b2 erythroblastic leukemia viral oncogene homolog 2, neuro/glioblastoma derived oncogene homolog (avian)	Growth Factor Receptors	-12.9609	-3.69609
ERBB3	V-erb-b2 erythroblastic leukemia viral oncogene homolog 3 (avian)	Growth Factor Receptors	-8.7333	-3.12653
ESR1	Estrogen receptor 1	Hormone Receptors	-14.5039	-3.85837
ESR2	Estrogen receptor 2 (ER beta)	Hormone Receptors	-8.7333	-3.12653
FGF2	Fibroblast growth factor 2 (basic)	Growth Factor Receptors	-2.91423	-1.54312
FOS	FBJ murine osteosarcoma viral oncogene homolog	Transcription Factors	-151.627	-7.24438
GSK3A	Glycogen synthase kinase 3 alpha	Drug metabolism	-5.36321	-2.4231
HIF1A	Hypoxia inducible factor 1, alpha subunit (basic helix-loop-helix transcription factor)	Transcription Factors	-2.57949	-1.36709
IGF1R	Insulin-like growth factor 1 receptor	Growth Factor Receptors	-8.7333	-3.12653

MSH2	MutS homolog 2, colon cancer, nonpolyposis type 1 (E. coli)	DNA damage and repair	-8.53527	-3.09344
MYC	V-myc myelocytomatosis viral oncogene homolog (avian)	Transcription Factors	-18.1028	-4.17814
NAT2	N-acetyltransferase 2 (arylamine N-acetyltransferase)	Drug metabolism	-8.7333	-3.12653
PPARD	Peroxisome proliferator-activated receptor delta	Hormone Receptors	-8.7333	-3.12653
PPARG	Peroxisome proliferator-activated receptor gamma	Hormone Receptors	-2.31272	-1.20959
RARA	Retinoic acid receptor, alpha	Hormone Receptors	-6.08013	-2.6041
RB1	Retinoblastoma 1	Drug resistance	-3.00881	-1.58919
SOD1	Superoxide dismutase 1, soluble	Drug metabolism	-2.25108	-1.17062
TOP1	Topoisomerase (DNA) I	Drug resistance	1.344652	0.427233
TP53	Tumor protein p53	Drug resistance	-8.7333	-3.12653
UGCG	UDP-glucose ceramide glucosyltransferase	Drug metabolism	-3.18955	-1.67335

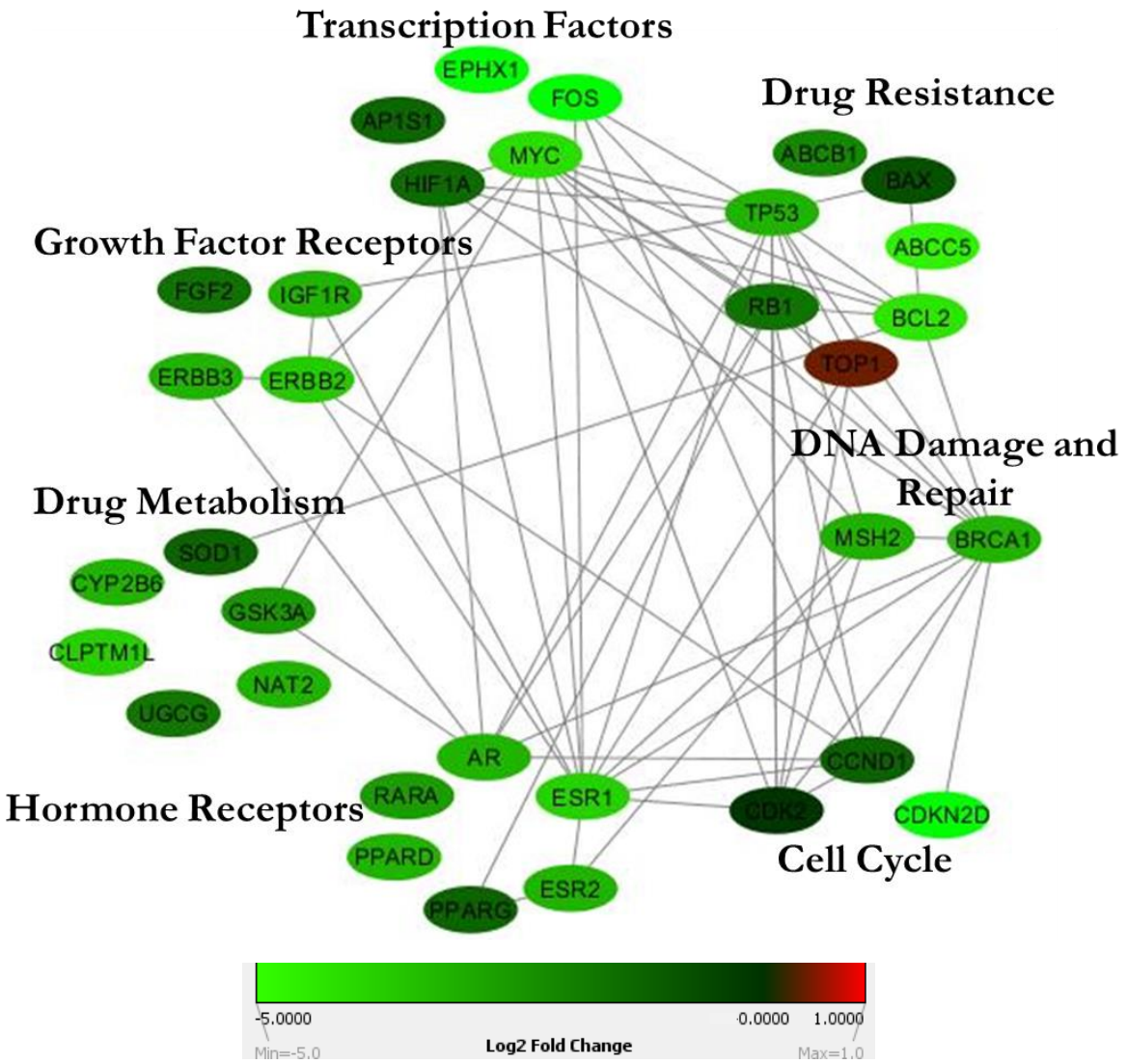


Figure 4.8: Network map of genes involved in cancer drug resistance in response to CETP knockdown.

A network map of genes involved in cancer drug resistance post-CETP knockdown was created using Cytoscape. Nodes (genes) were coloured according to Log_2 fold change (transfected/non-transfected MCF-7 cells) and potential gene interactions (links; coloured in grey) were generated using OmicsNet and visualised in Cytoscape. Genes were grouped according to their pathway they act in. Figure 4.8 displays several intra-pathway and inter-pathway interactions. All pathways were downregulated post-CETP knockdown, except for TOP1 in the drug resistance pathway.

5. Discussion

Targeting cholesterol as a potential therapeutic strategy to treat cancer is a relatively novel and promising field of study. This is particularly true for hormone receptor positive breast cancers that display an accumulated amount of cholesterol, which has been correlated to an increase in steroid hormone production (Esau et al., 2016; Sagar et al., 2014). Studies conducted by Sagar et al. (2014) and Esau et al. (2016) linked breast cancer occurrence and cholesterol accumulation in breast cancer cells, to a key cholesterogenic protein, CETP. Furthermore, CETP knockdown and treatment with cholesterol-depleting agents, such as AP, significantly increased cell death in MCF-7 (Esau et al., 2016). In addition, AP was found to decrease CETP mRNA expression (Esau et al., 2016), highlighting the effect CETP has on cholesterol homeostasis, but more importantly in the progression and aggressiveness of breast cancer. Furthermore, studies carried out by Gu (Master's dissertation, 2018) showed that CETP knockdown increased cell death and the apoptotic potential with reduced drug concentration (especially TAM) in cancer cells in the presence of AP, highlighting CETP's role as a drug resistance marker. Therefore, the present study sought to investigate the effect of CETP knockdown on cholesterol levels and expression of genes involved in lipoprotein signalling and cancer drug resistance, in MCF-7 breast cancer cells, thereby elucidating the molecular mechanisms underlying CETP's involvement in cancer, particularly, ER+ breast cancer.

5.1. CETP knockdown reduces MCF-7 cell viability and decreases cholesterol and CE content

CETP serves as cell survival gene in ER+ breast cancer aiding in cell proliferation and cholesterol uptake (Esau et al., 2016). Studies executed by Esau et al (2016) and Gu (Master's dissertation, 2018) displayed an increased growth inhibition in transfected MCF-7 cells, conjointly an increased apoptotic potential of approximately 30% compared to non-transfected cells (Esau et al., 2016; Gu, Master's dissertation, 2018). These results correlate with the cell viability count, where there was a 68.2% reduction in cell viability in transfected as compared to the non-transfected MCF-7 cells (Figure 4.6), highlighting the role of CETP in cancer cell survival.

As previously mentioned, breast cancer aggressiveness and drug resistance are fuelled by high levels of CE content (Esau et al., 2016; Peck and Schulze, 2014; Yue et al., 2014). In addition, due to their proliferative capacity, it is postulated that cancer cells maintain a high level of

cholesterol in order to rapidly synthesise cell membranes for their growth and division (Cruz et al., 2013; Tosi and Tugnoli, 2005). In the present study, filipin staining and the cholesterol assay revealed a 76.8% and 54% reduction in free cholesterol and CEs, respectively post-CETP knockdown (Figure 4.4, Figure 4.5). This result coincides with previous work conducted by Gu (2018), where a 70% - 90% reduction in CEs was observed in transfected MCF-7 cells treated with various cholesterol – depleting agents such as AP. Additionally, transfected cells treated with AP revealed a further reduction in CEs (Figure 4.5). AP, a cholesterol-depletory agent, is derived from PL and has been found to be less cytotoxic to normal cells while still highly effective in cancer cells (Sagar et al., 2014). Moreover, a 35% reduction in CETP mRNA expression was observed in breast cancer cells treated with AP(Esau et al., 2016), where AP was able to significantly increase the thermal stability of CETP, shown by a cellular thermal shift assay (Esau et al., 2016). These results collectively suggest a potential CETP-AP interaction.

Cholesterol homeostasis is a complex process, tightly regulated by various proteins and gene regulatory elements. However, this process is aberrant in many cancers, such as ER+ breast cancer where lipid metabolism is altered. The intracellular accumulation of CEs is potentially maintained by SREBP1, the key TF involved in *de novo* biosynthesis of cholesterol and ACAT, the enzyme that converts free cholesterol to CEs (Peck and Shulze, 2014).

SREBP1 binds to a specific sequence in the target gene promoter known as a sterol regulatory element (SRE), where it aids in transcribing the gene (Eberle et al., 2004; Shimano, 2001). SREBP1 target genes, that contain SREs, include *LDLR, HMG coA synthase, HMG coA reductase and farnesyl diphoshate synthase* all of which are involved in cholesterol synthesis (Shimano, 2001). Studies have emerged revealing that *CETP* contains a tandem repeat region known as the cholesterol response element (CRE) that is homologous to the SREs seen in SREBP1 target genes (Gauthier et al., 1999), providing a direct link between SREBP1 and CETP. Furthermore, the study conducted by Gauthier et al. (1999) revealed that SREBP1 through its interaction with the CRE, is involved in upregulation of CETP, in cholesterol-rich conditions (Gauthier et al., 1999). Under these conditions, upregulation of CETP may facilitate the transport of CEs from its site of synthesis to storage droplets. Therefore, cancer cells display an accumulated level of CEs maintained by CETP and a high cholesterol level maintained by SREBP1, since most of the free cholesterol is converted to CEs (by ACAT) and transported to storage droplets (by CETP). An increased activity of SREBP1 has been associated with several cancers and SREBP1 inhibition was shown to halt cancer cell growth and proliferation (Peck

and Schulze, 2014). Therefore, the decrease in cholesterol/CE levels that is observed in transfected MCF-7 cells could possibly suggest a reduced SREBP1 activity, as a result of CETP knockdown.

In addition, the accumulation of intracellular CEs results in an escalated PI3K-dependent SREBP1 activity, thus fuelling cancer aggressiveness (Peck and Schulze, 2014; Yue et al., 2014). It is therefore speculated that the surge in cancer cell growth inhibition and apoptosis in transfected MCF-7 cells, even when cells are treated with low concentrations of drugs, such as TAM and AP (Gu, Master's dissertation, 2018) could be due to a reduction in CEs, managing cancer aggressiveness and increasing response to cytotoxic agents or drugs.

Furthermore, high levels of intracellular CEs are associated with drug resistance (Peck and Schulze, 2014). Considering in normal cells, excess cholesterol stops SREBP1 and ACAT activity. However, in cancer cells, ACAT and SREBP1 are continuously producing CEs for storage, thus reducing intracellular toxicity of cytotoxic compounds (Peck and Schulze, 2014). Additionally, it was found that P-gp activity (involved in MDR) is directly correlated to cholesterol levels and a decrease in cholesterol content resulted in a reduced P-gp activity thus reducing drug resistance (Reungpatthanaphong et al., 2004). For these reasons, the growth inhibition, decreased cell viability and increased cell death in transfected MCF-7 cells (Esau et al., 2016; Gu, Master's dissertation 2018) that is observed could have been due to the reduction in intracellular CE levels and could possibly signify a decrease in drug resistance. However, alternative pathways activating other cholesterogenic proteins and enzymes may also be involved in intracellular cholesterol accumulation and drug resistance (Cruz et al., 2013), since cancer is a heterogenous disease.

5.2. Altered lipogenic expression profile in MCF-7 post-CETP knockdown

The lipogenic phenotype is one of the key characteristics of cancer cells (Silvente-Poirot and Poirot, 2014). Increasing evidence has shown that *de novo* biosynthesis of lipids, including cholesterol, is among many metabolic alterations or hallmarks of cancer (Guo et al., 2014), but has not been well-characterised. The potential of cancer cells to engage in independent lipid synthesis is a crucial route by which they escape host regulation (Maughan et al., 2010). An abundant supply of lipids is needed for rapid cancer cell proliferation (Cruz et al., 2013). Cholesterol and phospholipids provide structural integrity to cell membranes, while cholesterol and other lipid molecules serve as precursors to synthesise steroid hormones and second

messengers that regulate various signal transduction pathways (Silvente-Poirot and Poirot, 2014; Gibitova and Astsaturov, 2014). Additionally, FAs and TGs also act as energy substrates (Guo et al., 2014). Therefore, cholesterol and lipid accumulation in breast cancer cells is considered to promote cancer development and aggressiveness by not only aiding cell proliferation but also supporting cancer cell survival.

Since the molecular mechanisms underlying CETP's involvement in cancer particularly ER+ breast cancer is unknown, the following study through gene expression profiles provided a comprehensive understanding of various gene changes and interactions post-CETP knockdown. Considering the large cohort of genes in each array, only the relevant genes and pathways central to this study will be discussed. As mentioned, cholesterol biosynthesis takes place via the mevalonate pathway. Several key genes play a role in the synthesis of cholesterol, acting at various stages; Acetyl-CoA, produced during glycolysis, acts as the precursor in which two molecules are condensed to yield acetoacetyl-CoA (Buhaescu and Izzedine, 2007). This step is carried out by the enzyme HMG-CoA synthase. Subsequently, a second condensation step takes place, to form HMG-CoA and reduction of HMG-CoA (by HMG-CoA reductase) then produces mevalonate, which through a series of enzymatic steps is converted to cholesterol (Buhaescu and Izzedine, 2007). Interestingly, the genes encoding HMG-CoA synthase (encoded by *HMGCS1*) and HMG-CoA reductase (encoded by *HMGCR*) were both downregulated by -3.87- and -3.89-fold changes post-CETP knockdown. This directly suggests a reduction in cholesterol synthesis as a result of knocking down CETP. More importantly, CETP knockdown does not result in complete inhibition of HMG-CoA reductase, comparatively as statins act (Warita et al., 2014). HMG-CoA reductase performs the critical rate-limiting step in the mevalonate pathway, synthesising cholesterol for the needs of the cell. Statins block the synthesis of cholesterol and this causes a myriad of side-effects (Stroes et al., 2015). As mentioned, cholesterol is crucial for normal cellular functions, thus reducing excess cholesterol in cancer cells instead of completely blocking its synthesis is a more feasible option in treating cholesterol-rich cancers, such as ER+ breast cancer. For this reason, CETP knockdown presents a potentially more effective anti-cancer treatment than statins. This will not only reduce synthesis of cholesterol but will also limit the accumulation of CEs in the cancer cells. Furthermore, several other genes involved in cholesterol biosynthesis, such as mevalonate (diphospho) decarboxylase (encoded by *MVD* this enzyme catalyses the conversion of mevalonate pyrophosphate into isopentenyl pyrophosphate in one of the early steps in cholesterol, synthesis), NAD(P) dependent steroid dehydrogenase-like (encoded by

NSDHL is an enzyme that converts lanosterol to cholesterol*)*, mevalonate kinase (encoded by *MVK* is an enzyme that converts mevalonic acid to mevalonate 5-phosphate), etc are drastically downregulated (table 4.1), displaying the overall decrease in cholesterol synthesis genes post-CETP knockdown.

As mentioned SREBP1 is a master regulator of cholesterol synthesis, where its expression is regulated by endogenous sterol content in the cell via a negative feedback mechanism (Guo et al., 2014). When cholesterol levels decrease, SREBP1 (located in the membrane of the endoplasmic reticulum) is translocated by the SCAP chaperone (bound by INSIG) to the Golgi. In the Golgi, S1P and S2P proteases proteolytically activate SREBP1 and the active N-terminus of this TF then stimulates the transcription of various lipid-associated genes involved in cholesterogenesis (Shimano, 2001). In cancer, this process is deviant, as mentioned. Compellingly, there was a downregulation of genes involved in the above process post-CETP knockdown, including SREBP1 (encoded by *SREBPF1*), insulin- induced gene 1 (encoded by *INSIG1*) and S1P (encoded by *MBTPS1*) with fold changes of -1.57, -2.7 and -10.7, respectively. This data therefore displays that abrogating CETP, results in a reduction in cholesterol synthesis, not only downregulating SREBP1 but upstream genes involved in its regulation.

In addition to its role in connecting oncogenic signalling pathways to *de novo* lipid synthesis, SREBP1 has also been shown to directly participate in cell proliferation and cell cycle pathways (Wen et al., 2018). Therefore, it is unsurprising that SREBP1 is highly activated or upregulated in many cancers (Wen et al., 2018). Since, lipogenesis is crucial for the formation of new cellular membranes, it is not particularly surprising that cancer cells develop redundant molecular mechanisms to maintain SREBP1 stability and expression, to guarantee the ability to acquire abundant lipids for their rapid proliferation and growth (Cruz et al., 2013; Wen et al., 2018). The critical link between SREBP1 and cancer is the PI3K/Akt pathway (Guo et al., 2014). Besides being regulated by endogenous sterol content, SREBP1 is also activated and stabilised by this oncogenic signalling pathway (Guo et al., 2014). Firstly, activated Akt can stabilise the nuclear form of SREBP1 and sequentially promote its target gene expression by down-regulating an E3 ubiquitin enzyme that regulates SREBP1 N-terminus degradation (Guo et al., 2014). Secondly, PI3K/Akt signalling via the mammalian target of rapamycin complex 1 (mTORC1) regulates a phosphatidic acid phosphatase that controls SREBP1 transcriptional activity and nuclear localisation (Guo et al., 2014; Wen et al., 2018). However, SREBP1 regulation by the PI3K/Akt pathway appears to be much more complex in cancer cells;

mTORC1 in addition to other upstream oncogenic molecules, such as PI3K, Akt and EGFR notably regulate SREBP1 levels in the nucleus (Guo et al., 2014). Recent studies show that high SREBP1 expression is directly implicated with tumour metastasis and predicts poor prognosis in breast cancer patients (Wen et al., 2018). Furthermore, SREBP1 activation as a result of mTORC1 is shown to induce breast cancer cell proliferation and growth (Wen et al., 2018).

Furthermore, very little is known about how cancer cells sustain increased cholesterol levels. Both *de novo* synthesis and exogenous uptake of cholesterol contribute to cholesterol pools, however, the preferred route in cancer cells is unknown (Guo et al., 2014; Wen et al., 2018). Previous studies have shown that glioblastoma cells, prefer to take up exogenous LDL cholesterol in culture media while *de novo* cholesterol synthesis is used as a compensatory mechanism when exogenous cholesterol is scarce (Guo et al., 2014). More recently, an intriguing study revealed that anaplastic large cell lymphoma cell lines and primary tumours are solely dependent on the cholesterol uptake from the external environment. This is because these cancer cells lack squalene monooxygenase causing cholesterol auxotrophy (Garcia-Bermudez et al., 2019). In contrast, some cancer cells may also rely more on intracellular cholesterol synthesis rather than cholesterol uptake, such as in the highly aggressive prostate cancer (Stopsack et al., 2017). LDLR, is a prominent receptor involved in cholesterol uptake. When intracellular cholesterol levels are low, LDL, containing cholesterol, binds to LDLR, where the complex is internalised. Free cholesterol is then released into the cells, increasing intracellular cholesterol levels (Gahegher et al., 2017). Intriguingly, the gene expression of LDLR (encoded by *LDLR*) was downregulated by -3.96 post-CETP knockdown. Therefore, less LDL molecules can bind and be internalised by the cell, reducing intracellular cholesterol content. This result illustrates the significance of CETP knockdown, as it not only reduces intracellular cholesterol levels directly but acts on several genes and proteins that aid in endogenous cholesterol synthesis, as well as uptake of cholesterol from the external environment. This way, overall cholesterol levels are reduced both intra- and extra-cellularly. Therefore, displaying the important role of CETP in cholesterol homeostasis in cancer cells.

Moreover, the study by Guo et al. (2014) also showed that the EGFR-linked PI3K/Akt pathway drives cholesterol uptake through upregulation of LDLR. It was further elucidated that SREBP1 is a key mediator in the EGFR/PI3K/Akt oncogenic signalling pathway, while also being regulated by molecules involved in these pathways (Guo et al., 2014). Another study showed that hepatocytes of SREBP1 transgenic mice overproduced LDLs, but these molecules

were rapidly taken up via LDLRs, increasing endogenous cellular cholesterol content (Shimano, 2001). The high levels of SREBP1 thus support the continued expression of LDLR, allowing the constant uptake of cholesterol, even in cells whose cholesterol concentration is elevated (Dos Santos et al., 2014; Shimano, 2001). Additionally, in LDLR-deficient mice containing an SREBP1 transgene, TG and plasma cholesterol levels increased by approximately ten-fold (Shimano, 2001). Collectively, this data reveals that SREBP1 activation relies on LDLR expression, displaying the pathway and gene/protein-crosstalk and interaction in cholesterol homeostasis (Shimano, 2001; Gallhegher et al., 2017). However, as mentioned, alternative pathways activating other cholesterogenic proteins and enzymes may also be involved in intracellular cholesterol accumulation in these cancer cells (Cruz et al., 2013).

5.3. CETP knockdown reduces cancer drug resistance in MCF-7 cells

Although many types of cancers originally respond to available chemotherapies, over time they develop resistance (acquired resistance) through various mechanisms, such as increased drug efflux, drug inactivation, alterations to drug targets, DNA damage and repair and evasion of apoptosis (Mansoori et al., 2017; Longley and Johnston, 2005). Alternatively, cancer may be intrinsically resistant to chemotherapies (Mansoori et al., 2017). Drug resistance presents a major barrier in the effective treatment of cancer. Acquired resistance, in particular, is a major problem since cancers become resistant to drugs which was initially used to treat them. Moreover, the process of developing the drug and its placement in the market, takes 10 – 20 years (Esau et al., 2016), highlighting the need to combat drug resistance in cancer. Resistance to chemotherapy is believed to cause treatment failure in 90% of patients suffering with metastatic cancer (Longely and Johnston, 2005). As mentioned, due to the large cohort of genes in the arrays, only relevant genes and pathways will be discussed.

Notably, over 80% of breast cancers express ER alpha upon primary diagnosis (Simigdala et al., 2016). ER acts as a TF controlling proliferation and cell survival by binding and activating EREs (estrogen response elements) on target genes that control proliferation and survival (Housman et al., 2014). Currently, endocrine therapies are being administered to treat ER+ breast cancer. Available therapies include aromatase inhibitors that block the conversion of androgens to estrogen (Esau et al, 2016) and TAM that antagonistically binds to the ER, inhibiting estrogen from binding and recruiting nuclear corepressors (Maughan et al., 2010).

Despite the efficacy of endocrine targeted therapies, many patients relapse and develop acquired resistance or early in their treatment display intrinsic resistance (Rings and Dowsett, 2004). ER signalling has a complex interaction with other growth signalling pathways in breast cancer cells, thus enabling drug resistance through various mechanisms. For example, in cancers with active growth factor receptor signalling, for example HER2 amplification, TAM may lose its estrogen antagonist activity and acquire more agonist-like activity, resulting in cancer growth stimulation (Housman et al., 2014). Additionally, expression of EGFR and HER2, which are barely detected in ER+ breast cancers, was found to increase slightly with TAM and markedly increase when the cancer becomes resistant (Housman et al., 2014). Other studies suggest pathway cross-talk between the ER and growth factor receptors, such as HER2 (encoded by *ERBB2*) and the insulin-like growth factor-1 receptor (encoded by *IGF1R*), which may lead to ligand-independent activation of the ER or can change the phosphorylation state of the nuclear co-activators and alter the balance of ER TFs, thus enhancing transcription (Housman et al., 2014). Since cholesterol is a precursor molecule for the hormone estrogen, cholesterol can also be indirectly linked to cell proliferation and drug resistance pathways. Fascinatingly, CETP knockdown resulted in a downregulation of *ESR1, IGF1R* and *ERBB2*, with fold changes of -14.5, -8.73 and -12.96, respectively. CETP knockdown thus results in a decrease in the expression of the *ER*, stunting proliferative signals. Furthermore, the downregulation of *IGF1R* and *HER2/ERBB2* post-CETP knockdown potentiates a possible halt in drug resistance in ER+ breast cancer, since these receptors also play a role in drug resistance. Thus, data obtained by Gu (Master's dissertation, 2018), displaying an increased efficacy of TAM in MCF-7 cells, even at low concentrations could be due to the downregulation of genes encoding the ER, IGF1R and HER2 when CETP is abrogated. Additionally, CETP knockdown results in a reduction in CE content, which has also been linked to cancer drug resistance and breast cancer aggressiveness. Furthermore, there was a downregulation of the androgen receptor gene (*AR*) displaying a fold change downregulation of -8.73. Since the biological activity of androgens is mediated by androgen receptors and CETP knockdown results in a decrease in the expression of *AR*, the level of androgens is reduced. As mentioned, the conversion of androgens to estrogen is therefore halted, reducing the progression of ER+ breast cancer.

Several cell membrane transporter proteins have been linked to resistance to commonly used chemotherapeutics by promoting drug efflux. Most notably, the ABC transporter family of transmembrane proteins regulate the flux across the plasma membrane of multiple structurally

and mechanistically unrelated chemotherapeutic agents (Assaraf et al., 2019). The most widely studied ABC, involved in drug efflux is the multi-drug resistance protein 1 (MDR1), also known as P-gp, which is encoded by *ABCB1* (Housman et al., 2014). MDR1 is overexpressed in many tumours (thus causing intrinsic drug resistance) and the expression of MDR1 can be induced by chemotherapy (thus also resulting in the acquired development of MDR) (Holohan et al., 2013). MDR1 overexpression has been associated with chemotherapy failure in many cancers, including kidney, colon and liver, prostate, lung and breast cancers, as well as leukaemias and lymphomas (Mansoori et al., 2017). MDR1 inhibitors such as tariquidar have high potency and specificity; however, results from clinical trials show that tariquidar had limited activity in a small cohort of women with stage III–IV breast carcinoma, whereas a Phase II study in breast cancer found no additional benefit in overall survival, progression-free survival (Holohan et al., 2013). Interestingly, CETP knockdown resulted in a downregulation of *ABCB1*, with a fold change downregulation of -4.15.

Combination therapy, including DNA-damaging agents together with inhibiting DNA damage repair in cancer cells has become a promising treatment for cancer (Assaraf et al., 2019). Moreover, cancers frequently have a dysfunction in at least one DNA damage repair pathway, which can lead to complete dependence on an alternative repair pathway that is functionally redundant in normal cells and therefore can be inhibited to induce cancer-cell-specific death. The mismatch repair (MMR) system is crucial for maintaining genomic integrity, and mutations in MMR genes such as MutS Homolog 2 (MSH2) can lead to the microsatellite instability phenotype (Holohan et al., 2013). Moreover, MMR upregulation has been linked to the resistance to various cytotoxic chemotherapies, for example MSH2-defiencent mice displayed a better response to the drug methotrexate, which targets the MMR system in cancer cells (Holohan et al., 2013). CETP knockdown resulted in a downregulation of *MSH2* (-8.53fold change downregulation), together with a downregulation of *BRCA1* post-CETP knockdown, displaying the DNA damaging effects on MCF-7 cancer cells.

Evasion or deregulation of apoptosis in cancer cells presents a major barrier in drug resistance. The role of BCL-2 family members in regulating responses to chemotherapy has been extensively studied. Studies showed that the overexpression of BCL-2 renders leukaemic cells and mouse thymocytes resistant to cytotoxic chemotherapeutic agents (Holohan et al., 2013). This suggests that despite diverse mechanisms of action, cytotoxic drugs all signal to a common pathway of cell death. This pathway involves mitochondrial outer membrane permeabilization (MOMP) and can be blocked by BCL-2 (Holohan et al., 2013). Various other BCL-2 family

proteins have since been demonstrated to have roles in regulating chemotherapy-induced apoptosis. These include the anti-apoptotic BCL-2 and pro-apoptotic family members BAX, BAD and BAK, as well as various BH3-only proteins that can antagonize the anti-apoptotic BCL-2 family members (Housman et al., 2014; Assaraf et al., 2019). It is the interplay between members of this family that is critical in determining the fate of the cell by either inhibiting or facilitating MOMP induction. Studies conducted by Gu (Matster's dissertation, 2018) showed a 30% increase in apoptosis in transfected MCF-7 cells, while the study conducted by Esau et al. (2016) showed an increase in mitochondrial mediated apoptosis, shown by an increase in caspase 3/7 activity. The downregulation of *BCL2*, with a drastic fold change of -20.69, not only supports the data of Esau et al (2016) and Gu (2018), but displays the pro-apoptotic potential of CETP when knocked down, since BCL2 is anti-apoptotic. This again illustrates CETP's role in targeting not only cholesterol pathways but pathways, such as apoptosis is dually overcoming breast cancer aggressiveness and cancer drug resistance.

p53 is known to play a major role in anti-cancer pathways, such as apoptosis. However, p53 is mutated and overexpressed in 50% of cancers and when mutation of this gene renders it non-functional, cancer progression and drug resistance can follow (Perri et al., 2016). Therefore, it can be noted that the downregulation of tumour-suppressor p53 (encoded by *TP53*) post-CETP knockdown (fold change downregulation of – 8.73), in MCF-7 cells can be seen as beneficial in combatting the high proliferative capacity of this disease.

Dysregulation of the regulatory network that controls cell cycle progression is a hallmark of cancer (Hanahan and Weinberg, 2011). A major point of dysregulation is the gateway of cell cycle entry, controlled by the retinoblastoma (Rb) protein. Rb causes cell cycle arrest by binding and supressing E2F TFs, inhibiting the progression of G1 into S-phase (Portman et al., 2019). However, phosphorylation of Rb, by cyclin-dependent kinase 4/6 (CDK 4/6) releases E2F TFs, committing the cell to G1 exit. Subsequently, a cascade of events take place, promoting the activity of CDK2 complexes, leading into progression in S-phase and DNA replication. Ultimately, cell proliferation occurs (Portman et al., 2019). Furthermore, CDK 4/6 become active when they form heterodimers with D-type cyclins (Portman et al., 2019). Intriguingly, overexpression of these cyclins and CDKs have been shown to increase the proliferative capacity of several cancers, including breast cancer (Portman et al., 2019). However, CETP knockdown results in a downregulation of *CCND1* (fold change downregulation of – 2.20) and *CDK2* (fold change downregulation of – 1.01). For this reason, CETP abrogation disturbs both the upstream (targeting cyclin-D1) and downstream (targeting

CDK2) processes of cell cycle progression, displaying CETP's pro-survival effect in ER+ breast cancer. Furthermore, the downregulation of Rb (encoded by *RB1*) post-CETP knockdown coincides with the above result. Regulation of CDK 4/6 activity is key to deactivation of Rb; an example of CDK 4/6 inhibitor is cyclin-dependent kinase inhibitor-2D (CDKN2D) or p19 (encoded by *CDKN2D*). p19 selectively inhibits CDK 4/6 to induce cell cycle arrest senescence (Portman et al., 2019). Dysregulation of cyclin-CDK-Rb axis is characteristic of many cancers. Therefore, upregulation of these inhibitors may be beneficial in targeting cancer. However, some studies show that overexpression of p19 enhances DNA repair and cell viability (Felisiak-Golabek, 2013). In cell lines deprived of p19, DNA damage was impaired, and apoptosis was increased (Felisiak-Golabek, 2013). In a previous study, p19-deficient mice did not develop cancer and apoptosis was enhanced (Felisiak-Golabek, 2013). Therefore, a downregulation of p19 may decrease the efficiency of DNA repair processes, which may result in a higher level of DNA damage and the activation of apoptosis. Furthermore, studies show that p19 enhances cell survival and viability after UV treatment and silencing p19 enhances the sensitivity of cancer cells to genotoxic agents (Felisiak-Golabek, 2013). Thus, CETP knockdown resulted in a drastic decrease in *CDKN2D* expression (fold change = - 1405. 56), displaying the apoptotic and DNA damage potential of abrogating CETP in cancer. Furthermore, CETP knockdown resulted in a decrease in cell viability and this could have been due to the downregulation of p19. Moreover, a complex interplay between cell cycle and apoptosis exists, where CETP abrogation targets both processes in an effort to decrease cell viability in ER+ breast cancer.

6. Concluding remarks and future perspectives

CETP knockdown in combination with a cholesterol-depleting agent – AP, drastically reduces intracellular cholesterol content in cancer cells, which ultimately results in changes in expression of genes involved in lipoprotein signalling and cancer drug resistance. Abrogating CETP results in a downregulation of endogenous cholesterol synthesis genes, as well as genes involved in uptake of cholesterol from the extracellular environment. Drug resistance mechanisms, such as genes involved in DNA damage and repair, and evasion of apoptosis is drastically downregulated, displaying CETP's role as a cell survival and drug resistance marker. Furthermore, the downregulation of *ESR1* and *ESR2* potentiates CETP's role in limiting ER-presence, since it the abundance of this receptor that promotes ER+ breast cancer

progression. Moreover, CETP knockdown results in a downregulation of genes involved in cell cycle progression, illustrating the anti-proliferative effect of CETP abrogation.

It will be compelling to observe protein expression of the aforementioned genes, either through Western blotting or protein arrays to functionalise the role of CETP in ER+ breast cancer, since gene expression might not always coincide with protein expression. Furthermore, it will be interesting to observe the effect of overexpression of CETP on gene and protein expression *in vitro* and *in vivo.*

7. Successes and limitations of the study

The study validated every result, for example CETP knockdown was confirmed by RT-qPCR, Western blotting and immunofluorescent staining. Additionally, cholesterol levels were measured using filipin staining as well as the cholesterol assay. Since, the RT^2 Profiler PCR Arrays were expensive, gene expression could only be performed once in transfected and non-transfected MCF-7 cells. Repeating the gene expression studies would have given much more confidence in the results. Moreover, gene expression does not necessarily coincide with protein expression, therefore it is not easy to functionalise with absolute certainty that CETP knockdown produces the above results. However, future studies will include measuring protein expression post-CETP knockdown. Furthermore, this study included *in vitro* studies, and this does not necessarily reflect what is taking place *in vivo*, since cancer is such a heterogenous disease. However, this study does pave the way in understanding the molecular basis of CETP abrogation in ER+ breast cancer. Further studies, including overexpression of CETP, protein expression analysis (post-CETP knockdown or when CETP is overexpressed) and *in vivo* validation will give a more holistic view in elucidating the molecular mechanisms of CETP's involvement in breast cancer.

8. Troubleshooting

siRNA transfection

Western blotting analysis revealed problems in the transfection process. Firstly, the protein bands, including β-tubulin which normally is detected as thick dark bands, were faint. Conclusively, it was found that not enough cells were being seeded and therefore protein levels were reduced, resulting in the faint bands. The number of cells were then increased from 50,000 to 300,000 cells. This prompted transfection reagent to be increased in the reaction mixture in accordance to the manufacturer's protocol. However, the transfection reagent, especially polymer-based transfection reagents, become toxic to the cells and as a result no bands were observed on the Western blots. Reducing the volume of transfection reagent from 6 µl to 3 µl and increasing the number of cells, produced much higher quality and workable Western blots.

qPCR

Melt curve analysis for the first qPCR reaction showed non-specific amplification and/or the presence of primer-dimers. Additionally, CETP mRNA was detected at very late cycles, indicative of the high Ct values. This was expected since CETP is expressed at vey low levels in the cell. However, increasing the denaturation time from 5 to 6 seconds and the extension step from 15 to 20 seconds, as well as increasing the cell cycle number from 40 to 45 cycles, eliminated all the above problems and produced more accurate and reliable Ct values. RNA quality (purity and integrity) was only examined in the present study, due to limited sample amounts. However, future works should include quality checks for PCR products (from the cDNA synthesis step, as well as after the qPCR process, from both target gene (CETP) and refence gene (GAPDH)). Furthermore, variability between replicates was observed in the first qPCR reaction. However, this was eliminated by thoroughly pipetting each qPCR reaction mixture (at least 30 times) thereafter.

BCA assay

The BCA assay detected low protein levels, even when cell number was increased to 300,000 cells. It was then discovered that the lysis procedure was ineffective in the disruption of the cell membranes and thus cellular contents, including protein was not released by the cells or only some cells were subjected to lysis. The lysis procedure was then optimised by firstly

mixing the lysis buffer and cell pellets thoroughly, followed by brief vortexing every 5 minutes for a 20 minutes period. Tubes were kept on ice during the entire lysis procedure, since lysis buffer works more efficiently at -4°C. Previously, cell lysis was carried as follows: cold lysis buffer was added to cell pellets and mixed a few times at room temperature, before being used in downstream experiments.

Western blotting

The principal issue in Western blotting for the present study was during transfer of the proteins to the PVDF membrane. Non-definitive bands or blots with no bands were observed initially. It was only later discovered that membranes and gels were too dry or air bubbles were present during transfer, resulting in the above problems. These issues were ceased by placing more transfer buffer on both the membrane and gel (to prevent drying out) and gently rolling any air bubbles out using a roller. This allowed efficient transfer of protein from the gel to the membrane. In addition, background noise was eliminated by increasing washes and wash times between antibody changes or when different proteins were detected on the same blot.

Cholesterol Assay

Standardisation of the cholesterol assay was done by testing different volumes of various components in the assay for optimal results. These included; Ampliflu red (Sigma Aldrich, UK), cholesterol esterase and cholesterol oxidase. In addition, the assay was performed with and without catalase and it was found that with catalase, the background noise was reduced.

Filipin staining

Filipin staining is still in the process of being standardised. However, since filipin is a fluorescent dye, every step was performed in the dark to prevent photobleaching. Plates were wrapped in foil and only taken out when needed. Furthermore, increased incubation time with the filipin stain from 30 minutes to an hour and concentration was increased. Additionally, washes were increased to prevent background noise.

9. References

Acconcia, F., Barnes, C. J., and Kumar, R. (2006). Estrogen and TAM induce cytoskeletal remodeling and migration in endometrial cancer cells. *Endocrinology*, *147*(3), 1203-1212.

Ahern, T.P., Lash, T.L., Damkier, P., Christiansen, P.M., and Cronin-Fenton, D.P. (2014). Statins and breast cancer prognosis: evidence and opportunities. *The Lancet Oncology*, *15*, 1-19.

Ampuero, J., and Romero-Gomez, M. (2015). Prevention of hepatocellular carcinoma by correction of metabolic abnormalities: Role of statins and metformin. *World Journal of Hepatology*, *7*, 1105-1111.

Arita, Y., Nishimura, S., Ishitsuka, R., Kishimoto, T., Ikenouchi, J., Ishii, K., Umeda, M., Matsunaga, S., Kobayashi, T., and Yoshida, M. (2015). Targeting cholesterol in a liquid-disordered environment by theonellamides modulates cell membrane order and cell shape. *Chemistry and Biology*, *22*(5), 604-610.

Ahern, T. P., Lash, T. L., Damkier, P., Christiansen, P. M., and Cronin-Fenton, D. P. (2014). Statins and breast cancer prognosis: evidence and opportunities. *The Lancet Oncology*, *15*(10), e461-e468.

Assaraf, Y. G., Brozovic, A., Gonçalves, A. C., Jurkovicova, D., Linē, A., Machuqueiro, M. and Vasconcelos, M. H. (2019). The multi-factorial nature of clinical multidrug resistance in cancer. *Drug Resistance Updates*, *46*, 100645.

Barter, P. J., Caulfield, M., Eriksson, M., Grundy, S. M., Kastelein, J. J., Komajda, M., and Shear, C. L. (2007). Effects of torcetrapib in patients at high risk for coronary events. *New England Journal of Medicine*, *357*(21), 2109-2122.

Bots, M.L., Visseren, F.L., Evans, G.W., Riley, W.A., Revkin, J.H., Tegeler, C.H., Shear, C.L., Duggan, W.T., Vicari, R.M., and Grobbee, D.E. (2007). Torcetrapib and carotid intimamedia thickness in mixed dyslipidaemia (RADIANCE 2 study): a randomised, double-blind trial. *The Lancet*, *370*, 153-160.

Boudreau, D.M., Yu, O., and Johnson, J. (2010). Statin use and cancer risk: a comprehensive review. *Expert Opinion on Drug Safety*, *9*, 603-621.

Boyer, J. L. (2013). Bile formation and secretion. *Comprehensive Physiology*, *3* (5),1035-1078.

Buhaescu, I., and Izzedine, H. (2007). Mevalonate pathway: a review of clinical and therapeutical implications. *Clinical Biochemistry*, *40*(9-10), 575-584.

Campbell, M.J., Esserman, L.J., Zhou, Y., Shoemaker, M., Lobo, M., Borman, E., Baehner, F., Kumar, A.S., Adduci, K., and Marx, C. (2006). Breast cancer growth prevention by statins. *Cancer Research, 66*, 8707-8714.

Cao, G., Beyer, T. P., Yang, X. P., Schmidt, R. J., Zhang, Y., Bensch, W. R., and Eacho, P. I. (2002). Phospholipid transfer protein is regulated by liver X receptors in vivo. *Journal of Biological Chemistry*, *277*(42), 39561-39565.

Chan, K.K., Oza, A.M., and Siu, L.L. (2003). The statins as anticancer agents. *Clinical Cancer Research, 9,* 10-19.

Chang, T. Y., Li, B. L., Chang, C. C., and Urano, Y. (2009). Acyl-coenzyme A: cholesterol acyltransferases. *American Journal of Physiology-Endocrinology and Metabolism*, *297*(1), E1-E9.

Chen, T., Sun, M., Wang, J. Q., Cui, J. J., Liu, Z. H., and Yu, B. (2017). A novel swine model for evaluation of dyslipidemia and atherosclerosis induced by human CETP overexpression. *Lipids in Health and Disease*, *16*(1), 169.

Chirasani, V. R., Sankar, R., and Senapati, S. (2016). Mechanism of inhibition of cholesteryl ester transfer protein by small molecule inhibitors. *The Journal of Physical Chemistry B*, *120*(33), 8254-8263.

Clark, R. W., Sutfin, T. A., Ruggeri, R. B., Willauer, A. T., Sugarman, E. D., Magnus-Aryitey, G., and Perlman, M. E. (2004). Raising high-density lipoprotein in humans through inhibition of cholesteryl ester transfer protein: an initial multidose study of torcetrapib. *Arteriosclerosis, Thrombosis, and Vascular Biology*, *24*(3), 490-497.

Cleator, S., Heller, W., & Coombes, R. C. (2007). Triple-negative breast cancer: therapeutic options. *The Lancet Oncology*, *8*(3), 235-244.

Cronin-Fenton, D. P., Damkier, P., and Lash, T. L. (2014). Metabolism and transport of tamoxifen in relation to its effectiveness: new perspectives on an ongoing controversy. *Future Oncology*, *10*(1), 107-122.

Cruz, P. M., Mo, H., McConathy, W., Sabnis, N. A., and Lacko, A. G. (2013). The role of cholesterol metabolism and cholesterol transport in carcinogenesis: a review of scientific findings, relevant to future cancer therapeutics. *Frontiers in Pharmacology*, *4*, 119.

Dean, M., Hamon, Y., and Chimini, G. (2001). The human ATP-binding cassette (ABC) transporter superfamily. *Journal of Lipid Research*, *42*(7), 1007-1017.

Didichenko, S. A., Navdaev, A., Cukier, A. M., Gille, A., Schuetz, P., Spycher, M. O., Therond, P., Chapman, M.J., Kontush, A., and Wright, S. D. (2016). Enhanced HDL functionality in small HDL species produced upon remodeling of HDL by reconstituted HDL, CSL112: effects on cholesterol efflux, anti-inflammatory and antioxidative activity. *Circulation Research*, CIRCRESAHA-116.

Dos Santos, C. R., Domingues, G., Matias, I., Matos, J., Fonseca, I., de Almeida, J. M., and Dias, S. (2014). LDL-cholesterol signaling induces breast cancer proliferation and invasion. *Lipids in Health and Disease*, *13*(1), 16.

Duncan, R.E., El-Sohemy, A., and Archer, M.C. (2005). Statins and cancer development. *Cancer Epidemiology and Prevention Biomarkers*, *14*, 1897-1898.

Eberle, D., Hegarty, B., Bossard, P., Ferré, P., and Foufelle, F. (2004). SREBP transcription factors: master regulators of lipid homeostasis. *Biochimie*, *86*(11), 839-848.

Esau, L., Sagar, S., Bangarusamy, D., and Kaur, M. (2016). Identification of CETP as a molecular target for estrogen positive breast cancer cell death by cholesterol depleting agents. *Genes and Cancer*, *7*(9-10), 309.

Fazio, S., Major, A. S., Swift, L. L., Gleaves, L. A., Accad, M., Linton, M. F., and Farese, R. V. (2001). Increased atherosclerosis in LDL receptor–null mice lacking ACAT1 in macrophages. *The Journal of Clinical Investigation*, *107*(2), 163-171.

Felisiak-Golabek, A., Dansonka-Mieszkowska, A., Rzepecka, I. K., Szafron, L., Kwiatkowska, E., Konopka, B., and Kupryjanczyk, J. (2013). p19INK4d mRNA and protein expression as new prognostic factors in ovarian cancer patients. *Cancer Biology & Therapy*, *14*(10), 973-981.

Forrest, M. J., Bloomfield, D., Briscoe, R. J., Brown, P. N., Cumiskey, A. M., Ehrhart, J., and Messina, E. (2008). Torcetrapib-induced blood pressure elevation is independent of CETP inhibition and is accompanied by increased circulating levels of aldosterone. *British Journal of Pharmacology*, *154*(7), 1465-1473.

Frank-Kamenetsky, M., Grefhorst, A., Anderson, N. N., Racie, T. S., Bramlage, B., Akinc, A., and Gamba-Vitalo, C. (2008). Therapeutic RNAi targeting PCSK9 acutely lowers plasma cholesterol in rodents and LDL cholesterol in nonhuman primates. *Proceedings of the National Academy of Sciences*, *105*(33), 11915-11920.

Fu, Y., Hoang, A., Escher, G., Parton, R.G., Krozowski, Z., and Sviridov, D. (2004). Expression of caveolin-1 enhances cholesterol efflux in hepatic cells. *Journal of Biological Chemistry, 279*, 14140-14146.

Fujimoto, M., Higuchi, T., Hosomi, K., and Takada, M. (2015). Association between statin use and cancer: data mining of a spontaneous reporting database and a claims database. *International Journal of Medical Sciences, 12*, 223-233.

Gabitova, L., Gorin, A., and Astsaturov, I. (2014). Molecular pathways: sterols and receptor signaling in cancer. *Clinical Cancer Research*, *20*(1), 28-34.

Gallagher, E. J., Zelenko, Z., Neel, B. A., Antoniou, I. M., Rajan, L., Kase, N., and LeRoith, D. (2017). Elevated tumor LDLR expression accelerates LDL cholesterol-mediated breast cancer growth in mouse models of hyperlipidemia. *Oncogene*, *36*(46), 6462-6471.

Garcia-Bermudez, J., Baudrier, L., Bayraktar, E. C., Shen, Y., La, K., Guarecuco, R., and Chan, S. H. (2019). Squalene accumulation in cholesterol auxotrophic lymphomas prevents oxidative cell death. *Nature*, *567*(7746), 118-122.

Goard, C.A., Mather, R.G., Vinepal, B., Clendening, J.W., Martirosyan, A., Boutros, P.C., Sharom, F.J., and Penn, L.Z. (2010). Differential interactions between statins and P-glycoprotein: Implications for exploiting statins as anticancer agents. *International Journal of Cancer, 127*, 2936-2948.

Goldstein, M.R., Mascitelli, L., and Pezzetta, F. (2008). Do statins prevent or promote cancer? *Current Oncology*, *15*, 76-77.

Gui, T., Sun, Y., Shimokado, A., and Muragaki, Y. (2012). The roles of mitogen-activated protein kinase pathways in TGF-β-induced epithelial-mesenchymal transition. *Journal of Signal Transduction, 2012*, 1-10.

Guo, D., Hlavin Bell, E., Mischel, P., and Chakravarti, A. (2014). Targeting SREBP-1-driven lipid metabolism to treat cancer. *Current Pharmaceutical Design*, *20*(15), 2619-2626.

Ho, C.-C., Kuo, S.-H., Huang, P.-H., Huang, H.-Y., Yang, C.-H., and Yang, P.-C. (2008). Caveolin-1 expression is significantly associated with drug resistance and poor prognosis in advanced non-small cell lung cancer patients treated with gemcitabine-based chemotherapy. *Lung Cancer*, *59*, 105-110.

Hodges, L. C., Cook, J. D., Lobenhofer, E. K., Li, L., Bennett, L., Bushel, P.R., Aldaz, C. M., Afshari, C. A. and Walker, C. L. (2003). TAM Functions as a Molecular Agonist Inducing Cell Cycle-Associated Genes in Breast Cancer Cells. *Molecular Cancer Research, 1(4),* 300-311.

Holohan, C., Van Schaeybroeck, S., Longley, D. B., and Johnston, P. G. (2013). Cancer drug resistance: an evolving paradigm. *Nature Reviews Cancer*, *13*(10), 714-726.

Horton, J. D., Goldstein, J. L., and Brown, M. S. (2002). SREBPs: activators of the complete program of cholesterol and fatty acid synthesis in the liver. *The Journal of Clinical Investigation*, *109*(9), 1125-1131.

Housman, G., Byler, S., Heerboth, S., Lapinska, K., Longacre, M., Snyder, N., and Sarkar, S. (2014). Drug resistance in cancer: an overview. *Cancers*, *6*(3), 1769-1792.

Ikonen, E. (2008). Cellular cholesterol trafficking and compartmentalization. *Nature Reviews Molecular Cell Biology*, *9*(2), 125.

Izem, L., and Morton, R. E. (2007). Possible role for intracellular cholesteryl ester transfer protein in adipocyte lipid metabolism and storage. *Journal of Biological Chemistry*, *282*(30), 21856-21865.

Kang, M. H., Zhang, L. H., Wijesekara, N., de Haan, W., Butland, S., Bhattacharjee, A., and Hayden, M. R. (2013). Regulation of ABCA1 protein expression and function in hepatic and pancreatic islet cells by miR-145. *Arteriosclerosis, Thrombosis, and Vascular Biology*, *33*(12), 2724-2732.

Kaur, M. and Esau, L. (2015). Two step-protocol for preparing adherent cells for high-throughput flow cytometry biotechniques. *BioTechniques*, *59(3)*, 119-126.

Kurien, B. T., and Scofield, R. H. (2006). Western blotting. *Methods*, *38*(4), 283-293.

Lagace, T. A. (2014). PCSK9 and LDLR degradation: regulatory mechanisms in circulation and in cells. *Current Opinion in Lipidology*, *25*(5), 387.

Lavie, Y., and Liscovitch, M. (2000). Changes in lipid and protein constituents of rafts and caveolae in multidrug resistant cancer cells and their functional consequences. *Glycoconjugate Journal*, *17*, 253-259.

Li, X., Zhang, S., Blander, G., Jeanette, G. T., Krieger, M., and Guarente, L. (2007). SIRT1 deacetylates and positively regulates the nuclear receptor LXR. *Molecular Cell*, *28*(1), 91-106.

Li, Y. C., Park, M. J., Ye, S. K., Kim, C. W., and Kim, Y. N. (2006). Elevated levels of cholesterol-rich lipid rafts in cancer cells are correlated with apoptosis sensitivity induced by cholesterol-depleting agents. *The American Journal of Pathology*, *168*(4), 1107-1118.

Longley, D. B., and Johnston, P. G. (2005). Molecular mechanisms of drug resistance. *The Journal of Pathology: A Journal of the Pathological Society of Great Britain and Ireland*, *205*(2), 275-292.

Lu, W. J., Desta, Z., and Flockhart, D. A. (2012). Tamoxifen metabolites as active inhibitors of aromatase in the treatment of breast cancer. *Breast Cancer Research and Treatment*, *131*(2), 473-481.

Luchetti, G., Sircar, R., Kong, J. H., Nachtergaele, S., Sagner, A., Byrne, E. F., and Rohatgi, R. (2016). Cholesterol activates the G-protein coupled receptor Smoothened to promote Hedgehog signaling. *Elife*, *5*, 1-22.

Mahammad, S., and Parmryd, I. (2015). Cholesterol depletion using methyl-β-cyclodextrin. In *Methods in Membrane Lipids*. Humana Press, New York, NY. 91-102.

Mandal, C. C., and Rahman, M. M. (2014). Targeting intracellular cholesterol is a novel therapeutic strategy for cancer treatment. *Journal of Cancer Science & Therapy*, *6*(12), 510.

Mansoori, B., Mohammadi, A., Davudian, S., Shirjang, S., and Baradaran, B. (2017). The different mechanisms of cancer drug resistance: a brief review. *Advanced Pharmaceutical Bulletin*, *7*(3), 339.

Marcuzzi, A., De Leo, L., Decorti, G., Crovella, S., Tommasini, A., and Pontillo, A. (2011). The farnesyltransferase inhibitors tipifarnib and lonafarnib inhibit cytokines secretion in a cellular model of mevalonate kinase deficiency. *Pediatric Research*, *70*(1), 78-82.

Martín, M. G., Pfrieger, F., and Dotti, C. G. (2014). Cholesterol in brain disease: sometimes determinant and frequently implicated. *EMBO Reports*, e201439225.

Masson, D., Staels, B., Gautier, T., Desrumaux, C., Athias, A., Le Guern, N., and Tall, A. (2004). Cholesteryl ester transfer protein modulates the effect of liver X receptor agonists on cholesterol transport and excretion in the mouse. *Journal of Lipid Research*, *45*(3), 543-550.

Maughan, K. L., Lutterbie, M. A., and Ham, P. S. (2010). Treatment of breast cancer. *Chemotherapy*, *51*, 53.

Mohammad, N., Malvi, P., Meena, A. S., Singh, S. V., Chaube, B., Vannuruswamy, G., and Bhat, M. K. (2014). Cholesterol depletion by methyl-β-cyclodextrin augments tamoxifen induced cell death by enhancing its uptake in melanoma. *Molecular Cancer*, *13*(1), 204.

Moosmann, B., and Behl, C. (2004). Selenoprotein synthesis and side-effects of statins. *The Lancet*, *363*, 892-894.

Mostaghel, E.A., Solomon, K.R., Pelton, K., Freeman, M.R., and Montgomery, R.B. (2012). Impact of circulating cholesterol levels on growth and intratumoral androgen concentration of prostate tumors. *PloS One, 7*, 1-8.

Mourits, M. J., De Vries, E. G., Willemse, P. H., Ten Hoor, K. A., Hollema, H., and Van der Zee, A. G. (2001). TAM treatment and gynecologic side effects: a review. *Obstetrics and Gynecology*, *97*(5), 855-866.

Nissen, S. E., Tardif, J. C., Nicholls, S. J., Revkin, J. H., Shear, C. L., Duggan, W. T., and Tuzcu, E. M. (2007). Effect of torcetrapib on the progression of coronary atherosclerosis. *New England Journal of Medicine*, *356*(13), 1304-1316.

Nowosielski, M., Hoffmann, M., Wyrwicz, L. S., Stepniak, P., Plewczynski, D. M., Lazniewski, M., and Rychlewski, L. (2011). Detailed mechanism of squalene epoxidase inhibition by terbinafine. *Journal of Chemical Information and Modeling*, *51*(2), 455-462.

Ohashi, R., Mu, H., Wang, X., Yao, Q., and Chen, C. (2005). Reverse cholesterol transport and cholesterol efflux in atherosclerosis. *Qjm*, *98*(12), 845-856.

Peck, B., and Schulze, A. (2014). Cholesteryl esters: fueling the fury of prostate cancer. *Cell Metabolism*, *19*(3), 350-352.

Peng, J., Sengupta, S., and Jordan, V. C. (2009). Potential of selective estrogen receptor modulators as treatments and preventives of breast cancer. *Anti-Cancer Agents in Medicinal Chemistry (Formerly Current Medicinal Chemistry-Anti-Cancer Agents)*, *9*(5), 481-499.

Perri, F., Pisconti, S., and Scarpati, G. D. V. (2016). P53 mutations and cancer: a tight linkage. *Annals of Translational Medicine*, *4*(24).

Portman, N., Alexandrou, S., Carson, E., Wang, S., Lim, E., and Caldon, C. E. (2019). Overcoming CDK4/6 inhibitor resistance in ER-positive breast cancer. *Endocrine-related Cancer*, *26*(1), R15-R30.

Ravnskov, U., Rosch, P.J., and McCully, K.S. (2015). Statins do not protect against cancer: quite the opposite. *Journal of Clinical Oncology*, *33*, 810-811.

Repa, J. J., Liang, G., Ou, J., Bashmakov, Y., Lobaccaro, J. M. A., Shimomura, I., and Mangelsdorf, D. J. (2000). Regulation of mouse sterol regulatory element-binding protein-1c gene (SREBP-1c) by oxysterol receptors, LXRα and LXRβ. *Genes and Development*, *14*(22), 2819-2830.

Repa, J. J., and Mangelsdorf, D. J. (2002). The liver X receptor gene team: potential new players in atherosclerosis. *Nature Medicine*, *8*(11), 1243.

Reungpatthanaphong, P., Marbeuf-Gueye, C., Le Moyec, L., Salerno, M. and Garnier-Suillerot, A. (2004). Decrease of P-glycoprotein activity in K562/ADR cells by MβCD and filipin and lack of effect induced by cholesterol oxidase indicate that this transporter is not located in rafts. *Journal of Bioenergetics and Biomembranes*, *36*(6), 533-543.

Ring, A., and Dowsett, M. (2004). Mechanisms of TAM resistance. *Endocrine-related Cancer*, *11*(4), 643-658.

Sakao, K., Fujii, M., & Hou, D. X. (2009). Acetyl derivate of quercetin increases the sensitivity of human leukemia cells toward apoptosis. *Biofactors*, *35*(4), 399-405.

Rosenson, R.S., Brewer, H.B., Davidson, W.S., Fayad, Z.A., Fuster, V., Goldstein, J., Hellerstein, M., Jiang, X.-C., Phillips, M.C., and Rader, D.J. (2012). Cholesterol efflux and atheroprotection. *Circulation, 125*, 1905-1919.

Sagar, S., Esau, L., Moosa, B., Khashab, N. M., Bajic, V. B., and Kaur, M. (2014). Cytotoxicity and apoptosis induced by a plumbagin derivative in estrogen positive MCF-7 breast cancer cells. *Anti-Cancer Agents in Medicinal Chemistry (Formerly Current Medicinal Chemistry-Anti-Cancer Agents)*, *14*(1), 170-180.

Sandur, S. K., Ichikawa, H., Sethi, G., Ahn, K. S., and Aggarwal, B. B. (2006). Plumbagin (5-hydroxy-2-methyl-1, 4-naphthoquinone) suppresses NF-κB activation and NF-κB-regulated gene products through modulation of p65 and IκBα kinase activation, leading to potentiation of apoptosis induced by cytokine and chemotherapeutic agents. *Journal of Biological Chemistry*, *281*(25), 17023-17033.

Seo, T., Oelkers, P. M., Giattina, M. R., Worgall, T. S., Sturley, S. L., and Deckelbaum, R. J. (2001). Differential modulation of ACAT1 and ACAT2 transcription and activity by long chain free fatty acids in cultured cells. *Biochemistry*, *40*(15), 4756-4762.

Shimano, H. (2001). Sterol regulatory element-binding proteins (SREBPs): transcriptional regulators of lipid synthetic genes. *Progress in Lipid Research*, *40*(6), 439-452.

Shimano, H., Shimomura, I., Hammer, R. E., Herz, J., Goldstein, J. L., Brown, M. S., and Horton, J. D. (1997). Elevated levels of SREBP-2 and cholesterol synthesis in livers of mice homozygous for a targeted disruption of the SREBP-1 gene. *The Journal of Clinical Investigation*, *100*(8), 2115-2124.

Silvente-Poirot, S., and Poirot, M. (2014). Cholesterol and cancer, in the balance. *Science*, *343*(6178), 1445-1446.

Simigdala, N., Gao, Q., Pancholi, S., Roberg-Larsen, H., Zvelebil, M., Ribas, R. and Martin, L. A. (2016). Cholesterol biosynthesis pathway as a novel mechanism of resistance to estrogen deprivation in estrogen receptor-positive breast cancer. *Breast Cancer Research*, *18*(1), 58.

Simões, A. E., Pereira, D. M., Amaral, J. D., Nunes, A. F., Gomes, S. E., Rodrigues, P. M., and Borralho, P. M. (2013). Efficient recovery of proteins from multiple source samples after trizol® or trizol® LS RNA extraction and long-term storage. *BMC Genomics*, *14*(1), 181.

Sinzinger, H., Wolfram, R., and Peskar, B.A. (2002). Muscular side effects of statins. *Journal of Cardiovascular Pharmacology, 40*, 163-171.

Soccio, R. E., and Breslow, J. L. (2004). Intracellular cholesterol transport. *Arteriosclerosis, Thrombosis, and Vascular Biology*, *24*(7), 1150-1160.

Srinivas, P., Gopinath, G., Banerji, A., Dinakar, A., and Srinivas, G. (2004). Plumbagin induces reactive oxygen species, which mediate apoptosis in human cervical cancer cells. *Molecular Carcinogenesis: Published in cooperation with the University of Texas MD Anderson Cancer Center*, *40*(4), 201-211.

Stancu, C., and Sima, A. (2001). Statins: mechanism of action and effects. *Journal of Cellular and Molecular Medicine, 5*, 378-387.

Stopsack, K. H., Gerke, T. A., Andrén, O., Andersson, S. O., Giovannucci, E. L., Mucci, L. A., and Rider, J. R. (2017). Cholesterol uptake and regulation in high-grade and lethal prostate cancers. *Carcinogenesis*, *38*(8), 806-811.

Stroes, E. S., Thompson, P. D., Corsini, A., Vladutiu, G. D., Raal, F. J., Ray, K. K., and Bruckert, E. (2015). Statin-associated muscle symptoms: impact on statin therapy—European Atherosclerosis Society consensus panel statement on assessment, aetiology and management. *European Heart Journal*, *36*(17), 1012-1022.

Tontonoz, P., and Mangelsdorf, D. J. (2003). Liver X receptor signaling pathways in cardiovascular disease. *Molecular Endocrinology*, *17*(6), 985-993.

Tosi, M. R., and Tugnoli, V. (2005). Cholesteryl esters in malignancy. *Clinica Chimica acta*, *359*(1-2), 27-45.

Tsoumpra, M. K., Muniz, J. R., Barnett, B. L., Kwaasi, A. A., Pilka, E. S., Kavanagh, K. L., and Oppermann, U. (2015). The inhibition of human farnesyl pyrophosphate synthase by nitrogen-containing bisphosphonates. Elucidating the role of active site threonine 201 and tyrosine 204 residues using enzyme mutants. *Bone*, *81*, 478-486.

Tsubaki, M., Yamazoe, Y., Yanae, M., Satou, T., Itoh, T., Kaneko, J., Kidera, Y., Moriyama, K., and Nishida, S. (2011). Blockade of the Ras/MEK/ERK and Ras/PI3K/Akt pathways by statins reduces the expression of bFGF, HGF, and TGF-β as angiogenic factors in mouse osteosarcoma. *Cytokine, 54*, 100-107.

Van Wyhe, R.D., Rahal, O.M., and Woodward, W.A. (2017). Effect of statins on breast cancer recurrence and mortality: a review. *Breast Cancer: Targets and Therapy, 9*, 559-565.

Wang, C. C., Chiang, Y. M., Sung, S. C., Hsu, Y. L., Chang, J. K., and Kuo, P. L. (2008). Plumbagin induces cell cycle arrest and apoptosis through reactive oxygen species/c-Jun N-terminal kinase pathways in human melanoma A375. S2 cells. *Cancer Letters*, *259*(1), 82-98.

Warita, K., Warita, T., Beckwitt, C. H., Schurdak, M. E., Vazquez, A., Wells, A., and Oltvai, Z. N. (2014). Statin-induced mevalonate pathway inhibition attenuates the growth of mesenchymal-like cancer cells that lack functional E-cadherin mediated cell cohesion. *Scientific Reports*, *4*, 7593.

Webb, P., Lopez, G. N., Uht, R. M., and Kushner, P. J. (1995). TAM activation of the estrogen receptor/AP-1 pathway: potential origin for the cell-specific estrogen-like effects of antiestrogens. *Molecular Endocrinology*, *9*(4), 443-456.

Yancey, P.G., Bortnick, A.E., Kellner-Weibel, G., De la Llera-Moya, M., Phillips, M.C., and Rothblat, G.H. (2003). Importance of different pathways of cellular cholesterol efflux. *Arteriosclerosis, Thrombosis, and Vascular Biology, 23*, 712-719.

Yue, S., Li, J., Lee, S. Y., Lee, H. J., Shao, T., Song, B., and Cheng, J. X. (2014). Cholesteryl ester accumulation induced by PTEN loss and PI3K/AKT activation underlies human prostate cancer aggressiveness. *Cell Metabolism*, *19*(3), 393-406.

Yvan-Charvet, L., Wang, N., and Tall, A. R. (2010). Role of HDL, ABCA1, and ABCG1 transporters in cholesterol efflux and immune responses. *Arteriosclerosis, Thrombosis, and Vascular Biology*, *30*(2), 139-143.

Zhao, C., and Dahlman-Wright, K. (2010). Liver X receptor in cholesterol metabolism. *Journal of Endocrinology*, *204*(3), 233-240.

Zidovetzki, R., and Levitan, I. (2007). Use of cyclodextrins to manipulate plasma membrane cholesterol content: evidence, misconceptions and control strategies. *Biochimica et Biophysica Acta (BBA)-Biomembranes*, *1768*(6), 1311-1324.

Websites

BreastCancer.org. (2019). http://www.breastcancer.org/symptoms/diagnosis/hormone_status (Accessed 30 October 2019).

CANSA. (2019). http://www.cansa.org.za/south-african-cancer-statistics/ (Accessed on: 28 October 2019).

National Cancer Institute. (2019). http://www.cancer.gov/types/breast/breast-hormone-therapy-fact-sheet (Accessed 30 October 2019).

ThermoFisher Scientific. (2019). https://www.thermofisher.com/za/en/home/life-science/cell-culture/transfection/rnai-transfection.html (Accessed 30 October 2019).

World Health Organisation. (2019). http://www.who.int/mediacentre/factsheets/fs297/en/ (Accessed 20 October 2019).